Food Structure

Volume 2 | Number 2 Article 1

1983

Food Microstructure

Follow this and additional works at: https://digitalcommons.usu.edu/foodmicrostructure

Recommended Citation
(1983) "Food Microstructure," *Food Structure*: Vol. 2 : No. 2 , Article 1.
Available at: https://digitalcommons.usu.edu/foodmicrostructure/vol2/iss2/1

This Article is brought to you for free and open access by the Western Dairy Center at DigitalCommons@USU. It has been accepted for inclusion in Food Structure by an authorized administrator of DigitalCommons@USU. For more information, please contact digitalcommons@usu.edu.

ISSN 0730-5419
CODEN – FMICDK
Vol. 2, No. 2, 1983

FOOD MICROSTRUCTURE

An International Journal on the Microstructure and Microanalysis of Foods, Feeds and their Ingredients

Published semiannually by

Scanning Electron Microscopy, Inc.
AMF O'Hare (Chicago), IL 60666
U.S.A.

FOOD MICROSTRUCTURE

An International Journal on the Microstructure and Microanalysis of Foods, Feeds and their Ingredients

EDITORS

M. Kalab, Food Research Institute, Agriculture Canada, Ottawa, Ontario, Canada K1A 0C6 (613-995-3700 x 272)

S.H. Cohen, Science and Advanced Technol. Lab., U.S. Army Natick R&D Labs, Natick, MA, 01760 USA (617-651-4578)

E.A. Davis, Dept. of Food Science & Nutrition, Univ. of Minnesota, St. Paul, MN 55108 USA (612-373-1158)

D.N. Holcomb, Kraft Inc., R&D, 801 Waukegan Rd., Glenview, IL 60025 USA (312-998-3724)

MANAGING EDITOR

Om Johari, SEM Inc. (312-529-6677)

ASSOCIATE EDITOR

Sudha A. Bhatt, SEM Inc.

PUBLISHER: Scanning Electron Microscopy Inc., P.O. Box 66507, AMF O'Hare (Chicago), IL 60666 USA

EDITORIAL BOARD

W. Buchheim, Bundesanst. Milchforsch., Kiel, W. Germany
R.J. Carroll, Eastern Reg. Res. Ctr., USDA, Philadelphia, PA
V.E. Colombo, Hoffmann-La Roche & Co, Basle, Switzerland
C.L. Davey, Meat Ind. Res. Inst., Hamilton, New Zealand
R.G. Fulcher, Agriculture Canada, Ottawa,Canada
D.J. Gallant, Ministry of Agriculture, Nantes, France
H.D. Geissinger, Univ. of Guelph, Ontario, Canada
A.M. Hermansson, The Swedish Food Inst., Goteborg, Sweden
R. Moss, Bread Res. Inst., North Ryde, Australia
Y. Pomeranz, U.S. Grain Marketing Res. Ctr., Manhattan, KS
J.S. Pruthi, M.S. Kold-Hold Industries, New Delhi, India
P. Resmini, Inst. di Industrie Agrarie, Milano, Italy
M.W. Ruegg, Fed. Dairy Res. Inst., Liebefeld-Berne, Switzerland
K. Saio, National Food Res. Inst., Ibaraki, Japan
M.V. Taranto, ITT Continental Baking Co., Rye, NY
M.A. Tung, Univ. of British Columbia, Vancouver, Canada
E. Varriano-Marston, Univ. of Pennsylvania, Philadelphia, PA
J.G. Vaughan, Queen Elizabeth College, London, U.K.
C.A. Voyle, Meat Research Inst., Bristol, U.K.
W.J. Wolf, USDA Northern Reg. Res. Lab., Peoria, IL

Annual Subscription Rates:
(Including postage and handling)

U.S. $50.00 (U.S. delivery)
U.S. $55.00 (elsewhere)

Business Communications:

Address all communications regarding subscriptions, change of address, etc. to Dr. Om Johari at SEM Inc.

Editorial Correspondence and Inquiries:

Submit papers (see instructions to authors, inside back cover), news items, books for review, etc. to one of the editors or to SEM Inc.

Copyright © 1983 Scanning Electron Microscopy, Inc., except for contributions in the public domain. All rights reserved. See Page 204.

Where necessary, permission is granted by the copyright owner for libraries and others registered with Copyright Clearance Center (CCC) to photocopy, provided that the base fee of $1.00 per copy of the article, plus .05 per page is paid directly to CCC, 21 Congress Street, Salem, MA 01907. Copying done for other than personal or internal reference use, without the expressed permission of the SEM, Inc. is prohibited. Those articles without a fee-code are not included in the CCC service.
Serial fee code: 0730-5419/83$1.00+.05.

FOOD MICROSTRUCTURE, Vol. 2 (1983), pp. 119-133
SEM Inc., AMF O'Hare (Chicago), IL 60666 U.S.A.

SENSORY AND INSTRUMENTAL TEXTURE PROPERTIES OF FLAKED AND FORMED BEEF

Armand V. Cardello, Ronald A. Segars, John Secrist,*
Joseph Smith*, Sam H. Cohen, and Robert Rosenkrans*

Science and Advanced Technology Laboratory
and
Food Engineering Laboratory*
U.S. Army Natick Research & Development Laboratories
Natick, Massachusetts 01760

Abstract

Four experiments were conducted to assess the sensory textural properties, consumer acceptability and instrumental-sensory correlates of flaked and formed beef steaks. In Experiment 1, the effects of additions of NaCl, TPP and soy isolate on the texture of steaks were examined using a trained texture profile panel, and the texture of these steaks was compared to that of intact muscle (ribeye) steaks. Results showed large differences between the flaked and formed samples and the ribeye steak, as contrasted to small differences among the flaked and formed samples treated with different levels of NaCl, TPP and/or soy isolate.

In Experiments 2 and 3 the effect of flake size on the texture of flaked and formed beef was examined. In Experiment 2, instrumental shear data and SEM data were collected and compared to the sensory data. In Experiment 3, a comparison was made of the texture of these products to both ribeye steak and ground beef patties. Systematic differences in a variety of textural attributes were observed as a function of flake-size. In general, the smallest flake-size produced a texture most like ground beef, whereas certain intermediate and large flake sizes produced a texture most like whole-muscle steak. Simple and multiple linear regression equations were established between sensory and shear stress measures on these steaks, and these data, combined with the SEM data, suggested that tenderization of these meats is attributable to mechanical disruption of the tissue and not to an enzymatic process.

In Experiment 4, a consumer test was conducted to assess the effect of flake-size on the acceptability of flaked and formed steaks, and to assess consumer perception of the similarity of the texture of these products to other beef products. Although few significant differences in the acceptability of the flaked and formed products were observed, maximal acceptability ratings were found for the intermediate flake sizes. In addition, it was found that consumers do not associate the texture of flaked and formed steaks with any one of a variety of traditional beef products.

Initial paper received March 16, 1982.
Final manuscript received October 20, 1983.
Direct inquiries to A.V. Cardello.
Telephone number: 617-651-4720.

Key Words: texture, flaked and formed, sensory, instrumental, NaCl, tripolyphosphate, soy isolate, flake-size, beef, restructured meat

Introduction

In recent years the rising cost of beef has forced consumers to search for lower quality grades and cuts of beef to provide them and their families with red meat entrees. The development of the comminution method of flake-cutting has helped to close the gap between consumer desires for beef products and the amount of these products that can be borne by the family budget. This has been achieved by enabling the use of lower quality grades and cuts of beef to produce products that have the functionality and sensory properties of higher grades and cuts. As the largest single purchaser of beef and other meat products in the world, the United States military has interest in the improvement of the flaked and formed process. This interest has led to a continuing research and development program at the U.S. Army Natick Research and Development Laboratories (NLABS), aimed at improving the flaked and formed process. Over the years, research has been conducted on the ingredients, processing variables, chemical properties, rheological properties and sensory properties of flaked and formed beef, lamb, pork and veal. In the case of flaked and formed beef, one aim of this research has been to optimize the textural characteristics of the product to match that of intact-muscle steak. The present paper is a summary of recent research conducted in our laboratory on the sensory textural properties of flaked and formed beef, on their sensory–instrumental correlates, and on consumer judgments of their acceptability.

The process of flake-cutting involves impelling meat across a stationary cutting-head comprised of a circular array of cutting surfaces. After the meat has been flake-cut, a steak-like product can be prepared by mixing the comminuted meat with NaCl and sodium tripolyphosphate (TPP) and submitting the meat to a sustained pressure. Some parameters of importance in this process are the flake-size (determined by the width and spacing of blades on the cutting head), the temperature at which the meat is flaked, the levels of salt and TPP added to the mixture, the mixing temperature and time, and the pressure and temperature during forming. Of these parameters, NaCl/TPP concentration and flake-size were investigated in our laboratory for their effects on the textural properties of these products. Also, the addition of a soy isolate to improve binding of the meat was examined.

A great number of studies have examined the effects of NaCl/TPP concentration on the properties of meat (Hellendoorn, 1962; Shults and Wierbicki, 1973; Ohashi and Sugano, 1973; Shults et al., 1976; Schwartz and Mandigo, 1976; Neer and Mandigo, 1977; Theno et al., 1978; Huffman et al., 1981; Hand et al., 1981). These studies have demonstrated increased tenderness, cooking yield, water-holding capacity, cohesiveness, juiciness, flavor and acceptability of meat with the addition of NaCl and TPP at varying concentrations. In the study by Neer and Mandigo (1977) the effect of NaCl (0–3%) and TPP (0–0.5%) levels were examined in a flaked, cured pork product. They found increased cooking yield and water-binding capacity, as well as improved appearance, flavor, and acceptability with increasing NaCl levels. As TPP levels were increased, flavor desirability increased, while appearance, color and acceptability increased then decreased (Neer and Mandigo, 1977). A synergistic effect between NaCl and TPP was proposed to explain the interaction effects that resulted in a maximum acceptability at intermediate levels of both NaCl and TPP (Neer and Mandigo, 1977). This synergistic effect was observed previously by Schnell et al., (1970), Flesch and Bauer (1965), and Schwartz and Mandigo, 1976. Huffman and Cordray (1979) have reported improvements in the flavor, tenderness, juiciness and connective tissue of restructured (chunked) pork products with the addition of 0.75% NaCl, and improvements in juiciness with the addition of 0.25% TPP. However, their data show that these effects were not statistically significant. Cooking losses were decreased most by the addition of both 0.75% NaCl and 0.25% TPP. Huffman et al., (1981), working with flaked and formed beef patties, also found improved flavor, cohesiveness and juiciness with the addition of 0.75% NaCl, but little effect of the addition of 0.30% TPP on any measured property. They also found that the addition of NaCl and TPP improved most sensory properties of the meat more than did the addition of NaCl or TPP alone. Most recently, Hand et al., (1981) have shown improved juiciness, cohesiveness, flavor and ease of fragmentation with the addition of NaCl (0.44%), TPP (0.25%), and hydrolyzed vegetable protein (0.31%) to restructured beef steaks.

Although the addition of soy protein to beef has been frequently investigated, the addition of soy protein to flaked and formed products has only recently been studied. Claims of increased water and/or fat retention and improved binding of meat particles by addition of soy isolate (Anonymous, 1979; Schweiger, 1974; Morris, 1980) makes this a potentially important area for improving flaked and formed products. However, in a recent study by Hand et al., (1981) addition of soy protein isolate to restructured beef steaks significantly increased off-flavors, while having no effect on the sensory textural properties of the meat.

The effect of flake-size on the sensory properties of flaked and formed meat products has also not been thoroughly investigated, although the claim has been made that the "bite" of these products can be varied from a "hamburger-like" texture to a "steak-like" texture by varying the flake-size (Anonymous, 1977). In studies by Popenhagen et al., (1973) and Popenhagen and Mandigo (1978) flake-size was investigated for its effects on the sensory properties of flaked and formed pork. For products flaked at −5.6°C, significantly lower tenderness was found with a 3.0 mm than with a 6.9 mm or 12.7 mm flake-size. For products flaked at 2.2°C, significantly lower scores were found for juiciness, cohesiveness and overall acceptability with the smallest flake-size (Popenhagen and Mandigo, 1978). Chesney et al., (1978) have also examined the effect of flake-size on the sensory properties of flaked and formed pork. In their work, they found large flake sizes (12.7 mm) to result in a product that is less cohesive than products made with smaller flake sizes (3.0 mm and 6.9 mm). Juiciness and tenderness were also found to decrease with increasing flake-size, and the overall acceptability of the products was significantly lower for the product made with the largest flake-size. At present, no studies have examined the effect of flake-size in a flaked and formed beef product, and no studies have made comparisons of the sensory characteristics of these products to an intact-muscle steak. Such information is essential for developing a flaked and formed product with steak-like texture.

General Materials and Methods

Processing of Flaked and Formed Steaks

All steaks were made from USDA Choice, yield grade 2 or 3, square-cut chucks that had been boned and trimmed of fat to 18 ± 2%. The boneless meat was tempered to 0°C and flake-cut with an Urschel Comitrol, Model 3600 (Urschel Laboratories, Inc., Valparaiso, IN 46383) using one of several specified cutting heads. The list of cutting heads is shown in Table 1, along with conformational data on each. The meat was mixed eight minutes in a ribbon-type mixer (Keebler, Chicago, IL 60636) under vacuum with salt (NaCl) and sodium tripolyphosphate ($Na_5P_3O_{10}$). The levels of salt and sodium tripolyphosphate were experimentally manipulated in Experiment 1 and held constant at 0.5% NaCl and 0.25% $Na_5P_3O_{10}$ in Experiments 2–4. The meat was stuffed into polyethylene tubing (lay-flat dimension = 13.3 cm) under vacuum (Vemeg Robot 100 S2 Type 116, Robert Pfiser and Co., Inc., Boston, MA 02210) clipped and pre-shaped to approximate the die shape. The meat log (2.7 – 3.6 kg) was frozen to −18°C and tempered to −3°C. The meat was then pressed at 8.75×10^4 N/m^2 in die #452 (Ribeye) using a Bettcher press, Model #70 (Bettcher Industries, Inc., Vermillion, OH 44089). The formed log was sliced on a Bettcher cleaver, Model #39 (Bettcher Industries, Inc., Vermillion, OH 44089) to produce a 6 oz. steak. The steaks were separated with patty paper, placed in sealed polyethylene bags, frozen immediately to −18°C and stored at −18°C until time of testing.

Table 1. Cutting heads used in preparation of flaked and formed steaks and conformational data about each.

Cutting Head Designation	Comitrol Designation	# of Cutting Posts on 152.4 mm Circumference	Opening Size (mm)
060	2K–020060	28	1.524
510	2J–030510	20	12.954
750	2J–030750	20	19.050
1628	2–0001600–28	28	40.640
1620	2–0001600–20	20	40.640
1614	2–0001600–14	14	40.640
1610	2–0001600–10	10	40.640

Cooking

In Experiments 1, 2 and 3, all samples were broiled from the frozen state on Farberware electric broilers, model

455N (S.W. Faber, Yonkers, NY) to an internal temperature of 69°C (internal temperature probe) turning once. In the consumer test of Experiment 4, samples were cooked on a flat grill. Details on the cooking procedure used in that test can be found in the Methods section of Experiment 4.

Sensory Panels

Texture Profile Panel. In all the experiments reported here, with the exception of Experiment 4, the flaked and formed products were evaluated by a trained texture profile panel. This panel, which consisted of 6–10 members during the period of these tests, was formed in June of 1977 and has operated within the Behavioral Sciences Division of the Science and Advanced Technology Laboratory at the U.S. Army Natick R&D Laboratories since that time. Each member of the panel was trained in the General Foods' Texture Profile Method, and all members have had extensive experience in evaluating the textural properties of a broad range of products, including fish, gelatins, breads, ground beef and other meat products.

As a descriptive/analytical panel, the first task of the panel was to develop a set of sensory attributes important for characterizing the texture of these products, as well as that of whole-muscle steak. These attributes were established through examination of a wide range of flaked and formed and whole-muscle steaks. Table 2 is a list of the important attributes and the operational definitions of each, as developed by the panel. Each attribute was evaluated at a specific time during mastication. "Coarseness" of the cooked surface was evaluated first, "springiness" was evaluated next during a partial compression with the molar teeth, "hardness," "cohesiveness" and "moisture/oil release" were evaluated during the first bite into the product, "chewiness," "size of particles," "moistness," "cohesiveness of the mass" and "amount of connective tissue" were evaluated during chewing, and "oily mouth coating" and "number of particles remaining in the mouth" were evaluated after swallowing.

Table 2: Definitions of textural attributes developed by texture profile panel for characterizing flaked and formed beef products.

Coarseness:	The perceived degree of roughness of the cut surface (characterized by large, uneven particles).
Springiness:	The perceived degree (extent) to which the sample returns to its original shape after slight compression with the molar teeth.
Hardness:	The perceived force required to compress the sample between the molar teeth.
Cohesiveness:	The perceived degree to which the sample holds together as a single mass upon biting.
Moistness:	The perceived amount of water and/or oil in the sample.
Moisture/Oil Release:	The perceived amount of water and/or oil released from the sample during mastication.
Chewiness:	The total perceived force required to reduce the sample to a consistency ready for swallowing when chewed at constant rate of force application.
Size of Particles:	The perceived volume of individual particles.
Cohesiveness of the Mass	The perceived degree to which the sample holds together as a single mass during mastication.
Amount of Connective Tissue:	The perceived volume of connective tissue (gristle) in the sample.
Oily Mouthcoating:	The perceived degree of oil left on the teeth and palate after swallowing.
Number of Particles Remaining:	The perceived number of particles left on the teeth, gums and oral cavity after swallowing.

Consumer Panel. In Experiment 4 a volunteer laboratory consumer panel was used. This panel was drawn from a population of 450 employees of NLABS who have volunteered to participate in consumer taste tests. None of the panelists had prior experience with these flaked and formed products, although some may have had experience with commercially available flaked steaks. All panelists had participated in previous consumer acceptance tests on a variety of food products.

Experiment 1

The first experiment was designed to compare the textural characteristics of flaked and formed beef steaks to those of intact muscle steak, and to assess the effect of the addition of TPP, NaCl and soy isolate on the texture of these products.

Samples

The samples tested appear in Table 3. All were processed with the 750 (intermediate size) cutting-head (see Table 1). The tested levels of TPP were 0.0 and 0.50%, reflecting both the fact that the maximum phosphate level allowed in meat is 0.50% (U.S.D.A., 1975) and the fact that preliminary triangle tests showed no significant differences between samples with 0.25% TPP and either 0.0% or 0.5% TPP. NaCl levels of 0.0% and 0.50% were chosen on the basis of prior information concerning the necessary level for proper binding of the meat particles and on the basis of triangle tests, which showed that samples prepared with 0.0% and 0.50% NaCl were significantly different. The choice of 0.0% and 1.0% soy isolate levels was based on product usage recommendations.

Table 3: Concentrations of NaCl, TPP and soy isolate for the sample used in Experiment 1.

	Concentration (%)		
	NaCl	TPP	Soy Isolate
Treatment 1	0.0 %	0.50%	0.0%
Treatment 2	0.50%	0.0 %	0.0%
Treatment 3	0.50%	0.50%	0.0%
Treatment 4	0.0 %	0.0 %	1.0%
Treatment 5	0.0 %	0.50%	1.0%

Procedure

The five sets of samples of flaked and formed beef were prepared and cooked as described under Materials and Methods. A sixth set of samples, consisting of whole-muscle ribeye steak, was also included for evaluation and cooked in the same manner. The rib-eye cut was chosen for comparison with the flaked and formed steaks, since it is an intermediate quality cut of beef and serves as a good target product for these steaks. After cooking, samples were halved and placed on heated ceramic dishes for evaluation by the profile panel. Each member received all six samples and was instructed to evaluate them for each of the attributes listed in Table 2. All panelist judgments were made independently.

The psychophysical method of magnitude estimation was used to judge the perceived magnitude of each attribute in the products. All panelists had prior experience with this method. The ribeye sample was used as a standard and was assigned a modulus of 10.0 for each of the textural attributes. Panelists were instructed to first sample the ribeye, and to then evaluate each of the other samples relative to this standard. Panelists were instructed to assign numerical ratings according to the ratio of perceived magnitudes between the test sample and the standard. Thus, if the

chewiness of a test sample was perceived to be twice that of the standard (ribeye), the panelist would assign the number 20.0 to it; if it was one-third as chewy as the standard, he/she would assign to it the number 3.33, etc. Each sample was evaluated once for each attribute by each panelist and all test samples were evaluated in random order.

Results

The magnitude estimates assigned to each sample for each attribute were averaged across panelists by calculating the geometric mean of the magnitude estimates. The geometric mean was used, because magnitude estimates have been shown to be log-normally distributed (Stevens, 1957; Marks, 1974). Figure 1 shows the texture profiles for the three samples containing only TPP and/or NaCl. Each of the textural attributes appears along the bottom of the figure. The ordinate is the geometric mean magnitude estimate for each attribute. The solid horizontal line represents the value assigned to the standard (ribeye) steak for each attribute. The dotted horizontal lines represent 25% deviation from the standard. Although the data points for each sample reflect geometric mean ratings for different attributes, the data points have been joined to facilitate comparison of the profiles.

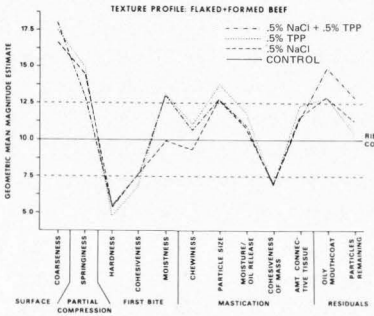

Figure 1. Texture profiles for flaked and formed beef products containing 0.5% NaCl, 0.5% TPP or 0.5% NaCl and 0.5% TPP. The ordinate is the geometric mean magnitude estimate for each texture attribute listed along the abscissa.

Overall, the profiles for the flaked and formed samples are very similar to one another, and all are quite different from that for the ribeye steak. Comparison of the logarithms of the magnitude estimates assigned to each test sample with the logarithms of the modulus assigned to the standard (Z-test) revealed that all three flaked and formed products were significantly ($p<0.05$) more coarse, less firm (hard), and less cohesive (during mastication) than the ribeye sample. In addition, the 0.0% NaCl/0.5% TPP sample was less cohesive (during first bite) and had greater moisture/oil release than the ribeye ($p<0.05$), and the 0.50% NaCl/0.0% TPP and 0.5% NaCl/0.50% TPP samples were both perceived as more oily than the ribeye sample ($p<0.05$). Other apparent differences in Figure 1 were not statistically significant due to within sample variability.

Figure 2 shows the profiles for the two soy-added samples relative to the ribeye. Only the sample with both soy and TPP was significantly different from the control. This sample was significantly less firm (hard) and had more moisture/oil release and more particles remaining after swallowing than the ribeye sample ($p<0.05$).

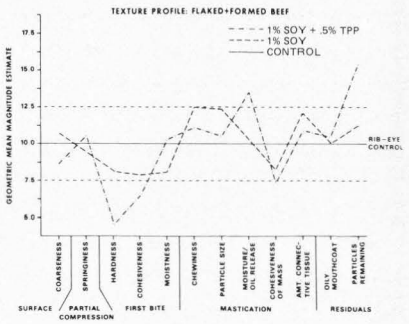

Figure 2. Texture profiles for flaked and formed beef products containing 1% soy isolate or 1% soy isolate and 0.5% TPP.

Figure 3 is a composite of Figures 1 and 2, showing the similarity among all of the five flaked and formed products. Analysis of variance applied to the logarithms of the magnitude estimates assigned to the five test samples showed no significant differences among any of the flaked and formed products treated with different levels of NaCl, TPP and soy isolate.

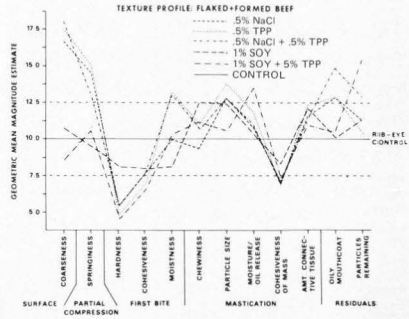

Figure 3. Composite of Figures 1 and 2.

Discussion

The texture profiles shown in Figures 1–3 provide useful information from which one can assess the textural differences between the flake-cut beef products of this test and intact muscle (ribeye) steak. The small differences among the five different flaked and formed samples suggest that variations in the levels of NaCl and TPP between 0 and 0.5% produce only slight differences in the texture of these products, as compared to the differences observed between these products and intact muscle steak. The failure to find significant effects of NaCl and TPP level on the texture of these products is surprising in light of previous research, but is consistent, for example, with the failure to find significant effects of these ingredients in restructured pork (Huffman and Cordray, 1979).

In view of the fact that all of the samples with 0.50% TPP had higher geometric mean ratings for moistness and moisture/oil release than the control (Figure 3) and moisture/oil release was significantly higher for the 0.0% NaCl/0.50% TPP and the 1.0% soy isolate/0.50% TPP samples than for the control, it was decided that the level of TPP could be reduced below 0.50%. Since the binding properties of the meat during processing were adequate with 0.25% TPP addition, 0.25% TPP was selected for use in subsequent processing of these products.

The fact that the sample with only 1.0% soy isolate produced a texture that was no different from the NaCl and TPP-added samples, suggests that the soy-isolate assisted in the binding of the meat flakes, as has been suggested previously (Morris, 1980; Anonymous, 1979). In addition, since some improvement was observed in the coarseness and springiness of the soy-isolate-added samples (Figure 3), reason exists for giving further study to the addition of soy isolates to these products.

Experiment 2

The second major processing variable having direct influence on the textural properties of flaked and formed products is flake-size. This experiment was designed to provide information on the magnitude of these effects using three greatly different flake sizes. Both sensory and instrumental (Instron shear tests and scanning electron microscopy (SEM)) data were collected.

Samples

Samples of flaked and formed beef processed with three different cutting heads were used as test products. Cutting heads were chosen to enable a comparison of the two extreme flake sizes with the flake-size used in preparing the samples in Experiment 1. The three cutting heads chosen for testing were the 060 (small flake), 750 (intermediate flake) and 1610 (large flake).

Procedure

Samples were cooked, prepared and served in the same manner as in Experiment 1, except for certain instrumental measures that were made on raw samples, as described below.

Sensory Data. The textural attributes evaluated were reduced from the 12 used in Experiment 1 to include only the mechanical properties perceived during partial compression, first bite and mastication. The surface and residual properties were not evaluated, because they were not deemed important to the differentiation of these three products. The attributes of moisture/oil release and cohesiveness of the mass were found to be redundant with the moistness and cohesiveness attributes, respectively, and so they were also eliminated.

Samples were presented simultaneously to members of the texture profile panel and all ratings were made independently of one another. The method of magnitude estimation was used and the sample processed with the 750 head-size was designated as the standard and assigned the number 100.0 on all attributes. Panelists evaluated the 750 head-size first and then evaluated the other two samples in random order. Five replicates were conducted.

Shear Data. The punch shear data were obtained with an Instron Universal Testing Machine equipped with a Punch and Die test cell (Segars et al., 1975). A 2 cm diameter flat-end punch travelling at 5 cm/min was forced through the cooked steak and maximum shear stress (punch shear), stress at yield, energy to rupture and stiffness were determined from the resulting force-deformation curves.

SEM Data. Small pieces of meat approximately 1 cm^3 were cut from an area adjacent to where the Instron punch had passed through the sample and were put into 2.5% glutaraldehyde fixative overnight (approximately 16 hrs). The pieces were then cut into smaller 0.2 cm^3 pieces and stored in the fixative for 24 hrs. Samples were then dehydrated through 100% ethyl alcohol and critical point dried using liquid CO_2.

The dried samples were mounted on specimen stubs with conductive silver paint, sputter coated with gold-palladium, and then examined in a Nanometrics SEM at 20 kV. Polaroid type 55 film was used.

Results

Sensory Data. Figure 4 shows the geometric mean magnitude estimates assigned to each sample for each attribute. The attribute ratings for the sample processed with the 750 head-size are all designated by a single point at 100.0 on the ordinate, representing the modulus (standard number) assigned to that sample.

In order to test whether ratings for the samples processed with either the 1610 or 060 head-size were significantly different from that of the 750 head-size, the magnitude estimates were normalized by taking the logarithm of the values, and the normalized values were then used to statistically test the hypothesis that they did not differ from a value of 2.0 (log of 100). The results of these Z-statistics (two-tailed) are shown by the brackets in Figure 4, which show the attribute ratings that were found to be significantly different from 100 ($p<0.05$).

The sample processed with the 1610 head-size had ratings significantly above 100 for all attributes except "moistness." In contrast, the sample processed with the 060 head-size had attribute ratings significantly below 100 for the attributes of "cohesiveness," "chewiness," "size of particles," and "amount of connective tissue."

Shear Data. Data from the Instron Punch and Die tests are shown in Table 4. The maximum shear stress, stress at yield and energy to rupture all reflect the effort required to cause separation and tearing of the meat structure. In general they reflect the "toughness" of the meat and show increases as flake size increases. Standard deviations are also included and show an increase as flake size increases. A previous study (Segars et al. 1983; unpublished manuscript) has demonstrated a linear relationship between the mean and standard deviation of maximum shear stress data; the data in Table 4 also show this linear relationship.

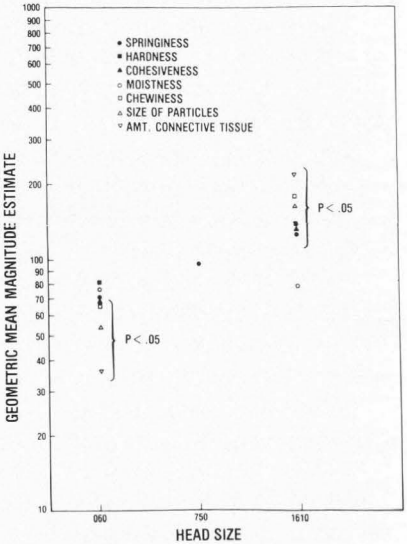

Figure 4. **Geometric mean magnitude estimates of seven textural attributes for flaked and formed beef prepared with the 060 and 1610 cutting head sizes. Data are compared to a modulus of 100.0 that was assigned to represent the intensity of each attribute for a product made with the 750 head size.**

The stiffness parameter, also in Table 4, reflects the initial firmness or resistance to indentation of the steak, and it is much less affected by flake size than either the maximum shear stress, stress at yield or energy to rupture. Although the initial firmness of the steaks does not change significantly with flake size, it is lowest with the intermediate flake size.

Table 4. Means ± standard deviations for Instron punch and die shear data obtained from the samples tested in Experiment 2

Head Size	n	Maximum Shear Stress N/cm^2	Stress At Yield N/cm^2	Stiffness N/cm^2	Energy To Rupture N/cm
060	16	5.822 ± 0.690	5.770 ± 0.732	10.966 ± 2.492	3.475 ± 0.897
750	16	8.404 ± 1.362	7.023 ± 1.496	9.871 ± 1.060	6.977 ± 0.604
1610	16	12.172 ± 1.895	10.499 ± 2.233	12.175 ± 1.349	8.828 ± 1.269

SEM Data. Scanning electron micrographs representing the three products in both raw and cooked states are shown in Figure 5.

Samples a and d in Figure 5 were prepared from meat cut with the 060 cutting head, meat for samples b and e was cut with the 750 cutting head and the meat for samples c and f was cut with the 1610 cutting head. Samples a, b and c were raw, samples d, e and f were cooked.

Discussion

Sensory Data. Overall, the sensory data demonstrate an increase in the "springiness," "hardness," "cohesiveness," "chewiness," "size of particles," and "amount of connective tissue" for flaked and formed beef products processed with increasingly larger cutting heads. Moreover, the magnitude of these differences were on the order of 6 to 1 for some attributes, e.g., amount of connective tissue. These data underscore the importance of flake-size in establishing a desired texture for flaked and formed products.

Shear Data. The instrumental shear measurements (Table 4) show that the products become firmer and less homogeneous as flake size increases. Increases in the maximum shear stress, stress at yield, and energy to rupture reflect a toughening of the meat, and are, therefore, in agreement with the sensory data.

SEM Data. The field of view shown in the micrographs of Figure 5 is approximately 100 micrometers wide. The scale of flake sizes, even for the smallest flakes produced with the 060 cutting head, is approximately 1500 micrometers in its largest dimension. Thus the photographs represent only one-tenth of the surface of the smallest flakes, and effects from macroscopic changes (flake size) should not be visible in the pictures. Any effects observed would presumably stem from secondary effects caused by differences in the quantity of enzyme released and changes in the amount of surface area available for enzymatic action. Both quantities should be greatest for the smallest flakes (060), since these flakes required the greatest amount of cutting. Hence the 060 samples should show the greatest amount of structural damage or interruption of the normal state. This damage might be expected to decrease progressively as the flake size increases.

The micrographs of Figure 5 do not show distinct change in the fiber due to interruption or other structural damage as flake size is altered. It thus appears that enzymatic breakdown of the meat tissue is not affected by the flaking process, either because the released enzymes have not reached a level sufficient to produce observable structural changes, or under the experimental processing conditions, the enzymes had neither the time nor the proper environment in which to act. In any case it seems that the tenderization produced by the flaking process is due, in this experiment, primarily to a mechanical disruption and breaking of the connective tissue and muscle fibers. The more disruption and breakage that occurs from mechanical means, the more tender the product.

In Experiment 1 of this report, whole muscle rib-eye steaks were compared to flaked and formed steaks. In that experiment, the hardness and cohesiveness of the flaked and formed product (made using the 750 cutting head) were lower and the chewiness was greater than in the rib-eye steak. In the next experiment to be reported (Experiment 3), flaked and formed steaks made with seven different cutting heads, ground beef, and rib-eye steaks were evaluated on the same three sensory attributes. The textural changes occurring with increasing flake size paralleled the changes observed in the present experiment.

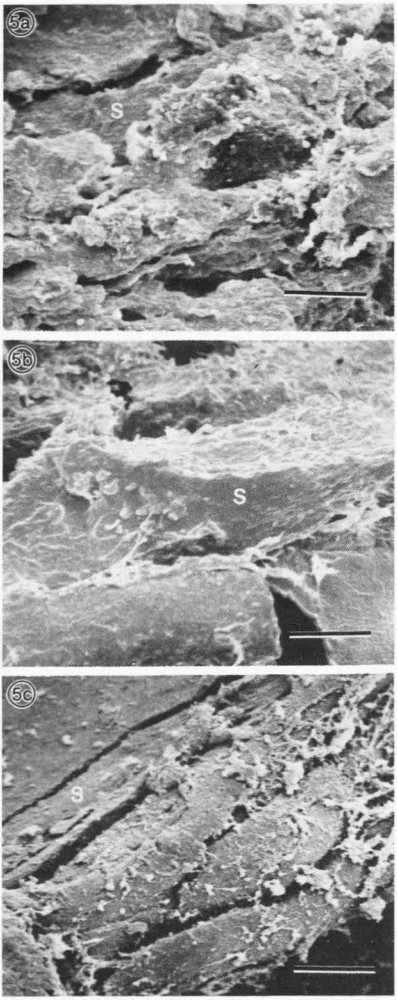

Figure 5. SEM micrographs of raw samples used in Experiment 2. 5a, 5b and 5c were processed with the 060, 750 and 1610 cutting heads, respectively. The muscle fiber surface (S) appears normal. Bar = 20μm.

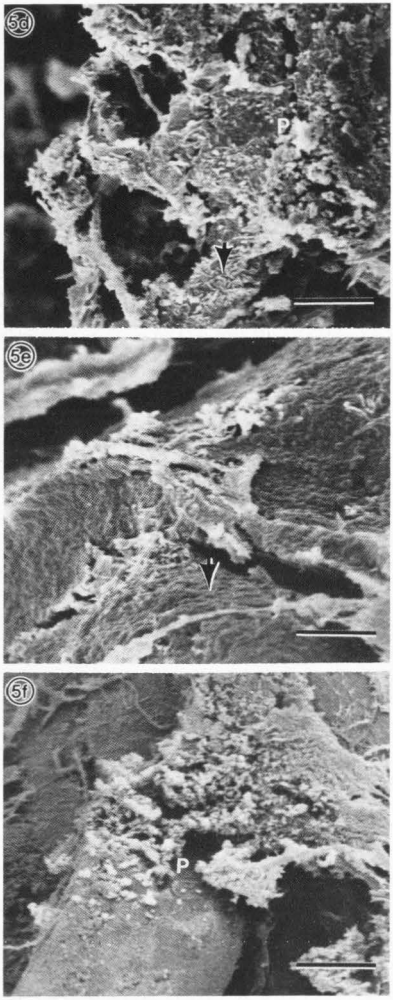

Figure 5. (cont'd). SEM micrographs of cooked samples used in Experiment 2. 5d, 5e and 5f were processed with the 060, 750 and 1610 cutting heads, respectively. Heat causes coagulation (P) and degradation (arrows) of the muscle fiber surface. Bar = 20μm.

Although the discrepancy between chewiness judgments, on the one hand, and hardness and cohesiveness judgments, on the other, may seem perplexing, it can be explained on the basis of the fact that chewiness is evaluated throughout the mastication process, and is, therefore, greatly influenced by the textural characteristics of the individual pieces of meat within the sample.

The attributes of hardness and cohesiveness are evaluated only upon first bite and, thus, are much less affected by the texture of the individual pieces of meat in the sample. Since the SEM studies in this experiment showed that the individual pieces were not visibly affected by the flaking process, one would then expect that the chewiness of flaked and formed steaks, which are made from the tougher meat of square-cut chuck, would be greater than the chewiness of rib-eye steaks. This was, in fact, what was found.

The conclusions from the present study are that flake size has a significant effect on the texture of flaked and formed meat and that natural chemical or enzymatic action plays only a minor role in the tenderization of flaked and formed meats. The major role in tenderization is played by the mechanical disruption itself. This stands in contrast to a previous study of flaked and formed meat (Cohen et al., 1982) which showed that various textural parameters, including amount of connective tissue, were improved with the addition of lysosomal proteolytic enzymes (cathepsins) during preparation. In that study, enzymes were added to an already flake-cut meat, which issued a much higher enzyme level than in the present study. These high enzyme levels, coupled with a longer mixing time of 15 minutes (8 minutes was used in the present study), could explain why the effect of enzyme was found only in the previous work. This suggests that the present processing methods for flaked and formed products could be modified (longer mixing times, holding at enzyme active temperatures etc.) to take advantage of the tenderization offered by the small amounts of natural enzymes released during the flaking process.

Experiment 3

Experiment 3 was aimed at a parametric examination of the effects of flake-size on the texture of flaked and formed beef and a comparison of these products to ground beef and ribeye steak. In addition, the relationship between sensory and instrumental measures of these products was assessed by obtaining Instron punch-shear data (maximum shear force, maximum strain and stiffness) and single blade shear (Food Technology Corp, Rockville, MD 20852) data (force per unit area) on these samples.

Samples

The samples consisted of seven treatments of flaked and formed beef, one sample of ribeye steak and one sample of ground beef. The flaked and formed beef samples were all processed as described under Materials and Methods, except that each set of samples was processed with a different cutting head. Table 1 lists the seven cutting-head sizes that were used. The ground beef was prepared from similar meat, ground through a 3.175 mm plate, stuffed into casings (with no salt or TPP), pressed, sliced and packaged in the same manner as the flaked and formed samples.

Procedure

Samples were cooked, prepared and served in the same manner as described in the previous experiments. Since testing of these products was to continue for an extended period and no suitable sensory reference standards were available for these products, it was necessary to identify a simple and reliable scalar method that could be used to evaluate these products without the need for an invariant reference. A 7–point category scale method was chosen for this purpose. Of the seven points, three were labeled. The three labeled points were 1–slight, 4–moderate and 7–extreme. Zeros were allowed to reflect absence of an attribute in the sample.

Samples were presented randomly to panelists over several sessions. During each session, three samples were presented. Each panelist rated each sample on the same attributes used in Experiment 2. In addition, two visual attributes were judged. These were the "coarseness of the cut surface" and the "size of fat deposits on the cooked surface." All samples were evaluated on five separate occasions by each panelist.

Results

The mean panel ratings for each sample and each attribute were calculated and appear in Table 5. Analysis of variance performed on the data revealed significant effects ($p<0.01$) of cutting-head size on all of the judged attributes. These results, as well as the results of Neuman–Keuls contrast tests performed on the differences in mean ratings among samples are shown in Table 5. In order to visually compare the mean ratings of the flaked and formed products to the ratings assigned to the ribeye, a difference score was calculated for each sample. The difference score was the mean panel rating assigned to the test sample minus the mean panel rating assigned to the ribeye sample. Thus, a score of zero represents identity with the ribeye steaks, scores greater than zero indicate that the sample had more of the attribute than the ribeye, and scores less than zero indicate that the sample had less of the attribute. These difference scores are plotted by attribute and appear in Figures 6–8. Figure 6 is a plot of the scores for the visual attributes of "coarseness" and "size of fat deposits," Figure 7 is a plot of the mechanical attributes and Figure 8 is a plot of the geometric and moisture attributes.

Figure 6 shows a steady increase in the "perceived size of fat deposits" on the cooked surface of these products, starting with ground beef and progressing through increasing flake sizes. In all cases the size of fat deposits is smaller for the flaked and formed products than for ribeye steak, although the 1614 and 1610 head sizes were not significantly smaller (Table 5). A large difference can be seen between the "coarseness" of the flaked and formed product processed with the smallest cutting-head (060) and those processed with larger head sizes. Ground beef was significantly more coarse than any of the flaked and formed samples (Table 5) and all of the flaked and formed products were more similar in coarseness to the ribeye steak than to ground beef.

Figure 7 shows a steady increase in the perceived "hardness," "chewiness," "cohesiveness upon first bite," and "cohesiveness of the mass" in progressing from ground beef through increasing flake (cutting-head) sizes of the flaked and formed products. The "springiness" of the products, however, tended to decrease with increasing head-size. Both ribeye and ground beef were significantly less springy than any of the flaked and formed products (Table 5).

Figure 8 shows an increase in both the "amount of connective tissue" and the perceived "size of chewed pieces" with increasing head-size in the flaked and formed products.

In both instances a greater increase is observed within the smaller head sizes. Also, in both instances, ground beef falls between the smallest (060) head-size and the others. The "moisture/oil content" of the samples did not vary greatly among any samples, showing few significant differences (Table 5).

Table 5. Mean ratings assigned to each sample on each attribute and results of ANOVA's and Neuman-Keuls contrasts tests for the data obtained in Experiment 3. Mean ratings in the column with the same superscript (a,b,c,d,e) are not significantly different ($p < .05$)

Coarseness

Ground Beef	5.69^{a}
1620	4.31^{b}
1610	4.00^{b}
1614	3.87^{b}
510	3.80^{b}
Rib-Eye	3.05^{bc}
750	3.00^{bc}
1628	2.20^{cd}
060	1.73^{d}

Size of Fat Deposits

Rib-Eye	5.66^{a}
1614	4.93^{ab}
1610	4.78^{ab}
1620	4.13^{bc}
750	3.36^{cd}
1628	3.13^{cd}
510	2.40^{de}
Ground Beef	1.50^{e}
060	1.45^{e}

Springiness

060	5.45^{a}
750	4.64^{ab}
1620	4.63^{ab}
1628	4.40^{ab}
510	4.20^{b}
1614	4.07^{b}
1610	3.67^{b}
Ground Beef	2.56^{c}
Rib-Eye	1.66^{d}

Hardness

1610	5.33^{a}
Rib-Eye	4.77^{ab}
1614	4.60^{ab}
750	4.36^{ab}
1628	4.27^{ab}
1620	4.19^{ab}
510	4.13^{ab}
060	3.60^{bc}
Ground Beef	2.69^{c}

Cohesiveness

Rib-Eye	6.16^{a}
1610	5.22^{ab}
1614	4.80^{b}
750	4.55^{b}
1620	4.50^{b}
1628	4.47^{b}
510	4.33^{b}
060	3.70^{b}
Ground Beef	2.44^{c}

Chewiness

1610	6.11^{a}
1614	5.73^{a}
1620	5.50^{a}
750	5.18^{ab}
1628	5.00^{ab}
510	4.47^{b}
Rib-Eye	4.44^{b}
060	4.10^{b}
Ground Beef	3.25^{c}

Size of Chewed Pieces

Rib-Eye	5.95^{a}
1610	5.67^{ab}
1614	5.27^{ab}
750	5.09^{ab}
1620	4.88^{b}
1628	4.67^{bc}
510	4.20^{bc}
Ground Beef	3.69^{c}
060	2.30^{d}

Moistness

1620	5.19^{a}
1614	5.13^{a}
1628	4.87^{ab}
510	4.87^{ab}
750	4.82^{ab}
1610	4.78^{ab}
060	4.60^{ab}
Rib-Eye	4.00^{b}
Ground Beef	3.81^{b}

Cohesiveness of Mass

Rib-Eye	5.51^{a}
1610	5.11^{a}
1614	4.93^{a}
1620	4.06^{b}
750	3.73^{bc}
1628	3.40^{bc}
510	3.40^{bc}
060	2.90^{c}
Ground Beef	1.63^{d}

Amount of Connective Tissue

1610	5.89^{a}
1614	5.67^{a}
1620	5.19^{a}
510	3.87^{b}
750	3.73^{b}
1628	3.40^{b}
Ground Beef	2.40^{c}
Rib-Eye	2.13^{cd}
060	1.30^{d}

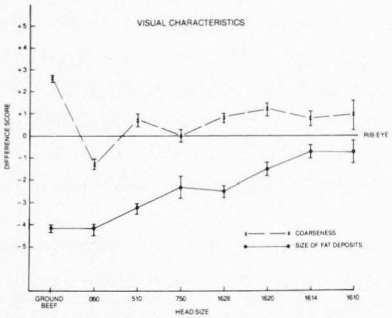

Figure 6. A plot of difference scores for the two visual attributes judged in Experiment 3. The difference score is the rating assigned to the test sample minus the rating assigned to the ribeye control.

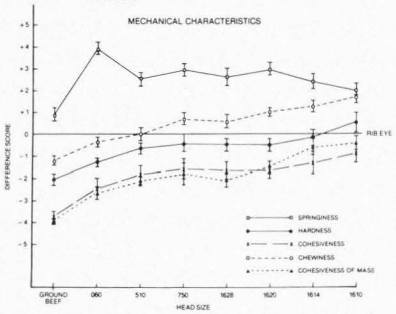

Figure 7. Same as Figure 6, but for the mechanical texture attributes.

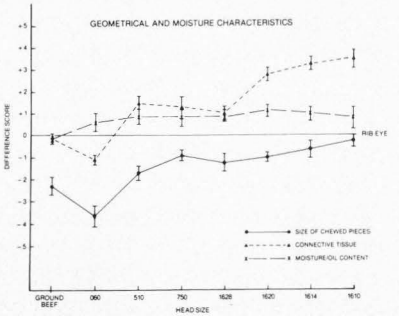

Figure 8. Same as Figure 6, but for the geometrical and moisture attributes.

Table 6 shows Spearman rank-order correlation coefficients for the relationships between head-size and each of the judged sensory attributes. Significant positive correlation coefficients were observed for all sensory attributes except "springiness," which shows a non-significant negative correlation with cutting-head size.

In order to index the degree of similarity of each flaked and formed sample to the ribeye control, the average absolute deviation of the mean ratings for each test sample from the control was calculated across all attributes. These average deviations appear in Table 7. As can be seen, the smallest absolute deviations were found for the 1610, 1614, and 750 cutting-head sizes.

Although the 1610 and 1614 cutting heads produced samples that were very similar to one another on all attributes, these two samples differed greatly from the 750. Examining Figure 6, one can see that the visual appearance of the samples prepared with the 750 cutting head were different from those prepared with the 1614 and 1610 cutting heads, the former having smaller fat deposits on the cooked surface and looking less similar to ribeye steak. Similarly, Figure 7 shows that the samples processed with the 750 head-size were less like the control in cohesiveness. On the other hand, the 750 is more similar to the control than either the 1610 or 1614 on the attributes of chewiness (Figure 7) and amount of connective tissue (Figure 8). Thus, while all three samples are about equally similar to the control, they are similar on different sensory dimensions.

Table 6. Spearman rank-order correlation coefficients for the relationship between cutting-head size and each of the judged textural attributes of the products.

ATTRIBUTE	
Size of fat deposits on cooked surface	0.96**
Coarseness of cut surface	0.86*
Springiness	−0.75
Hardness	0.96**
Cohesiveness	0.89*
Chewiness	0.96**
Size of chewed pieces	0.89*
Moisture/oil content	0.86*
Cohesiveness of the mass	0.96**
Amount of connective tissue	0.86*

** $p<0.01$
* $p<0.05$

Table 7. Average absolute deviation of the mean ratings for the flaked and formed and ground beef samples from the mean ratings for the ribeye sample. deviations are averaged across all sensory attributes.

Sample	Average Absolute Deviation
Ground beef	2.13
060	2.13
510	1.53
750	1.29
1628	1.41
1620	1.56
1614	1.24
1610	1.20

Table 8 shows the Pearson product-moment correlation coefficients among all pairs of judged sensory attributes. As can be seen, the visual attribute of "coarseness," as well as those of "springiness" and "moisture/oil content," were not significantly correlated with any other sensory attribute. On the other hand, the visual attribute of "size of fat deposits" had a significant positive correlation with "hardness," "cohesiveness," "size of chewed pieces," and "cohesiveness of the mass." In addition, "hardness" was significantly correlated with "cohesiveness," "chewiness," and "cohesiveness of the mass," "cohesiveness" was significantly correlated with "amount of connective tissue," and the "size of chewed pieces" was significantly correlated with "cohesiveness of the mass."

Table 9 shows the Pearson product-moment correlation coefficients between the four instrumental texture measures obtained on these products and each of the mechanical, geometric and moisture/fat-related sensory attributes. As can be seen, maximum strain (E) was not significantly correlated with any attribute. The stiffness (S) of the products had a significant ($p<0.01$) negative correlation with perceived "springiness." Maximum shear stress (γ) had significant positive correlations with "cohesiveness," "cohesiveness of the mass," and with the "size of the chewed pieces," while maximum shear force per unit area (F) was only significantly correlated with the "size of the chewed pieces."

Table 10 shows the multiple linear regression equations and multiple correlation coefficients (R) for predicting each of the sensory texture attributes from the instrumental measures obtained on the products. Improvements in the correlation coefficients over the simple linear coefficients can be observed for all attributes except "springiness" and "size of chewed pieces," for which the simple linear correlations with (S) or (F), respectively, are as high.

Discussion

The above data show the significant effects that flake-size can have on the perceived texture of flaked and formed beef products. For optimizing the texture of these products to that of an intact muscle steak, e.g., ribeye, these data suggest that either the 750 cutting-head or the 1610 and 1614 cutting heads are most suitable, albeit for different reasons. If the appearance or cohesiveness of the product is to be matched, then the 1610 or 1614 head sizes are better choices. If the chewiness or the amount of connective tissue is to be matched, then the 750 head-size is more suitable. The decision, while difficult, must necessarily take into account the acceptability of the products processed by these head sizes, since some one or combination of these textural attributes may be more important than others in affecting acceptability (see Experiment 4).

The correlation coefficients in Table 8 show a strong linear association between the sensory attributes of "hardness," "chewiness," "cohesiveness," and "cohesiveness of the mass." These correlations are indicative of an underlying perceptual factor that may be termed "toughness." The visual attribute of "size of fat deposits" is also linearly associated with these attributes, reflecting the fact that fat or connective tissue perceived visually in the products are also perceived by the oral-tactile sense. In contrast to the above, all other judged dimensions are relatively independent.

The simple linear correlation coefficients between sensory and instrumental measures suggest that the Instron maximum shear force (γ) may be used alone to predict either the "cohesiveness," "cohesiveness of the mass" or "size of

Table 8. Pearson product–moment correlation coefficients among all pairs of sensory attributes.

	Size of Fat Deposits	Springi–ness	Hard–ness	Cohesive–ness	Chewi–ness	Size of Chewed Particles	Moisture/ Oil Content	Cohesive–ness of Mass	Amount of Connective Tissue
Coarseness	0.01	-0.47	-0.28	-0.35	-0.12	0.19	-0.25	-0.19	0.32
Size of Fat Deposits		-0.40	0.83**	0.88**	0.69	0.91**	0.20	0.95**	0.60
Springiness			-0.04	-0.25	0.28	-0.50	0.74*	-0.24	0.12
Hardness				0.91**	0.85**	0.77	0.45	0.93**	0.65
Cohesiveness					0.62	0.77	0.23	0.95**	0.39
Chewiness						0.64	0.76	0.73	0.89**
Size of Chewed Particles							0.14	0.80**	0.64
Moisture/Oil Content								0.30	0.69
Cohesiveness of Mass									0.56

* $p < 0.05$
** $p < 0.01$

Table 9. Pearson product–moment correlation coefficients between the instrumental and sensory texture measures.

	Springiness	Hardness	Cohesiveness	Chewiness	Size of Chewed Particles	Moisture/0.1 Content	Cohesiveness of Mass	Amt Connective Tissue
E	0.68	-0.47	-0.74	-0.04	-0.57	0.43	-0.68	0.12
S	-0.82**	0.26	0.53	-0.05	0.53	-0.50	0.52	-0.06
γ	-0.43	0.75	0.83**	0.60	0.89**	0.23	0.87*	0.61
F	-0.42	0.50	0.58	0.48	0.80**	0.17	0.67	0.61

* $p < 0.01$ ** $p < 0.05$

Table 10. Multiple Linear regression equation coefficients and multiple correlation coefficients relating the instrumental texture measures to the sensory texture measures.

	E	S	γ	F	(c)	R
Springiness	1.906	-0.468	0.346	-0.100	3.967	0.85
Hardness	-6.415	-0.259	0.671	-0.137	8.912	0.94
Cohesiveness	-13.544	-0.267	0.752	-0.157	15.848	0.99
Chewiness	2.271	-0.278	0.726	-0.099	-0.118	0.87
Size Chewed Pieces	-3.371	-0.093	0.497		3.840	0.89
Moisture/Oil	3.711	-0.176	0.355	-0.051	0.015	0.93
Cohesiveness of Mass	-11.990	-0.267	0.817	-0.130	12.471	0.96
Amt Connective Tissue	20.361	-0.211	1.012	-0.022	-23.592	0.92

chewed particles" of the samples, and that the instrumental stiffness (S) of the sample may be used to predict its perceived springiness. Similarly, force per unit area (F) measures (from the Food Technology Corporation shear data) may also be used to predict the size of chewed particles. However, by using a multiple regression formula (Table 10), better predictive relationships can be established for most of the sensory attributes.

Experiment 4

Experiment 3 was aimed at identifying the similarities and dissimilarities in the textural properties of the flaked and formed products processed with different cutting heads and their relationship to whole-muscle steak. The present experiment was aimed at identifying which, if any, of the flaked and formed samples was most acceptable to consumers and how the acceptance of these products compared with ground beef or ribeye steak.

Samples

The same test samples as used in Experiment 3 were employed.

Procedure

The samples were cooked on a flat grill, preheated to 177°C and cooked to an internal temperature of 69°C. This method of cooking was chosen since it is the method that is used in most military dining halls.

The consumer panel was comprised of volunteer employees of the Food Acceptance Laboratory taste test panel. None of these panelists had prior experience with the flaked and formed products, although all had participated in previous acceptance tests with other products.

Fifty (50) randomly selected consumer panelists participated in each of the three test sessions. During each session, three of the nine test samples were presented for evaluation. Samples were presented randomly and sequentially to each panelist on preheated ceramic plates. All tests were conducted in individual light-controlled (white fluores-

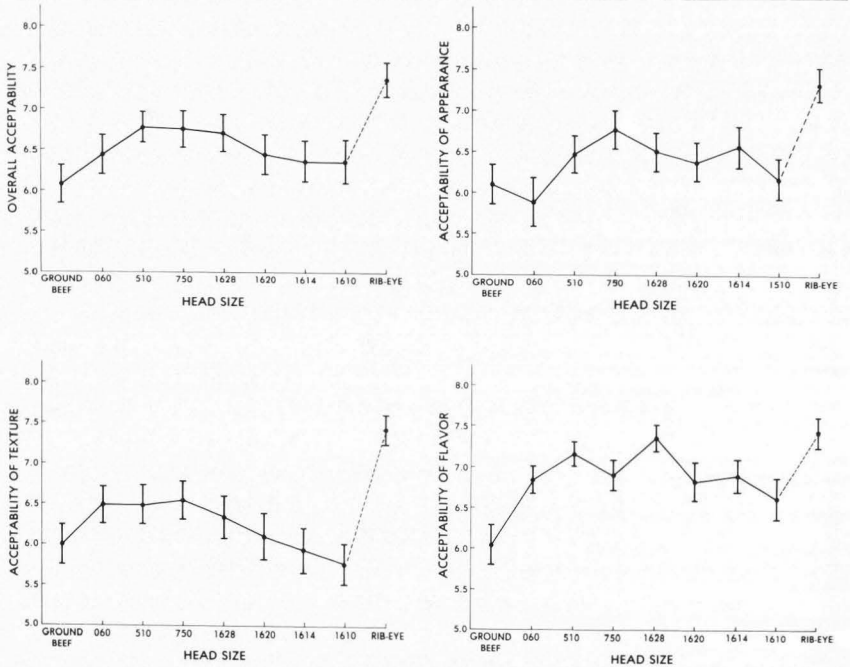

Figure 9. Mean ratings of "overall acceptability" (top, left), "acceptability of appearance" (top, right), "acceptability of texture" (bottom, left) and "acceptability of flavor" (bottom, right) for the flaked and formed beef products, ground beef patty and ribeye steak used in Experiment 4.

cent) sensory testing booths.

Panelists were asked to rate each sample for its "overall acceptability," "acceptability of texture," "acceptability of appearance" and "acceptability of flavor." A 9–point labeled hedonic scale was used. In addition, each panelist was asked to indicate on a printed ballot, whether the texture of the sample was most like that of "hamburger," "salisbury steak," "cubed steak," "swiss steak," or "ribeye or other intact muscle steak." A choice of "other" was also provided. The only information provided to the panelists was that they would be evaluating samples of "100% beef."

Results

The mean ratings obtained for each of the nine test samples on each of the judged attributes are shown in Figure 9. As can be seen, on "overall acceptability," all of the flaked and formed products were rated more acceptable than ground beef, but less acceptable than ribeye steak. Maximum acceptability was observed for the 510, 750 and 1628 head sizes. For "acceptability of texture" all of the flaked and formed samples were less acceptable than the ribeye, but, in addition, several of the largest head sizes were less acceptable than ground beef. The most acceptable texture among these samples was observed for the 060, 510, and 750 head sizes. On "acceptability of appearance" all of the flaked and formed samples were less acceptable than the ribeye steak and the 060 was less acceptable than ground beef. The most acceptable in appearance of the flaked and formed products was the sample prepared with the 750 cutting-head. "Acceptability of Flavor" showed lower mean ratings for the flaked and formed products than for the ribeye, but all flaked and formed samples were more acceptable than ground beef. The latter effect may be partly due to the absence of salt in the ground beef sample. The 1628 head size produced the most acceptable flavor.

Table 11: Results of consumer tests conducted on flaked and formed beef in Experiment 4. Mean ratings in the same column with the same superscript (a,b) are not significantly different ($p<0.005$).

Overall Acceptability

ANOVA:

F= 2.98, df = 8,392 $p<0.01$

Neuman-Keuls Contrasts:

$S_{\bar{Y}}$ = 0.0457 0.05 criterion = 0.1966

Rib-Eye	7.36^{a}
510	6.78^{ab}
750	6.74^{ab}
1628	6.70^{ab}
060	6.44^{b}
1620	6.44^{b}
1614	6.36^{b}
1610	6.36^{b}
Ground beef	6.06^{b}

Acceptability of Appearance

ANOVA:

F= 3.78, df = 8,392 $p<0.01$

Neuman-Keuls Contrasts:

$S_{\bar{Y}}$= 0.0475 0.05 criterion=0.2046

Rib-Eye	7.34^{a}
750	6.78^{ab}
1614	6.56^{b}
1628	6.50^{b}
510	6.46^{b}
1620	6.38^{b}
1610	6.18^{b}
Ground beef	6.10^{b}
060	5.88^{b}

Acceptability of Texture

ANOVA:

F=4.66, df=8,392 $p<0.01$

Neuman-Keuls Contrasts:

$S_{\bar{Y}}$=0.0513 0.05 criterion=0.2207

Rib-Eye	7.42^{a}
750	6.54^{b}
060	6.48^{b}
510	6.48^{b}
1628	6.34^{b}
1620	6.10^{b}
Ground beef	6.00^{b}
1614	5.94^{b}
1610	5.76^{b}

Acceptability of Flavor

ANOVA:

F=4.76, df=8,392 $p<0.01$

Neuman-Keuls Contrasts:

$S_{\bar{Y}}$=0.0367 0.05 criterion=0.1576

Rib-Eye	7.44^{a}
1628	7.36^{a}
510	7.16^{a}
1614	6.90^{a}
750	6.90^{a}
060	6.84^{a}
1620	6.84^{a}
1610	6.62^{a}
Ground beef	6.04^{a}

Table 11 shows the results of analyses of variance and Neuman–Keuls contrast tests conducted on these data. Significant effects were found for all four of the judged attributes. Neuman–Keuls contrasts revealed that the 510, 750, and 1628 head sizes were not significantly different from the ribeye steak on "overall acceptability," although they were also not significantly different from those made with other head sizes or from ground beef. For "acceptability of appearance," only the 750 head-size was not significantly different from the ribeye, although again, it was not significantly different from any other flaked and formed sample or ground beef. Concerning the "acceptability of texture," all flaked and formed products were significantly less acceptable than the ribeye sample, but none differed from any other test sample. Lastly, none of the flaked and formed products were significantly more acceptable than ground beef.

Figure 10 is a plot of the responses to the question asking about the similarity of the texture of the samples to various alternative cuts of meat. As can be seen, ground beef was "correctly" described as having a texture like that of "hamburger," and ribeye steak was "correctly" identified as "ribeye or some other intact muscle cut of meat." However, there was little agreement concerning the texture of the flaked and formed products. These products were randomly categorized as being like hamburger, ribeye steak, salisbury steak, etc.

Discussion

It is clear from the data that most of these flaked and formed beef products differed significantly from both ribeye steak and from ground beef patties. Based on the mean ratings of "overall acceptability," it would appear that intermediate flakes sizes (510, 750, 1628) produce the most acceptable products, although statistically significant differences between these samples and samples processed with other head sizes are not apparent. Notably, the acceptability of these products does not differ from intact muscle ribeye steak.

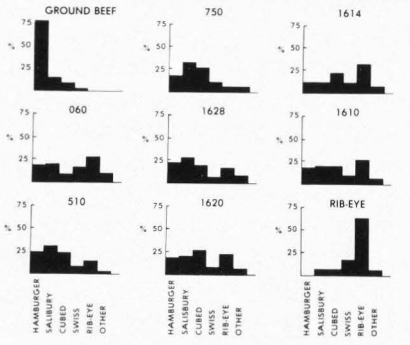

Figure 10. Percentage of consumers characterizing the texture of each of the test samples in Experiment 4 as "hamburger," "salisbury steak," "cubed steak," "swiss steak," "ribeye steak or other intact muscle steak" or "other."

The results shown in Figure 10 suggest that consumers do not perceive flaked and formed beef steaks as either intact-muscle cuts of meats or as hamburgers. Neither do they uniformly describe them as salisbury, cubed or swiss steak. Rather, it appears that consumers perceive these products as entirely new beef products. These data suggest that flaked and formed steaks should be marketed as an entirely new meat product, rather than as a substitute for existing products.

Summary and Conclusions

The studies reported here provide information on the effects of NaCl, TPP, soy isolate and flake-size on the sensory-instrumental texture properties, microstructure and/or consumer acceptability of flaked and formed beef products.

Results of this research show that flake-size has a more important effect on the perceived texture of flaked and formed products than does the addition of NaCl, TPP, or soy isolate. In particular, flake-size was shown to be significantly correlated with the hardness, cohesiveness, chewiness, moisture/oil content, cohesiveness of the mass, amount of connective tissue and size of chewed pieces, as well as with such visual attributes as the "size of fat deposits on the cooked surface" and the "coarseness of the cut surface." Taking all attributes together, the 750 head-size and the 1610 and 1614 head sizes produced products most similar to ribeye steak. The effects of the addition of various combinations of 0% and 0.5% NaCl, 0% and 0.5% TPP and 0% and 1% soy isolate were tested, and it was found that none of the samples were significantly different from one another.

Consumer tests of the products revealed that the 750 head size was a better choice than the 1610 or 1614 to produce a maximally acceptable product that does not differ significantly in acceptance from whole muscle meat. Sensory-instrumental correlations suggest that good prediction of the sensory texture of these products can be achieved using a multiple regression approach, and these data, combined with SEM data, showed that tenderization of these meats is primarily attributable to mechanical disruption of the tissue and not to an enzymatic process.

References

Anonymous (1977). New products from flake-cut meat. **Food Processing Industry**, 46(543): 23.

Anonymous (1979). Isolate improves tenderness and lowers cost of "chunked/formed" meat rolls. **Food Processing**, 40(11): 32–33.

Chesney, M.S., Mandigo, R.W., Campbell, J.F. (1978). Properties of restructured pork product as influenced by meat particle size, temperature and comminution method. **Journal of Food Science**, 43: 1535–1537.

Cohen, S.H., Segars, R.A., Cardello, A.V., Smith, J., Robbins, F.M. (1982). Instrumental and sensory analysis of the action of catheptic enzymes on flaked and formed beef. **Food Microstructure**, 1: 99–105.

Flesch, P., Bauer, G. (1965). Novel additives for sausages. French Patent 1,446,678.

Hand, L.W., Crenwelge, C.H., Terrell, R.N. (1981). Effects of wheat gluten, soy isolate and flavorings on properties of restructured beef steaks. **Journal of Food Science**, 46: 1004–1006.

Hellendoorn, E.W. (1962). Water-binding capacity of meat as affected by phosphates. I. Influence of sodium chloride and phosphate on the water retention of comminuted meat at various pH values. **Food Technology**, 16(9): 119–124.

Huffman, D.L., Cordray, J.C. (1979). Restructured fresh meat cuts from chilled and hot processed pork. **Journal of Food Science**, 44: 1564–1567.

Huffman, D.L., Cross, H.R., Campbell, K.J., Cordray, J.C. (1981). Effect of salt and tripolyphosphate on acceptability of flaked and formed hamburger patties. **Journal of Food Science**, 46: 34–36.

Marks, L.E. (1974). **Sensory Processes: The New Psychophysics.** New York: Academic Press.

Morris, C.E. (1980). Soy protein system binds fat. **Food Engineering**, 52(9): 28–29.

Neer, K.L., Mandigo, R.W. (1977). Effects of salt, sodium tripolyphosphate and frozen storage time on properties of flaked, cured pork product. **Journal of Food Science**, 42: 738–742.

Ohashi, T., Sugano, S. (1973). Combined effect of sodium chloride and polyphosphates on the water-holding capacity of various meats. **J. Japanese Society of Food and Nutrition**, 28(8): 497–499.

Popenhagen, G.R., Mandigo, R.W. (1978). Properties of restructured pork as affected by flake size, flake temperature and blend combinations. **Journal of Food Science**, 43: 1641–1645.

Popenhagen, G.R., Mandigo, R.W., Hansen, K.R., Chesney, M.S., Mahoney, L.C. (1973). Effect of temperature, flake size, and blending on flaked, formed and sectioned pork products. **Journal of Animal Science**, 37: 269–270.

*Robbins, F.M., Walker, J.E., Cohen, S.H., Chatterjee, S. (1979). Action of proteolytic enzymes on bovine myofibrils. **Journal of Food Science**, 44: 1672–1677, 1680.

Schnell, H.G., Vadehra, D.V., Baker, R.C. (1970). Mechanism of binding chunks of meat. 1. Effect of physical and chemical treatments. **Canadian Institute of Food Technology Journal**, 3(2): 44–48.

Schwartz, W.C., Mandigo, R.W. (1976). Effect of salt, sodium tripolyphosphate and storage on restructured pork. **Journal of Food Science**, 41: 1266–1269.

Schweiger, R.G. (1974). Soy protein concentrate and isolates in comminuted meat systems. **J. Am. Oil Chem. Soc.**, 51: 192–194.

Segars, R.A., Hamel, R.G., Kapsalis, J.G., Kluter, R.A. (1975). A punch and die test cell for determining the textural qualities of meat. **J. Texture Studies**, 6: 211–225.

Shults, G.W., Howker, J.J., Wierbicki, E. (1976). Effect of salt and sodium tripolyphosphate on texture, organic volatiles and sensory characteristics of irradiated and non-irradiated pork. **Journal of Food Science**, 41: 1096–1101.

Shults, G.W., Wierbicki, E. (1973). Effects of sodium chloride and condensed phosphates on the water-holding capacity, pH and swelling of chicken muscle. **Journal of Food Science**, 38: 991–994.

Stevens, S.S. (1957). On the psychophysical law. **Psychological Review**, 64: 153–181.

Theno, D.M., Siegel, D.G., Schmidt, G.R. (1978). Meat massaging: Effects of salt and phosphate on the microstructure of binding junctions in sectioned and formed hams. **Journal of Food Science**, 43: 493–498.

*See Discussion with Reviewers

U.S.D.A. (1975). Meat and Poultry Regulations. Animal and Plant Health Inspection Service. U.S. Dept. of Agriculture, Washington, D.C., Sec 318, 7(4).

Discussion with Reviewers

Reviewer #1: To draw the conclusion that enzymatic tenderization did not occur by using SEM photographs would have greater acceptance by this reviewer if a comparison to a known sample which had been enzymatically tenderized were shown. In other words, do we know if the changes due to enzymatic activity can be picked up on the SEM?

Authors: Although there have been several papers written on this subject, the one by Robbins et al. (1979) shows chemical, light microscopic and SEM evidence for the action of catheptic enzymes on muscle.

Reviewer #1: The authors' statement concerning the modification of processing variables, e.g., mixing time, to take advantage of tenderization by enzymes is only true from a point of view involving enzymatic activity. However, recommending longer mixing times without the consideration for mixing time effects of texture modification may mislead some readers. Mixing time effect on texture is a dramatic influence.

Authors: What our statement implied was that the modification of processing methods, including mixing time, would take advantage of enzymatic tenderization, thereby improving the textural qualities. Reviewer 1's comment concerning concomitant effects of these modifications is well taken.

FOOD MICROSTRUCTURE, Vol. 2 (1983), pp. 135-141
SEM Inc., AMF O'Hare (Chicago), IL 60666 U.S.A.

MORPHOMETRY OF MEAT BY SCANNING LIGHT MICROSCOPY

H.J. Swatland

Department of Animal and Poultry Science,
University of Guelph, Guelph, Ontario N1G 2W1, Canada

Abstract

Morphometric data can be collected from meat by using a scanning stage and a photometer, both controlled by a microcomputer. The passive counting of connective tissue boundaries is given as an example to show that enumerative data may be biassed by the ratio of the width of the subject of measurement to the projected diameter of the photometer aperture. In a second example, the scanning stage is actively directed by the observer and is used to map the radial distribution of succinate dehydrogenase (SDH) activity in different histochemical types of muscle fibers. This is accomplished by the arbitrary fitting by the microcomputer of reference features (plumb line and corners) to the muscle fiber perimeter. Concentric zones of the resulting data matrix are unpacked to calculate radial gradients of SDH activity within muscle fibers.

Initial paper received December 23, 1982.
Final manuscript received August 9, 1983.
Direct inquiries to H.J. Swatland.
Telephone number: 519-824-4120.

KEY WORDS: Meat, Morphometry, Stereology, Scanning light microscopy, Boundary detection, Succinate dehydrogenase, Histochemistry, Microcomputer, Microphotometry.

Introduction

There are several methods by which a scanning motion can be introduced into the formation of images by light microscopy. One of the simplest methods is to move the specimen with a scanning stage, and then to analyze the light that passes through a small measuring aperture in the optical axis of the microscope. This report describes how this simple configuration for scanning light microscopy can be used to collect morphometric data from meat. In the first example, the endomysial boundaries around individual muscle fibers are detected and counted. These data can be used stereologically to count the numbers of muscle fibers in a given cross sectional area and to detect anisotropy in the connective tissue framework of meat. In the second example, the activity of aerobic enzymes within the muscle fiber is mapped. This method can be used to quantify the degree of enzyme activity within a fiber, as in the categorization of histochemical fiber types, or may be used to study the radial distribution of enzyme activity within the fiber.

Apparatus

The following components were attached to a Zeiss type WL microscope with a specially strengthened base (Carl Zeiss, 7082 Oberkochen, West Germany): (1) a type SF photomultiplier, (2) a 0.5 μm step scanning stage, (3) a solenoid-operated shutter below the photomultiplier, (4) a solenoid-operated aperture to define the field stop, and (5) a motor-driven continuous interference filter monochromator. These components were operated from a Zeiss Zonax microcomputer programmed in Basic.

Muscle tissue for the examples illustrated in this report was obtained immediately post mortem from the longissimus dorsi of a Yorkshire gilt, live weight 86 kg. Samples were frozen in liquid nitrogen and serial sections were cut at a thickness of 10 μm at -20°C.

Sections were reacted for myofibrillar ATPase (Guth and Samaha, 1970) and for SDH (Zugibe, 1970).

Detection of Boundaries

With a rapid silver stain for frozen sections of meat (Swatland, 1979), epimysium and perimysium are stained brown or yellow, and reticular fibers in the endomysium and around adipose cells and blood vessels are stained black. When the stage is moved, stained connective tissue boundaries that interrupt the light path to the photometer cause a decrease in transmittance.

The speed of the scanning stage is important with respect to the time needed for analog to digital conversion, the time needed for replicate measurements to compensate for photometric error, and the characteristics of the photometer system. The decrease in transmittance associated with the passage of a boundary across the aperture is shown diagrammatically in Figure 1.

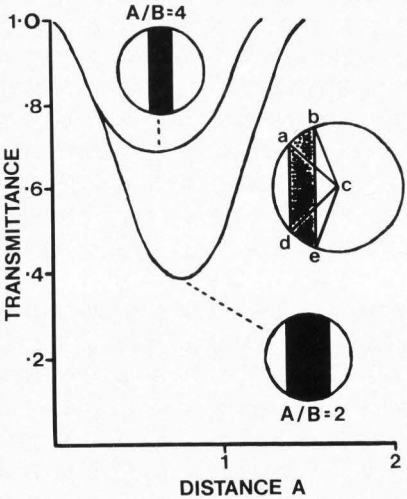

Figure 1. Transmittance changes caused by the passage of a boundary across the photometer aperture. The light that is stopped is proportional to the area of the boundary in the aperture (segment bce - segment acd) and to its absorbance.

The diameter of the aperture (A) relative to the width of the boundary (B) is described by the A:B ratio, for which two examples (A/B = 4 and A/B = 2) are illustrated. The x-axis indicates the distance travelled by the leading edge of the boundary across the aperture in units equal to the aperture diameter (A).

The amount of light that is stopped by the boundary depends on the width and position of the boundary relative to the aperture, and on the transmittance of the boundary. The diameter of the aperture (A) is divided by the width of the boundary (B) to obtain a ratio that describes the photometric result of passing the boundary across the aperture. In practice, the transmittance threshold for the detection of a boundary passing across the aperture is suprisingly complicated (Figure 2).

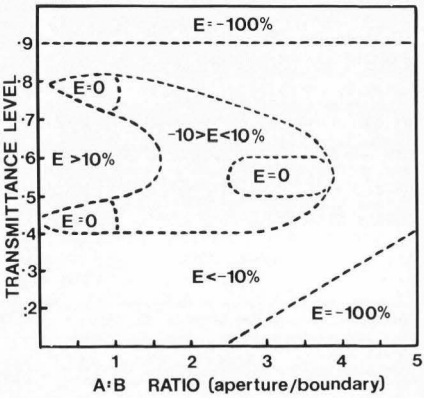

Figure 2. A typical contingency table for the magnitude of error (E) in the automated counting of boundaries. On the y-axis, the transmittance level is the threshold at which a boundary is detected as it passes across the aperture. The contour lines group together combinations of transmittance level and A:B ratio that produce a similar degree of error.

The upper zone where no boundaries are counted (error, E = -100%) is due to the background absorbance between the boundaries: the transmittance seldom rises above 0.9. The lower zone where no boundaries are counted (E = -100%) is due to thin boundaries: the transmittance

never drops low enough to reach the transmittance threshold. The left-side zone where many non-existent boundaries are counted (E > 10%) is due to uneven absorbance across the boundary: in a thick boundary, when the drop in transmittance forms a broad arc through the upper level of the threshold of transmittance, irregularities lead to multiple counting on a single boundary. A widespread zone of negatively biassed counting (E < -10%) is due to a combination of background absorbance, transmittance through the boundary, and thin boundaries relative to the aperture: the signal either dwells within, or seldom enters the transmittance threshold. Forming an island within the zones described above is an area in which moderate errors are more or less random (-10 > E < 10%): at three relatively small points in this area, boundaries are counted with no error (E = 0). The contours that outline the arbitrary error zones change with the scanning speed and with the degree of tissue staining. The boundaries often pass across the aperture obliquely or in pairs, and this produces an anomalous drop in transmittance. The most serious problem of all, however, is that there is a considerable biological range in the thickness of endomysial boundaries.

Muscle fiber size and number, and the number and orientation of connective tissue boundaries along a pathway can be estimated stereologically. For example (Swatland, 1979), when the scanning stage is moved so that the optical axis describes a square (with total length of sides = L) on the tissue section, the number of muscle fibers within the square area (mfrN/A) may be obtained from the number of endomysial boundaries that are transected along its sides (enN/L),

$$mfrN/A = (enN/L \ / \ 4)^2$$

However, since the photometer responds indiscriminately to all black boundaries of a similar type (bN/A), a correction factor is needed for non-endomysial boundaries. In pork chops from typical slaughter weight pigs the estimate of the number of muscle fibers per unit area is

$$mfrN/A = ((bN/L \ / \ 4)^2 \times 0.57) + 27.1$$

Mapping of Enzyme Activity

To define the perimeter of a cross-sectioned muscle fiber, the operator moves the meat section through the optical axis of the microscope using the scanning stage under direct control from the microcomputer keyboard. Cross-hairs in the microscope eyepiece are used to identify the X:Y coordinates of the perimeter as shown in Figure 3.

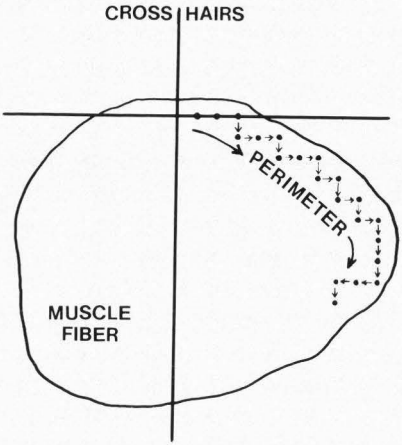

Figure 3. The definition of the perimeter of a muscle fiber. The stage is moved in y-axis or x-axis steps so that cross-hairs in the optical axis of the microscope trace a subsarcolemmal path.

Since measurements are to be taken along the perimeter, the perimeter pathway is subsarcolemmal in position, with clearance for the image of the measuring aperture to fall within the muscle fiber. For this purpose, the diameter of the photometer measuring aperture is marked on the cross-hairs. The perimeter is defined in a clockwise manner, starting at the highest point on the muscle fiber, as shown in Figure 3. The movements of the stage are recorded by the microcomputer as vectors that correspond to the numbers of steps to the left and to the right of a plumb line from the highest point on the muscle fiber (Figure 4).

Left or right movements of the section either increment or decrement (respectively) the position number (PN). On the descending clockwise segment of the perimeter, each upward movement of the stage causes the position number (PN) to be loaded as the line plus number of steps (LP) for the line that has just been completed (LN-1 when the line number incremented as the first step in the recording algorithm). The east corner (EC) of the perimeter is taken as the first movement

of the stage to the right (usually at about 3 o'clock on the perimeter). At the east corner, the position number (PN) is loaded as the line plus number of steps (LP) for that line. From then onwards and until the perimeter begins its clock-wise ascent, the position number (PN) is loaded for each new scanning line (LN when LN is incremented first in the algorithm).

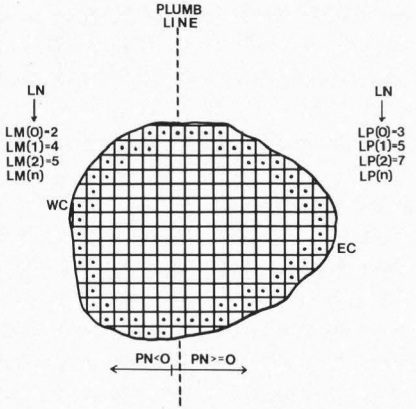

Figure 4. Salient features of the scanning matrix. LN = line number, LM = line minus number of steps, LP = line plus number of steps, PN = position number along x-axis, WC = west corner of perimeter, and EC = east corner of perimeter.

On the ascending clockwise segment of the perimeter, each downward movement of the stage causes the position number (PN) to be loaded as the line minus number of steps (LM) for the scanning line (LN+1 when LN is decremented first in the algorithm). The west corner (WC) of the perimeter is used to make the change from retrospective to advance loading of LM. The logical operations described above are summarized in Table 1.

Subroutines are used to cope with ellipsoidal perimeters in which the highest and lowest points are skewed with respect to the plumb line. As shown in Table 1, LM and LP then serve a second function. The lowest parts of these registers are unused if a perimeter is skewed (LM if the center of gravity is to the right of the plumb line and LP if the center of gravity is to the left of the plumb line). In these instances, the lower parts of these registers are loaded with a recognizable label (+1000 or -1000) combined with the number of steps outside of the muscle fiber that occur between the plumb line and the perimeter.

Table 1. Summary of logical operations for recording the perimeter of a fiber

Move stage	Position relative to plumb line	Position relative to corners	Operations
Left	PN>=<0	><EC, ><WC	PN=PN+1
Right	PN>=<0	><EC, ><WC	PN=PN-1
Up	PN>=0	<EC, <WC	LN=LN+1 LP(LN-1)=PN
Right	PN>=0	=EC, <WC	LP(LN)=PN PN=PN-1
Up	PN>=0	>EC, <WC	LN=LN+1 LP(LN)=PN
Down	PN<0	>EC, <WC	LN=LN-1 LP(LN+1)=PN
Left	PN<0	>EC, =WC	LM(LN)=PN PN=PN-1
Down	PN<0	>EC, >WC	LN=LN-1 LM(LN)=PN
Down	PN>0	>EC, <WC	LN=LN-1 LM(LN+1)=-1000-PN
Up	PN<0	>EC, <WC	LN=LN+1 LP(LN)=1000-PN

When the perimeter has been closed by the operator and checked for contiguity by the microcomputer, the microcomputer takes control to scan the field bounded by the subjectively defined perimeter. On each scan line, the stage steps to the right for the value of LM and then steps to the left for the value of LM + LP. Absorbance measurements for each step of LM + LP are collected in a matrix as shown in Figure 5. Measurements are made at the peak of the absorbance spectrum of the diformazan reaction product (590 nm). On completion of each scan line, the stage returns to the plumb line and steps upward to the level of the next scan line ready for the collection of more data. The specially labelled values of LM (<-1000) and LP (>1000) are used to adjust the scanning pattern for fibers that are skewed with respect to the plumb line.

Absorbance data are collected in a matrix with a straight left edge (Figure 5). This shape facilitates the later unpacking of the data in concentric zones with respect to the original perimeter. The outermost concentric zone is unpacked as follows: (1) all elements of the top row, (2) all elements of the bottom row,

and (3) the first and last elements of each row in-between the top and bottom rows. After each zone is unpacked, the data of the zone are replaced by zeros. The zeros then define the next outermost concentric zone to be unpacked, and so on. Branching instructions within the algorithm for unpacking can cope with a ragged right margin (should it occur on the data matrix) and with matrices containing either an odd or an even number of rows.

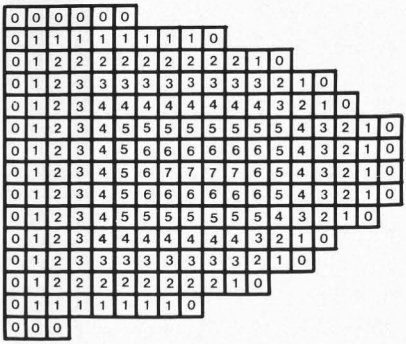

Figure 5. Shape of the data matrix derived from the scanning matrix. The digits at each point in the matrix indicate the allocation of that point to a concentric zone when the matrix is unpacked.

The main feature of this simple algorithm for the definition of concentric zones is that each zone is corrected for asymmetry. Although a few outer elements may be moved from one true concentric zone to another, the innermost zones are defined as a solid axial core rather than an attenuated shape that contradicts integrated diffusion gradients. The deviation of the concentric zones defined in this way from true concentric zones is monitored by calculating the degree of eccentricity. A least-squares linear regression is used to detect concentric gradients within the muscle fiber. A positive slope indicates that absorbance increases from the periphery to the axis, and vice versa. Since the outer zones contain many more observations than the inner zones, the slope of the regression is calculated from the means of the zones rather than from the original data. The null hypothesis that there is no slope is evaluated with a 't' test. The gradient per zone is multiplied by the number of zones in each fiber so as to obtain a radial gradient for each fiber which is independent of fiber size. Some preliminary results are shown in Table 2.

Table 2. Concentric distribution of SDH in three histochemical fiber types of the porcine longissimus dorsi muscle ($n = 10$)

Parameter	Histochemical fiber type		
	mfr:r	mfr:i	mfr:w
ATPase	weak	strong	strong
SDH	strong	medium	weak
Outer zone SDH	1.18	0.74	0.28
SD	0.17	0.32	0.05
Zonal gradient	-0.05	-0.04	-0.01
SD	0.01	0.02	0.01
Radial gradient	-0.67	-0.41	-0.13
SD	0.11	0.21	0.09
Eccentricity	1.06	1.15	1.1
SD	0.09	0.1	0.08

Unexpectedly, all three histochemical fiber types have a radial gradient in their SDH activity (a gradient in white fibers had not previously been recognized). The slope of the gradient might perhaps be proportional to the overall degree of SDH activity. Future progress with this technique may justify a more sophisticated three-dimensional analysis of the stored data.

Discussion

Information on the microstructure of meat is usually reported scientifically by means of a few sample micrographs. Not suprisingly, these usually support the conclusions and hypotheses that are advanced by the authors of the report. The reader of the report, therefore, has no way to evaluate the degree of variability of the microstructure and is, thus, denied access to data that might be open to some alternative explanation. The presentation of quantitative morphometric data can sometimes improve this situation, particularly if the data are abundant and collected objectively. The two examples presented in this report show the types of operations that are possible with a relatively inexpensive microcomputer system. Both examples can be easily modified to serve a number of other objectives. In the first example, the automatic counting of muscle fibers, the data could be used to estimate apparent fiber numbers in whole muscles. The apparent fiber number is the numerical

product of the cross sectional area of the whole muscle multiplied by the packing density of muscle fibers per unit area. Care must be taken to ensure that both the whole muscle section and the microscope sections are obtained in the same, or in nearby parallel planes. Similarly, care is needed to avoid, or to correct for any tissue shrinkage due to histological techniques. Apparent fiber numbers are extremely useful in comparing the potential meat yield of different breeds of animals. The same method, however, could easily be applied on a smaller scale to muscle samples for rheological testing. In this case, from the number of fibers present in the stump of the tested sample, it would be possible to correct for differences in fiber numbers between samples. Rheological data could even be expressed on a per fiber basis. The microstructural deformation caused by the rheological testing of meat samples has been described (Swatland, 1978) and could easily be expressed in quantitative terms by measuring the endomysial boundary frequency in different axes of the sample.

In the second example, measurement of the radial distribution of aerobic enzymes, the basic method of scanning within an area defined by the operator avoids one of the most serious difficulties encountered with more sophisticated image analysis systems - the difficulty of defining individual muscle fibers. The resolution of individual muscle fibers when they are closely packed and when they exhibit similar histochemical reactions is extremely difficult if not impossible to achieve by most image analysis systems. The human operator, however, has access to a large amount of subtle information obtained by slight variations in focus and, as a last resort, can refer to a serial section stained with silver to demonstrate endomysial boundaries. Scientifically, the technique of scanning within a defined area has a lot to offer in future research since it may be used for a variety of histochemical techniques.

References

Guth L, Samaha FJ, (1970) Procedure for the histochemical demonstration of actomyosin ATPase. Exp. Neurol. 28, 365-367.

Swatland HJ, (1978) Microstructure of cuts through the connective tissue framework of meat. Can. Inst. Food Sci. Technol. J. 11, 204-208.

Swatland HJ, (1979) Endomysial boundary scanning as a method of counting skeletal muscle fibres. Mikroskopie 35, 280-288.

Zugibe FT, (1970) Diagnostic Histochemistry, Mosby, Saint Louis, MO, p. 282.

Discussion with Reviewers

O.A. Young: What does the author think is the significance of a SDH activity gradient from the core to the periphery of muscle fibers?

Author: Oxygen is delivered to the muscle fiber surface by capillaries. Therefore, the axis of the fiber is farther from the supply of oxygen than is the subsarcolemmal zone. The intracellular availability of oxygen is mirrored in the distribution of mitochondria. This causes the descending centripetal gradient of SDH activity. There are two main features of this system that have some scientific significance. The first point is of theoretical interest. The classical model for the distribution of oxygen within muscles was proposed by Krogh in 1919 (Krogh, A. 1919. The number and distribution of capillaries in muscles with calculations of the oxygen pressure head necessary for supplying the tissue. J. Physiol. 52: 409-415). This model assumes that the supply of oxygen is predominantly a centrifugal system centered on the capillaries that wind between the muscle fibers. The SDH gradients reported here, however, show that there is little evidence of a centrifugal capillary-based diffusion system actually within the muscle. What appears to happen is that the effects due to the release of oxygen from discrete sites (the capillaries) on the muscle fiber surface are averaged over the whole surface of the muscle fiber. A likely explanation for this is that the muscle is constantly contracting. Thus, the position of capillaries on the muscle fiber surface is not constant with respect to the intracellular components of the muscle fiber. A centripetal fiber-based system might, therefore, be a more realistic model for the intracellular distribution of oxygen within skeletal muscles. The second feature of interest concerning SDH gradients has a more practical importance. Meat animals are constantly being bred for increased meat yield. This often results in animals with very large diameter muscle fibers. If a fiber becomes very large, is its axis likely to become anaerobic? The anaerobic axis, if it can survive in this manner, is likely to become specialized for anaerobic glycolysis. Thus, it may be no coincidence that solid cores of glycogen may sometimes be found in the axis of muscle fibers from heavy pigs (Swatland, H.J. 1975. Relationships between mitochondrial content and glycogen distribution in porcine muscle fibres. Histochem. J. 7: 459-469). The practical importance of this condition is that it is likely to lead to a rapid rate of glycolysis postmortem. As is well known, excessive lactate production in a hot carcass leads to the development of pale,

soft, exudative (PSE) pork. The measurement of SDH gradients, therefore, may be of some value in the investigation of muscle development in meat animals.

C.A. Voyle: The interpretation of Table I was not clear to me. Is this a summary of the operating programme in BASIC?
Author: Essentially, yes. The logical operators ("<", ">", and "=") used in Table I determine what operation will be carried out (extreme right column of Table I) for each direction of stage movement (extreme left column of Table I) when at different points around the perimeter. The point around the perimeter is described by reference to the plumb line and corners (center two columns of Table I). The alphabetical abbreviations in Table I correspond to those given in parentheses in the main text. For example, the position number is abbreviated to PN, and so on.

C.A. Voyle: In what terms would you make comparison of enzyme activity between normal and abnormal tissue? Can the system be calibrated against known standards?
Author: SDH activity in frozen tissue sections can be measured in biochemical terms provided that section thickness and histochemical conditions can be rigorously controlled. Section thickness causes the greatest problem. Since the tissue is frozen before the development of rigor mortis when it still contains abundant adenosine triphosphate, it is rather difficult to prevent contraction by filament sliding when the section is thawed. The damage caused to the sarcoplasmic reticulum by freezing and sectioning leads to the release of calcium ions. These then initiate extreme contraction on thawing. Since the histological sections are taken in a transverse plane, thaw-contraction causes an irregular change in the thickness of the section. Each muscle fiber is likely to change its thickness independently within the depth of the section. The cover slip that is added when a permanent preparation is made, merely sits like a lid over the whole irregular section. The end result is that the length of the light path is irregular, and the estimation of diformazan concentration from optical absorbance is not precise. There are many other technical problems that further confound the problem. The formation of the diformazan rection product in the reaction for SDH may not be linear with respect to time. The concentration of the reaction product into small granules allows an uninterrupted light path between the granules so that there is a distributional error. To cut a long story short, if a non-calibrated gradient can be satisfactorily used to compare different muscle fibers it is difficult to justify the considerable effort necessary to produce a biochemically calibrated gradient. If radial gradient measurements do, in fact, develop as a useful tool for the study of muscle fiber histochemistry, it might then be worthwhile to undertake the extra work necessary to express a gradient in biochemical terms.

Reviewer III: Please explain why the transmittance never drops low enough to reach the transmittance threshold.
Author: Very often it does. When it does not, this is because the boundary is too narrow or is too translucent relative to the arbitrary transmittance threshold.

R. Segars: Results obtained by the new described method should be compared with data obtained by previous methods to verify that the algorithms are appropriate and to establish their accuracy and reliability. For example, was the gradient observed for the white fibers verified by other means, or might it be an artifact of the method?
Author: I am not aware of any previous attempts to quantify the radial distribution of enzyme activity in skeletal muscle fibers. It is difficult, therefore, to compare the results reported here with those of any other studies. With regard to the possibility of the gradients being an artifact caused by the scanning method I do not think that this is the case. The method described here attempts to give a quantitative measurement of a phenomenon that is visible under the microscope. There is, therefore, no doubt that radial gradients exist. What cannot be so easily dismissed, however, is the possibility that radial gradient measurements are subject to some systematic source of error that reduces their usefulness. Only time and further research can settle this question.

FOOD MICROSTRUCTURE, Vol. 2 (1983), pp. 143-151
SEM Inc., AMF O'Hare (Chicago), IL 60666 U.S.A.

INFECTION OF ORIENTAL MUSTARD BY NEMATOSPORA: A FLUORESCENCE AND SCANNING ELECTRON MICROSCOPE STUDY

Richard A. Holley, Beverley E. Phipps-Todd and Suk H. Yiu

Food Research Institute
Research Branch
Agriculture Canada
Ottawa
Ontario, Canada K1A 0C6

Abstract

Fluorescence light microscopy and scanning electron microscopy were used to study penetration by the yeast Nematospora coryli through the seed coat and into the embryonic tissues of oriental mustard seed (Brassica juncea).

Infection of the seed was associated with its physical injury; however, it was evident that the yeast was capable of successfully invading healthy plant cells. The pathological process was followed in parallel using both the above types of microscopy. Foci of yeast infection on the seed coat outer surface were characterized by swelling of the infected epidermal cells. Nematospora hyphae were seen in the lumina of the seed coat palisade cells and spread laterally when the hyaline layer between the seed coat and embryo was reached. Sites of infection at the surface of cotyledon cells appeared as zones of localized erosion. Asci and spores were visible, embedded in disorganized and disintegrating plant tissue.

Initial paper received August 23, 1983.
Final manuscript received November 11, 1983.
Direct inquiries to R.A. Holley.
Telephone number: 613-995-5265.

KEY WORDS: Ascospore morphology; Fluorescence microscopy; Mustard; Nematospora; Plant pathogen; Scanning electron microscopy; Seed morphology; Spice; Yeast infection.

Introduction

It is not uncommon to find that spices are naturally contaminated with bacteria and fungi (Chandra et al. 1981, Ayres et al. 1980), to such an extent that in many countries their sterilization by treatment with ethylene oxide is routinely carried out. This is done mainly to reduce the risk of pathogenesis as well as early food spoilage by the introduction of large numbers of microorganisms during seasoning. Under normal circumstances most of the organisms present in spice seeds (e.g., anise, caraway, celery, coriander, cumin, nutmeg, dill, fennel, mustard, poppy, pepper, sesame) are on the surface of the seeds (Cowlen and Marshall 1982, Leistner et al. 1981, Pivnick 1980). Indeed, Leistner found that below the palisade layer of the peppercorn testa, the seed was essentially sterile. It should be noted that Chandra et al. (1981) found about 25% of seeds to be still infected following surface disinfection, although this may reflect storage at higher than normal humidity (Schans et al. 1982).

In spices several compounds, but, in particular, essential oils (e.g., isothiocyanates), are potent antimicrobial agents (Virtanen 1962, Pivnick 1980). It is believed that this is also true in oriental mustard with respect to Nematospora coryli (Holley and Timbers 1983). However, despite the natural toxicity of the seed to the infecting Nematospora it became of some interest to examine the development of yeast penetration into the seed, especially since the latter occurred spontaneously in the field.

Nematospora coryli is an internationally important plant pathogen capable of causing devastating damage to many crops in different parts of the world. Phytopathogenic Nematosporaceae are more frequently found in warmer parts of the world (Batra 1973) but recently were reported to occur in oriental mustard grown in a restricted area of western Canada (Burgess et al. 1983). Although at present the outbreak has abated, it has become important to examine the development of yeast penetration into the seed, especially in view of the expanding role mustard crops will probably play in Canadian agriculture. Concern is expressed that crop quantities larger than 80,000 hectares planted to mustard in Canada in 1982 may be at risk. In addition, should mustard serve as a

reservoir for infection of other susceptible crops, the potential for damage would be significant.

Materials and Methods

Electron microscopy

Oriental mustard seed (Brassica juncea) for these studies was obtained from a pocket of infestation in a field in southwestern Saskatchewan. In order to ensure that individual seeds for microscopic examination were infected with Nematospora, they were dissected approximately in half with a scalpel. One half was stored for later microscopic examination, the other was crushed in a sterile mortar with a pestle. The crushed seed was mixed with molten 50°C plate count agar (Difco) containing 50 ppm each of tetracycline and chloramphenicol to retard bacterial development. These additions of antibiotics, lower than the 100 ppm recommended (Speck 1976), were used because Nematospora growth was retarded by higher concentrations. The seed-agar mixture was allowed to solidify in a petri dish and incubated at 35°C under oxygen-free nitrogen for 4 to 5 days to further reduce competition from bacteria and filamentous fungi. The presence of typical subsurface cream-coloured and star-shaped colonies in the agar was taken to be indicative of Nematospora and this was confirmed by phase contrast light microscopy. Approximately 20% of seeds examined from this source were contaminated. Visual inspection and separation of mechanically damaged seeds was not an efficient or productive method for isolation of infected seeds. For comparative purposes, our original isolate of Nematospora coryli (Holley and Timbers 1983) which had been lyophilized, was used as a reference in pure culture work.

When it was determined from incubation of the halves of suspect seeds in agar that seeds were infected with Nematospora, the other half of the seed was bisected. Seed samples were fixed for 24 h at 4°C in 2.8% glutaraldehyde. Fixed seed was rinsed three times in distilled water, frozen in melting freon, transferred to liquid nitrogen, freeze-fractured, and then freeze-dried at -80°C (Speedivac-Pearce Tissue Dryer Model 1). Fractured seeds were mounted on aluminum stubs with silver cement, and coated with carbon and gold (20 nm) in a coating unit (Speedivac Model 12E6/1258, Edwards High Vacuum Limited, Crawley, Sussex, England). Specimens were examined in a Cambridge Stereoscan Mark 2A scanning electron microscope (SEM) at 20 kV.

Pure cultures of Nematospora grown on plate count agar (Difco) at 35°C for 3 to 7 days were removed from the agar surface and fixed in 2.8% glutaraldehyde for 4 h at 4°C in a test tube. The fixed culture, now a suspension, was transferred to freshly cleaved mica sheets (5 x 13 mm) which had been pretreated with 0.1% aqueous poly-L-lysine hydrobromide for 20 min and rinsed with water. Samples were applied before the mica dried. After 15 min exposure on the mica support, samples were rinsed in distilled water three times, frozen in melting freon, transferred to liquid nitrogen, and freeze-dried. Samples were mounted on SEM stubs and treated as described previously for SEM examination of seed.

Fluorescence microscopy

Mustard seeds were fixed and embedded in glycol methacrylate (GMA)(Eastman Kodak Co., Rochester, NY) using the method described by Yiu et al. (1982). Briefly, seed tissues were fixed in 3% glutaraldehyde in 0.025 M potassium phosphate buffer, pH 7.2, at 4°C for 48h, dehydrated through methyl cellosolve, ethanol, n-propanol and n-butanol, and infiltrated with GMA for 3 to 5 days prior to polymerization at 60°C in gelatin capsules. Sections were cut 3 to 7 µm thick using glass knives and affixed to glass slides for examination.

Mustard seed sections were stained with 0.05% (w/v) aqueous Aniline Blue (C.I. 42755, Polyscience Inc., Warrington, PA) in 0.07 M K_3PO_4 for 1 min and/or 0.001% (w/v) aqueous Calcofluor White M2R (American Cyanamide Co., Bound Brook, NJ) for 1 to 2 min. After a rinse in water they were air-dried, mounted in immersion oil, and examined for fluorescence using an exciter/barrier filter set with maximum transmission at 365 nm/>418 nm (FC I) or at 450-490 nm/>520 nm (FC II). Alternately, seed sections were stained 2 to 5 min in 0.01% (w/v) aqueous Congo Red (C.I. 22120, Fisher Scientific Co., Fairlawn, NJ). They were then rinsed in water, air-dried, and mounted in non-fluorescent immersion oil for fluorescence examination using either FC II or an exciter/barrier filter set with maximum transmission at 546 nm/>590 nm (FC III).

All sections were examined with a Zeiss Universal Research Microscope (Carl Zeiss Ltd., Montreal, Quebec) equipped with a III RS epi-illuminating condenser combined with an HBO 200 W mercury-arc illuminator for fluorescence analysis. The III RS condenser contained all three fluorescence filter combinations of FC I, II, and III. Photomicrographs were obtained using 35-mm Kodak Ektachrome 400 ASA daylight film.

Results

Scanning electron microscopy

Seed coat Normal uninfected mustard seed as viewed from the outer surface looked very much like a golf ball. The surface contained a semi-regular array of ridges which compartmented the seed coat to form a network that gave an almost honeycomb pattern (Figs. 1 and 2) with little apparent debris and no significant interruption of the surface pattern. Rarely, an ascospore could be seen on the outside surface of a normally appearing seed coat of an infected seed (Fig. 3).

Examination of Nematospora pure cultures by SEM revealed that as the culture aged beyond a week, hyphae and spindle-shaped ascospores predominated (Fig. 4). These latter ones were seen together with elliptical vegetative cells in infected seed tissue.

When seeds known to be infected by the yeast were examined further, most of the seed surface appeared to have the normal grid-like pattern; however, areas where this pattern was interrupted were visible at intervals on the seed coat (Fig. 5). Interruptions consisted of raised, somewhat smooth areas which were "pebbled" and appeared as if they were areas of seed epidermis swollen by the growth of an underlying yeast microcolony.

Globose and elliptical vegetative yeast cells were visible in the vicinity of these affected areas on the seed surface (Fig. 6). The contents of the raised areas were not amorphous as would be expected if it were mucilage.

Further examination revealed that these raised areas contained a tightly packed array of elliptical and globose yeast cells (Fig. 7).

It was usual to find sites of what appeared to be physical injury near where swollen yeast-infected tissue was seen at the surface of the seed coat (Fig.6).

Visible lesions were not clearly defined on the inside surface of the seed coat since this surface did not fracture cleanly. Often amorphous stringy debris would adhere to the exposed surface. Most spectacularly and in association with many infected cells, the hyaline layer was filled with vegetative yeast cells (Fig. 8). Occasionally mature asci and ascospores were also visible.

Cotyledon surface Cotyledon tissue was also affected by the development of the pathogenic Nematospora. Zones of eroded or partially digested tissue were evident in isolated areas across this surface and occurred only where the infecting yeast was present (Fig. 9). Frequently, evidence of extensive tissue damage due possibly to physical injury was present in the areas of the lesion (Fig. 10). Apparently undamaged cotyledon cells were also infected by the invading yeast. The presence of spores in these cells and the development toward disorganization of seed cell structure was also seen (Fig. 11).

Fluorescence microscopy

When a smear containing a 6-day old broth culture of Nematospora was prepared on a glass slide and was dried and stained with Aniline Blue, the results obtained were as shown in Fig. 12. Globose and elliptical cells were seen to have folds in their cell walls which fluoresced a pale green colour. The ascospores were also stained fluorescent, but with intensity at both the tip of the anterior (acuminate) end and the entire posterior half of the spore. No fluorescence was noted in the mid- to anterior region of the spore. It has been reported that Aniline Blue dye is specific for β-(1-3)-D-glucans (Fulcher 1982) which almost certainly occur in the vegetative cell walls and those of spores. However, the possibility that the dye may have affinity for other chemical groups cannot be ruled out. Certainly, the result obtained here reflects a difference between the anterior and posterior halves of the spores. Differential staining of these spores has been reported by others, with the anterior portion being refractile to staining with Acid Fast and cytoplasmic stains (Carmo-Sousa 1970, Batra 1973).

An examination of GMA-embedded serial sections of infected seed halves showed results similar to those found during SEM. Yeast on the

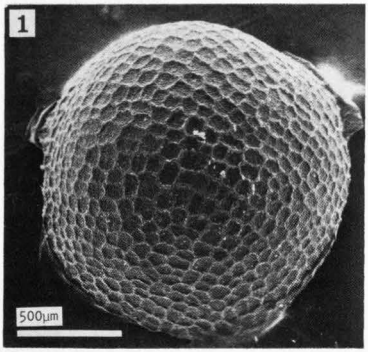

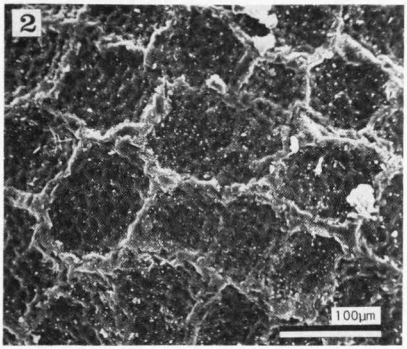

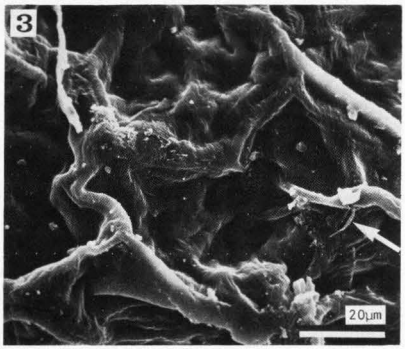

Fig. 1. Surface view of an uninfected oriental mustard seed by SEM.

Fig. 2. Seed coat of oriental mustard by SEM, showing semiregular network of surface ridges.

Fig. 3. Surface view of the seed coat from an infected mustard seed showing a single ascospore (arrow) of Nematospora.

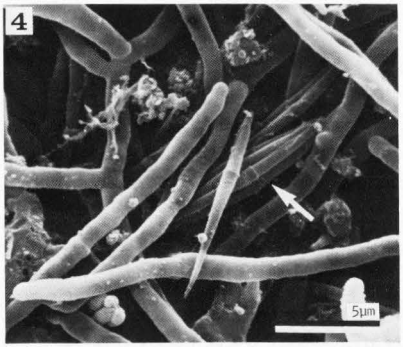

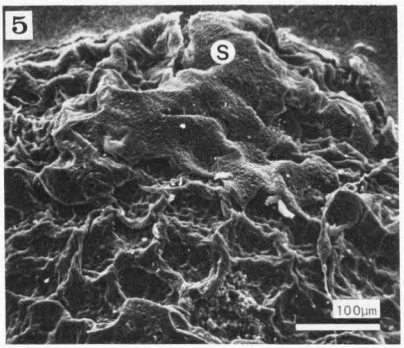

Fig. 4. Hyphae and pseudomycelium of Nematospora coryli also showing ascospores (arrow).

Fig. 5. Surface view of the seed coat from an infected mustard seed showing interruptions (S) in normal surface pattern which are believed to be areas of Nematospora involvement.

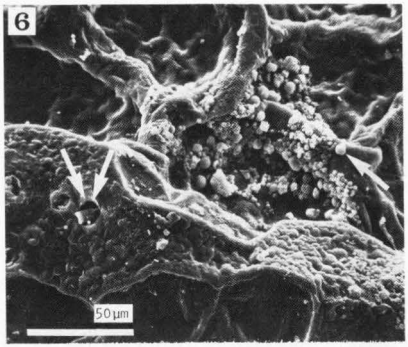

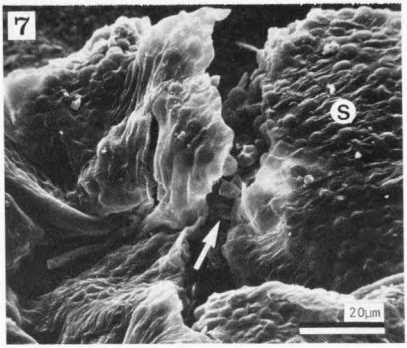

Fig. 6. Seed coat surface of an infected seed showing exposed yeast (arrow) and a swollen area of the seed surface where physical injury (double arrow) may have been inflicted.

Fig. 7. Seed coat surface of an infected seed showing an area where subsurface yeast growth has caused swelling (S). Vegetative yeast cells can be seen below the seed coat surface (arrow).

outside of the seed was integrated among cells of the mucilagenous epidermal layer (Fig. 13). This growth by the yeast mycelial form was observed to penetrate through the subepidermis into the palisade cells where yeast were visible in the lumina of the palisade cells (Fig. 14). A zone of eroded tissue or a site of physical injury was also visible. A cross sectional view of the seed coat is shown in Fig. 15. Fungal hyphae are visible in the mucilagenous epidermal tissue. Extensive damage can be seen in the pigment layer above the aleurone cells as well as in the latter tissue.

A cross-section of the seed coat below the epidermis is shown in Fig. 16. Significant damage was seen beneath the aleurone cells while the aleurone layer appeared largely unaffected. Yeast spores were seen to spread laterally throughout the hyaline layer and in some preparations actually circled the entire embryo. Tissue damage was also visible in the peripheral cells of the cotyledon (Fig. 17) and yeast spores with their characteristic arrangement in packets of eight were seen in cross-section inside some of the infected cotyledonous cells (Fig. 18). No infection was detected beyond the periphery of the cotyledonous tissue.

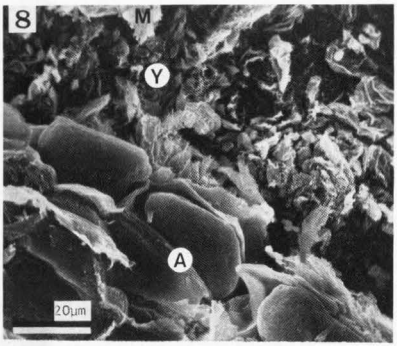

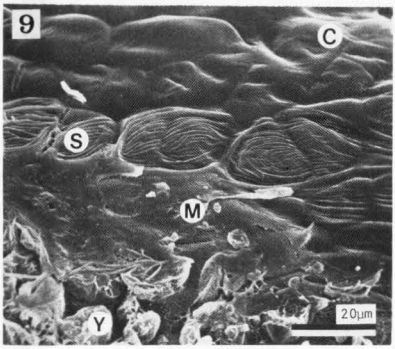

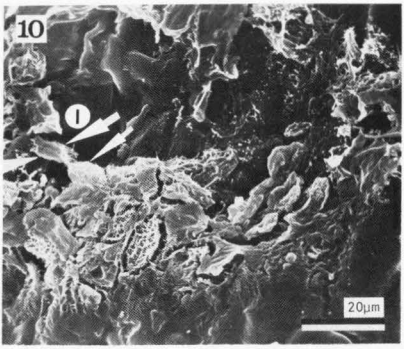

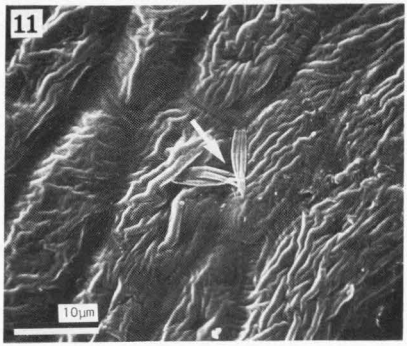

Fig. 8. A fracture of an infected oriental mustard seed tagential through the aleurone layer of the seed coat (A) through the hyaline layer showing vegetative yeast cells (Y) in a matrix (M) of amorphos material.

Fig. 9. View of the cotyledon surface of an infected mustard seed showing the progression of Nematospora infection of healthy tissue. Normal healthy cells (C), stressed cells (S), amorphous materia (M), and yeast cells (Y) are visible.

Fig. 10. Cotyledon surface from an infected seed illustrating tissue disorganization resulting from Nematospora infection from a site of physical injury (I). Yeast asci (arrows) are visible in necrotic tissue.

Fig. 11. Yeast ascospores (arrow) "exuding" from a cell of the surface of cotyledon tissue in an infected seed. Other adjacent cells appear distorted perhaps due to the yeast infection.

Discussion

Growth of Nematospora in pathological lesions of the seed or in laboratory culture resulted in the same diversity of cellular morphology. The distinct character of vegetative cells, mycelium, and ascospores was maintained in the two environments and equivalent yeast forms were observed in each milieu. The most striking morphological feature of the yeast was its spindle-shaped ascospores which possessed spiral ridges on the pointed or posterior end which resembled an auger (Fig. 4). In all probability this pattern on the surface of the spores was nothing more than the decoration that has been reported before on fungal spores (Martinez et al. 1982). The ridges may serve to some extent in the process of spore dissemination.

Seed coat - external

When seed rinse and surface sterilization procedures (Chandra et al. 1981) using 2% sodium hypochlorite were used, little evidence was obtained for the presence of contaminating Nematospora on the seed surface. An examination of contaminated seed by SEM and fluorescent light microscopy did result in the observation of surface contamination on the seed coat, usually, but not always, adjacent to foci of epidermal infection (Figs. 3, 6, and 13). The proportion of organisms on the seed surface easily removed by surface rinsing was small in relation to the total numbers of organisms present in infected seed (approx. 1%), although for surface-contaminated seed rinse-soak methods are recommended to routinely quantify microorganisms (Cowlen and Marshall 1982).

Oriental mustard seed surface topography (Figs. 1 and 2) resembled in a very general way images of Brassica napus published elsewhere (von Hofsten 1974), Brassica nigra (Vaughan et al. 1976), and also black pepper (Leistner et al. 1981) with differences noted in the following discussion. The predominating feature of the seed coat appearance was an informally arranged network of interconnecting ridges (Fig. 1). There were fewer ridges on the seed coat of black pepper than on oriental mustard. On B. napus surface ridges were closer together and valleys in between were deeper. With B. nigra the same pattern was evident but the ridges were not as conspicuous (Vaughan et al. 1976) and the surface was more like that of oriental mustard as seen by fluorescence microscopy (Fig. 13).

Surface contamination of oriental mustard by Nematospora was visible by both SEM (Figs. 3 and 6) and fluorescence microscopy (Fig. 13), and occurred mainly in areas where physical damage of the epidermis was visible (Fig. 6). If the latter were "puncture" damage, in all probability this physical injury was due to the feeding activity of insects like the false chinch bug (Nysius ericae) and others which have been implicated as vectors in disease transmission (Burgess et al. 1983, Heinrichs et al. 1976, Batra 1973). Prior physical injury is considered to be an important prerequisite for the establishment of infection in spice seeds (Leistner et al. 1981).

Foci of Nematospora infection on the outer seed coat surface appeared as elevated or swollen areas and interrupted the normal pattern of surface ridges (Fig. 5). These elevated areas had a "pebbled" appearance due to the underlying masses of globose and elliptical vegetative cells (Fig. 7). Engorged areas probably developed as a result of rapid yeast growth prior to seed maturation and desiccation in the seed pod. This hypothesis is consistent with the result obtained by Burgess et al. (1983) during laboratory infection of oriental mustard by infected insects. It is unlikely that swelling was due to hydration of mucilage since the underlying material contained structures resembling vegetative yeast cells (Fig. 7).

Seed coat penetration

Evidence for the spread of yeast infection through the seed coat was taken largely from results obtained using fluorescence microscopy techniques (Fulcher 1982, Yiu et al. 1982).

Images obtained in cross sections of the seed coat (Figs. 15 and 16) were identical in outline to those previously published for B. juncea (Aoba 1972, Vaughan et al. 1963) by light microscopy and were similar to those published for yellow mustard (Vaughan et al. 1976) and for rapeseed using fluorescence microscopy (Fulcher 1982, Schans et al. 1982, Yiu et al. 1982). In cross section, three major layers of cells were evident in the oriental mustard seed coat: the outer epidermal, underlying palisade layer, and inner aleurone cells (Fig. 15). The hyaline layer between the seed coat and cotyledon cells was also visible (Fig. 16) but detail of parenchymal tissue overlying the aleurone cells was not clear in infected specimens.

Yeast and mycelia were present on the outer epidermal layer (Figs. 6 and 13) and were believed to penetrate into and through the lumina of the palisade cells (Fig. 14), the aleurone layer (Fig. 15) and then to the underlying hyaline layers where lateral spread and multiplication of organisms occurred (Fig. 16). Shown in Fig. 8 is a comparable view by SEM, tangential to the hyaline layer through the aleurone layer. Vegetative cells of Nematospora were visible in large numbers. Often by both SEM and fluorescence microscopy the hyaline layer was seen to be filled with both vegetative cells (SEM) and spores (fluorescence).

Cotyledon penetration

Cotyledon tissue was heavily infected in some peripheral areas with localized foci of eroded and apparently necrotic tissue often in association with vegetative yeast cells (Fig. 9). In contrast with the swollen areas on the seed coat surface, these erosion zones (Fig. 10) resembled erosion troughs around the bacterium Alteromonas putrefaciens on pork skin (Butler et al. 1980). Results were interpreted to mean that foci of yeast infection developed in areas that had suffered physical injury, although the yeast appeared to be an invasive parasite. For example, amorphous tissue was often found in an area adjacent to a focus of infection. As one moved farther from the focus of infection, intact cotyledon cells could be seen which contained structures resembling maturing ascospores (Fig. 9). Thus, Nematospora appeared capable of infecting otherwise normal tissue - an observation made by Heinrichs et al. (1976) during a study of inoculated soybeans.

The pattern of oriental mustard seed infection by Nematospora seen here at each layer of tissue seemed to be associated with physical injury, and was likely caused by an insect vector (Burgess et al. 1983). There appears to be a consensus that physical injury, probably through insect feeding with consequent Nematospora inoculation of the damaged seed, is a necessary prerequisite (Burgess et al. 1983, Heinrichs et al. 1976, Batra 1973). On the other hand, at artificially high temperature and moisture, successful invasion of rapeseed with concomitant destruction of cotyledon cells by Aspergillus, Penicillium, and Verticillium was accomplished without prior physical damage to the seed (Schans et al. 1982). It is very probable that oriental mustard would be attacked by many fungi in a similar successful manner under the same abusive storage conditions without physical injury (Holley and Timbers 1983).

Schans et al. (1982) traced the invasion route and found that the inoculated fungi crossed the seed coat tissue and entered the rapeseed cotyledon without apparent difficulty. Once below the palisade cells of the seed coat, the fungi went laterally among the crushed parenchyma. In our study of infected oriental mustard, some lateral movement of the yeast hyphae may have taken place above the aleurone cells, but major lateral growth occurred below the aleurone layer and almost filled the entire hyaline layer. Intra- and extracellular growth of the fungi and yeast in cotyledonous cells was similar in both kinds of seed.

In contrast to results obtained by Heinrichs et al. (1976), who used soybeans inoculated with Nematospora, oriental mustard cotyledon tissue was not deeply penetrated by invading Nematospora. Substantial growth by the yeast occurred in the hyaline layer between the seed coat and embryo. It is possible that myrosine granules in cotyledon cells may play a role in the natural seed defence system to prevent deep penetration by microorganisms into cotyledon tissue. Work on the autotoxicity of mustard seed to the yeast Nematospora is continuing.

Conclusion

Support was obtained for the hypothesis that the infection process in the seed was initiated by physical injury. This injury was probably caused during the feeding activity of contaminated insects with piercing-sucking mouth parts. Areas of apparent physical injury were found adjacent to sites of yeast infection on the surface of the seed coat and on the cotyledon surface. Vegetative yeast cells and hyphae were seen to penetrate through the seed coat and to grow laterally at the hyaline layer between the seed coat and cotyledons. All morphological forms of the yeast were found both inter- and intracellularly with respect to the cotyledon cells.

Acknowledgments

Oriental mustard seeds with a high frequency of yeast infection were kindly provided by Dr. L. Burgess (Agriculture Canada, Saskatoon). Technical assistance provided by Mr. G.E. Millard and Mrs. Paula Allan-Wojtas is gratefully acknowledged. The authors wish to thank Drs. M. Kalab and R. G. Fulcher (Agriculture Canada, Ottawa) for their advice and assistance throughout this study. The Electron Microscope Centre, Research Branch, Agriculture Canada in Ottawa provided facilities for the SEM study.

This paper is Contribution 552 from Food Research Institute, Agriculture Canada, Ottawa.

References

1. Aoba R.(1972). Histological observations of seed coat in Brassica juncea Coss. Japan J. Breed. 22, 323-328.
2. Ayres JC, Mundt JO, Sandine WE.(1980). Spices and condiments, in: Microbiology of Foods. W.H. Freeman and Co., San Francisco, 249-260.
3. Batra LR. (1973). Nematosporaceae (Hemiascomycetidae): Taxonomy, Pathogenicity, Distribution and Vector Relations. U.S. Dept. Agriculture Tech. Bulletin No. 1469, 71 pp.
4. Burgess L, Dueck J, McKenzie DL. (1983). Insect vectors of the yeast Nematospora coryli in mustard, Brassica juncea, crops in southern Saskatchewan. Can. Entomologist 115, 25-30.
5. Butler JL, Vanderzant C, Carpenter ZL, Smith GC, Lewis RE, Dutson TR. (1980). Influence of certain processing steps on attachment of microorganisms to pork skin. J. Food Protect. 43, 699-705.
6. Carmo-Sousa L.(1970). Nematospora peglion, in: The Yeasts. J. Lodder (ed.), 2nd Edition, North-Holland Publ. Co., Amsterdam, 440-447.
7. Chandra S, Narang M, Srivastava RK. (1981). Studies on seed microflora of oilseeds in India. Part 1. Qualitative and quantitative estimations. International Biodeterioration Bull. 17, 71-75.
8. Cowlen MS, Marshall RT. (1982). Soaking of mustard seeds to release microorganisms in making plate counts. J. Food Protect. 45, 340, 344.
9. Fulcher RG. (1982). Fluorescence microscopy of cereals. Food Microstructure 1, 167-175.
10. Heinrichs EA, Lehman PS, Corso IC.(1976). Nematospora coryli, yeast-spot disease of soybeans in Brazil. Plant Disease Reporter 60, 508-509.
11. Holley RA, Timbers GE. (1983). Nematospora destruction in mustard seed by microwave and moisture treatments. Can. Inst. Food Sci. Technol. J. 16, 68-75.
12. Leistner L, Neumayr L, Forstmeier G. (1981). Verteilung von Mikroorganismen in und auf Gewürzen, am Beispiel Pfeffer. (Distribution of microorganisms in and on spices, as illustrated by pepper). Fleischwirtschaft 61, 630-632.
13. Martinez AT, Calvo MA, Ramirez C.(1982). Scanning electron microscopy of Penicillium conidia. Antonie van Leeuwenhoek 48, 235-255.
14. Pivnick H. (1980). Spices, in: Microbial Ecology of Foods. Vol. II. J.M. Silliker and R.P. Elliott (eds.), Acad. Press, New York, 731-751.
15. Schans J, Mills JT, van Caeseele L. (1982). Fluorescence microscopy of rapeseeds invaded by fungi. Phytopathology 72, 1582-1586.
16. Speck ML. (ed.), (1976). Compendium of Methods for the Microbial Examination of Foods. Am. Publ. Health Assocn., Washington, DC, 226-227.
17. Vaughan JG, Hemmingway JS, Schofield HJ. (1963). Contributions to a study of variation in Brassica juncea Coss and Czern. J. Linn. Soc. (Bot.) 58, 435-447.
18. Vaughan JG, Phelan JR, Denford KE. (1976). Seed studies in the Cruciferae, in: The Biology and Chemistry of the Cruciferae. J.G. Vaughan, A.J. MacLeod, and B.M.G. Jones (eds.). Acad. Press, New York, 119-144.
19. Virtanen AI. (1962). Some organic sulfur compounds in vegetables and fodder plants and their significance in human nutrition. Angew. Chem. Internat. 1, 299-308.

20. Von Hofsten A. (1974). The ultrastructure of seeds of some Brassica species - new sources of seed protein. Svensk Botanisk Tidskrift. 68, 153-163.
21. Yiu, SH, Poon H, Fulcher RG, Altosaar I. (1982). The microscopic structure and chemistry of rapeseed and its products. Food Microstructure 1, 135-143.

Discussion with Reviewers

D. N. Holcomb: Could you give more detail of the fluorescence microscopy technology and provide some warnings as to artefacts with this technique?
Authors: The formation and recognition of artefacts are important aspects of this and other techniques in microscopy. Substantial additional information on the applications and limitations of fluorescence microscopy are provided in the paper by Fulcher (1982) cited in the bibliography.

L. van Caeseele: In view of the differential color obtained by Schans et al. (1982) using Acridine Orange and Malachite Green, did you try combinations of stains such as this?
Authors: The major part of our work was done before the latter was published and thus the dyes mentioned were not used. In view of the success achieved by Schans et al. (1982) with rapeseed, they may be quite appropriate for use with mustard as well.

L. van Caeseele: Fig. 6 shows puncture marks (arrows). In the discussion you speculate that these may be caused by the false chinch bug. If this were so, would you expect smooth edges on the puncture hole? Would the holes vary in diameter? Is the diameter of the false chinch bug proboscis known?
Authors: Insects, which could be responsible for inflicting puncture damage upon these crops, vary in size and thus the lesions they cause also vary in their dimensions. Indeed,the male false chinch bug is significantly smaller than the female. The proboscis of the false chinch bug (the most likely insect to be involved) female measures approximately 50-80 µm in diameter. This includes an outer sheath which does not penetrate. Inside the sheath are 4 stilets, two of which cut the hole. The diameters of the "holes" in Fig. 6 are within the size range of those which would be produced by these insects (10-20 µm). The edge of these puncture wounds would initially be ragged, but as the seed matured and dried, one would expect changes to occur in the perimeter of these lesions.

J. G. Vaughan: Are the authors interested in carrying out a controlled experiment on yeast with healthy B. juncea seed?
Authors: Yes, and we would be especially interested in studying the progress of yeast infection during seed maturation. It is an interesting contradiction that the host seed is quite toxic toward the yeast parasite.

S. H. Humphreys: Could the folds shown in the vegetative yeast cells (Fig. 12) be artefacts of drying?
Authors: Undoubtedly this is true. Although less clearly resolved, irregular surfaces of vegetative yeast cells are also visible in the seed lesion viewed by SEM in Fig. 8.

Reviewer V: Is a reference strain of the infecting organism available?
Authors: Yes, the Nematospora culture studied has been deposited in the collection of the Centraal Bureau voor Schimmelcultures, Baarn, the Netherlands and has been assigned CBS#8199. The culture is also preserved at the National Mycological Herbarium, Ottawa, Ontario, Canada K1A 0C6, where it is given the number DAOM 187446.

Fig. 12. Aniline Blue-stained culture smear showing yeast cells and spores (arrow). Photographed using FC I.

Fig. 13. Congo Red-stained GMA-embedded paradermal section of infected mustard seed showing the epidermal mucilage (M) and the yeast (Y) structures. Photographed using FC III.

Fig. 14. Congo Red-stained GMA-embedded paradermal section of the palisade layer (P) of infected mustard seed penetrated by yeasts (Y) in an area of seed tissue showing signs of disorganization. Photographed using FC II.

Fig. 15. Aniline Blue - Calcofluor White-stained GMA section of infected mustard seed coat showing epidermis (E), palisade (P), pigment (arrow), aleurone (A), and hyaline (H) layers. Photographed using FC I.

Fig. 16. Congo Red-stained GMA section of infected mustard seed showing yeast spores (arrows) spreading throughout the hyaline (H), palisade (P), and aleurone (A) layers. Photographed using FC II.

Fig. 17. Congo Red-stained GMA section of infected mustard seed showing yeast cells (Y) at the periphery of the damaged cotyledonous cells (*). Photographed using FC II.

Fig. 18. Congo Red-stained GMA section of infected mustard seed showing yeast spores (arrows) inside an infected cotyledonous cell (*). Photographed using FC III.

Errata: The correct marker on Fig. 18 is 20 µm.

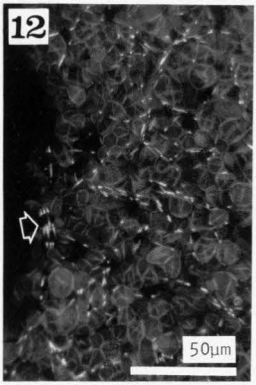
12
50µm

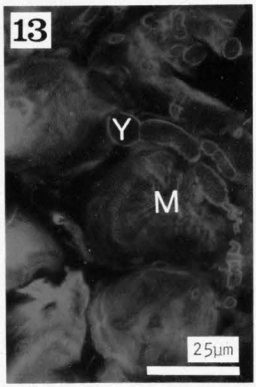
13
Y
M
25µm

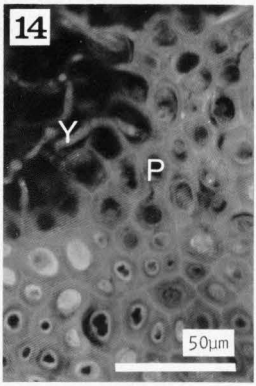
14
Y
P
50µm

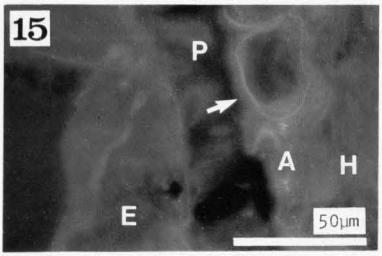
15
P
A
H
E
50µm

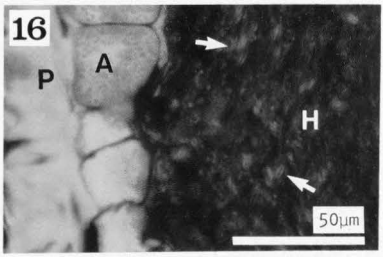
16
P
A
H
50µm

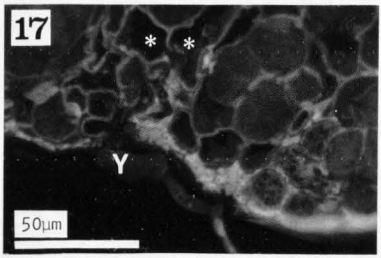
17
*
*
Y
50µm

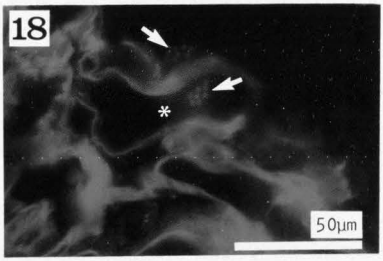
18
*
50µm

FOOD MICROSTRUCTURE, Vol. 2 (1983), pp. 153-160
SEM Inc., AMF O'Hare (Chicago), IL 60666 U.S.A.

EVALUATION OF SELECTED PROPERTIES OF CHLORINATED WHEAT FLOURS IN A LEAN CAKE FORMULATION

J. Grider, E.A. Davis and J. Gordon

University of Minnesota, Department of Food Science and Nutrition,
1334 Eckles Avenue, St. Paul, MN 55108

Abstract

Cake flours treated with different levels of chlorine were evaluated by use in a Kissell cake formulation. Flour particle size distributions varied with chlorination level, but pH and specific gravity of the batters did not differ. Batter viscosity differences were observed at specific temperatures during heating of total batters. Temperature profiles differed positionally in the cakes, but these patterns of heat penetration were not related to level of chlorine treatment. However, water loss rates differed depending on the level of chlorine treatment indicating a more pronounced effect of chlorination level on the water loss characteristics of the cakes during the baking process than on the temperature profiles. The largest cake volume, contour deviations, and least shrinkage from the pan sides occurred with a 0.93 g Cl_2/kg flour treatment (commercial level). The SEM micrographs on crumb showed larger starch particles with more continuous and extensive matrix development between starch particles as chlorine level increased. The aforementioned characteristics prior, during, and after baking were related to factors contributing to optimal cake structure.

Initial paper received September 29, 1983.
Final manuscript received November 14, 1983.
Direct inquiries to E.A. Davis.
Telephone number: 612-373-1158.

KEY WORDS: Flour - chlorinated, Heat and water transport - batters, Heat and water transport - cakes, chlorinated flour batter properties, Batter properties - chlorinated flour.

Introduction

Chlorine treatment of soft wheat flours has long been used to improve the baking performance of the flours used in cake making. Many researchers have studied the effects of chlorination on flour components and the functionality of flour in cake batter systems. Whistler et al. (1966) proposed a mechanism of starch depolymerization to explain the action of chlorine. Further work by Whistler and Pyler (1968) attempted to explain the action of chlorine on the polysaccharides found in flour. The work of Sollars (1961) and Gilles et al. (1964) was focused on determining the chlorine content of various flour fractions. Other workers have tried to evaluate changes in flour functionality that may be attributed to chlorine treatment. Youngquist et al. (1969) attributed the improving effect to an interaction between the chlorine and the lipids within the starch granules. Kissell et al. (1979) compared the functionality of lipids from untreated and chlorinated flours in white layer cake. Kulp et al. (1972) evaluated the changes in pasting characteristics, swelling power, extensibility, and water-binding capacity of the starch component after chlorination. Allen (1977) performed similar experiments but also included a study of the effect of chlorination on the heats of starch phase transitions. The changes in the functionality of the flour protein and subsequent effect on dough properties were examined by Tsen et al. (1971). Huang et al. (1982 a, b) examined the absorption of chlorine in starch and protein and found that the absorption of chlorine was a function of level of chlorination in protein but not starch. In isolated starch fractions, the response to chlorination depended on the stage of the phase transitions. For example, the initiation of the phase transition as measured by differential scanning calorimetry (DSC) was not influenced by level of chlorination, but swelling power after 80°C, and loss of birefringence at 90°C were affected. These studies have made major contributions to understanding the role of chlorine in individual components of the flours, although its precise action in baked products is not fully understood.

In this study, the functionality of the total cake flour which has been treated with different amounts of chlorine was evaluated in a research

cake formulation. Temperature profiles and water loss rates were recorded throughout the baking process as had been done in previous studies by Gordon et al. (1979) and Hsu et al. (1980). Also, various batter and cake characteristics such as pH, viscosity, specific gravity, volume index and particle size distribution were determined. Scanning electron microscopy (SEM) examination and chlorine analysis by X-ray microanalysis were also included. The combination of studies of water loss rates and temperature profiles with macro- and microstructural evaluation should lead to a better understanding of the specific role that chlorine plays in flour functionality.

Materials and Methods

Batter Formulation and Baking Procedure

A modified Kissell cake formulation as described by Gordon et al. (1979) was used to prepare the cake batters. All ingredients except the flour were purchased in the retail market. The flour, with an ash content of 0.28% and protein content of 7.31% on a dry weight basis, was prepared by General Mills, Inc. at the following levels of chlorine treatment (g Cl_2/kg flour): 0 g/kg (pH 5.17); 0.31 g/kg (pH 5.09); 0.62 g/kg (pH 4.86); 0.93 g/kg (pH 4.51); and 1.24 g/kg (pH 4.48).

The cakes were baked in a controlled environment oven (Godsalve et al., 1977) at 190°C ± 1°C with an airflow rate of 10.1 m^3/hr for 25 min. The temperature profiles were monitored by four thermocouples placed 5 mm above the bottom of the pan at the following positions: the center, 2.5, 5.1, and 6.9 cm radially from the center of the pan. The water loss rates from the cakes were calculated by monitoring the wet-bulb and dry-bulb temperatures of the airstreams flowing in and out of the oven throughout the baking process. These procedures were the same as those used by Gordon et al. (1979) for high starch cakes.

Flour Particle Size Analysis and Chlorine X-Ray Microanalysis in the SEM

The aluminum stubs used for particle size analysis were first coated with carbon paint, then covered with a thin layer of flour particles. The mounted samples were coated with carbon to minimize charging. These samples were then viewed in a Philips Model PSEM 500 scanning electron microscope operated at 6 kV. To ensure random selection of particles, measurements were taken at equidistant points along two perpendicular lines passing through the center of the stub. The areas of the particles were approximated by tracing the images of the particles as they appeared on the viewing screen of the microscope. The areas of these tracings were measured with a Hewlett Packard digitizer.

Chlorine analysis was performed on the flour particle components using energy dispersive X-ray microanalysis. The preparation of the sample stubs was similar to that described for particle size determinations. However, the samples were placed in a JEOL Model JSM-35 scanning electron microscope equipped with an Edax Model 711 microanalyzer. Random selection was accomplished by the same method described for particle size analysis. The X-ray intensity data were collected from the samples for 400 sec time periods. The method of Nasir (1976) was used to calculate mass concentration ratios of minerals in the samples.

For the collection of X-ray data, the electron beam of the SEM was focused on various micro-components within the clumps of dry flour particles mounted on carbon-coated SEM stubs. Analysis of the lipid fractions was not included because of the high risk of interference from other components due to the nature of the lipid fraction and the size of the beam penetration. The determinations were done for the most part on the granular starch and wedge-type protein. Due to the nature of the starch and protein fractions, potassium (K) was used as the basis for the calculation of mass concentration ratios in starch fractions; sulfur (S), for protein fractions.

Determinations Made on the Batter

The pH of the complete batter was measured on a Corning Model 7 pH meter. A Fischer-Grease pycnometer was used to determine the specific gravity of the batter. A preliminary study of viscosity was performed on a flour-water slurry (1:9) in a Model AV-30 Brabender amylograph viscograph. Flour (50 g) and distilled water (450 g) were initially mixed and used with a 350 cm-g cartridge at a rotational speed of 75 RPM for 42.5 min at a rate of temperature change of 1.5°C per min (0 time is 30°C). The viscosity of the batter was determined in a Model RV2 Haake rotoviscometer with an MVII cylinder set. The unit was operated at 2 RPM in the temperature range 75-95°C. Readings were taken at 5, 10 and 15 min.

Measurement of the Final Cake Characteristics

Cross-sectional areas of the bisected cakes recorded using a Hewlett Packard digitizer (average of three tracings) were used as a volume indicator. The diameter of the cross-section was used as an index of shrinkage. Contour index was defined as the differences between center height and the average of the two side heights of the cross-sectional tracings.

Scanning Electron Microscopy Evaluation of Cake Crumb

Samples to be viewed by SEM were taken from cakes at four positions: the center bottom, the center top, mid-point (3.5 cm from the center), and the mid-point of the outer edge of the cake. Using a razor blade, the samples of crumb were cut as elongated triangles (4 mm x 5 mm) which were 1 mm thick. After transferring the crumb onto an aluminum stub coated with a thin layer of silver paint, the sample was placed in a desiccator and exposed overnight to osmium vapors. The fixed samples were then coated with palladium gold prior to viewing in a Philips Model PSEM 500 scanning electron microscope operated at 6 kV or 12 kV.

Results

Flour Particle Size Analysis and Chlorine Content

Figure 1 shows the size distributions of flour particles for 0 g/kg and 1.24 g/kg level of chlorine treatment. The distribution suggests that chlorination increases the clumping tendency of the flour as evidenced by larger areas recorded for the 1.24 g/kg flour. Furthermore, a bimodal distribution is evident for the 0 g/kg level. Looking at the 0 g/kg sample, only 49% of the par-

ticles measured fell into the size range greater than 10 x 10^{-5} cm^2, while in the 1.24 g/kg sample, 72% were in this size range. The increased clustering with increased chlorination is also evident in the intermediate levels of treatment. It is difficult to determine if the increased association of the flour particles observed in the dry state is maintained during the batter preparation and cake baking. Although Seguchi and Matsuki (1977) found marked clustering of chlorinated samples in suspension, the clumping tendency may already have been established in the dry form. In Fig. 2 we see that the chlorine is taken up by starch more gradually than in the protein fraction of the same flour samples. Sollars (1961) found little chlorine located in the extracted starch fraction, although starch functionality seemed to be greatly affected after chlorine treatment. Gilles et al. (1964) confirmed that little chlorine is associated with the starch. After they made corrections for the lipids on the starch granules, the starch fraction showed no consistent increase with increased chlorine treatment. However, they found a slight increase in the chlorine content for the gluten fraction. In the present study, the correction for lipids was not made, possibly explaining the slight increase in chlorine uptake observed in the starch components in Fig. 2. We see, then, that the flour particle sizes are somewhat larger in the chlorine treated samples and that the chlorine uptake is somewhat greater for protein than for starch.

Batter Characteristics

It was found that the pH of the batters did not vary greatly from one level of chlorine to the next (Table 1). The batters were at 7.3-7.4 pH at all times. The pH of flour-water slurries decreased as the level of chlorine treatment was increased (pH 5.17 for 0 level and 4.48 for 1.24), but the pH of the batter was not affected by these initial differences. Localized areas may be affected by a lowering of pH, but this could not be detected in our batter pH measurements. The values for specific gravity of the batters were within the range of 0.98-0.99 regardless of the level of chlorine treatment.

A preliminary viscosity study of flour-water slurries on the Brabender amylograph (Fig. 3) showed that as the level of chlorine treatment was increased to 0.93 g/kg, the maximum viscosity of the flour-water slurries increased, but at the 1.24 g/kg level, the viscosity was lower than that of the 0.93 g/kg level. Unpublished data by B.M. Dirks did not have similar differences in peak viscosity. The reason for the differences found by those researchers is not obvious. Allen (1977) showed that the differential effects of chlorine on viscosity as measured by the Brabender amylograph are dependent on starch concentration. Therefore, the Haake rotoviscometer was used for batters so that determinations could be made on the undiluted batters. Table 2 shows the viscosities that are recorded over a range of temperatures for the batters prepared from untreated and commercially treated flours. The differences between the batter systems were not as dramatic as the results obtained for the flour-water slurries done by the Brabender amylograph method. The increase in viscosity is not measurable until the temperatures approach the gelatinization temperatures of the starch in high sucrose batter

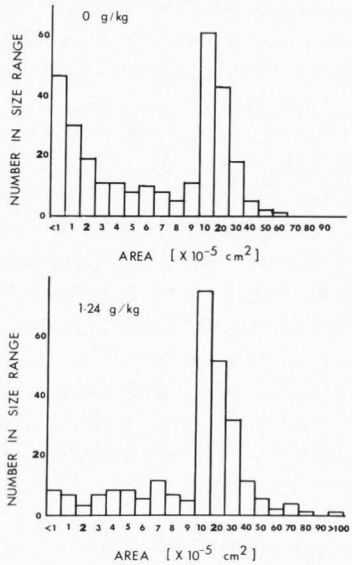

Fig. 1 Size distributions of flour particles for 0 and 1.24 g Cl_2/kg flour treatment.

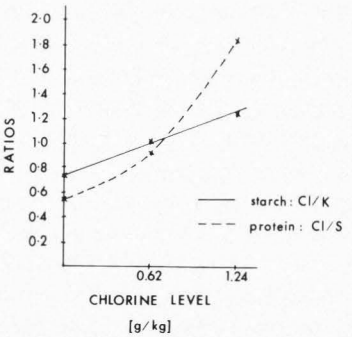

Fig. 2 Relative amounts of chlorine taken up by starch (Cl/K) and protein (Cl/S) for 3 different levels of chlorine treated flour.

Table 1. Summary of physical measurements on batters and final cakes.

Measurement	Level of chlorine g/kg				
	0	0.31	0.62	0.93	1.24
pH batter	7.4	7.4	7.3	7.4	7.4
Specific gravity (batter)	0.98	0.98	0.99	0.99	0.98
Cake cross-sectional area (cm^2)	22.12	24.45	28.64	41.02	39.47
Cake contour index	-.28	-.025	0.18	0.81	0.60
Cake diameter (cm)	13.1	13.6	13.6	14.3	13.9

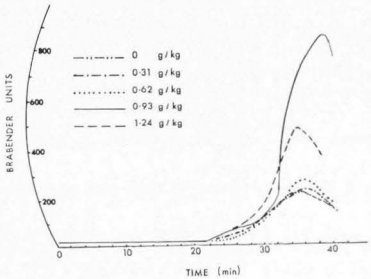

Fig. 3 Brabender viscosity curves for flour-water slurries.

systems. Slight differences between the samples were observed when viscosities are measured at 85°C. There is a suggestion that the increase in viscosity as temperature increases is more rapid in the chlorinated samples. This trend is also evident when the batters are held at 90°C. It appears that the level of chlorine treatment (up to 0.93 g/kg) does not dramatically influence the final viscosity of the batter, but that the rate of viscosity development may be more rapid due to chlorination. Although other workers have emphasized the importance of batter viscosity in relation to the development of the final cake structure, it is not known whether the more rapid increase in viscosity in the chlorinated sample is responsible for the improvement in the final cake structure.

Table 2. Viscosity (Poise) of batters made with flour chlorinated at two levels.

Temperature C°	Level of Chlorine (g/kg)	Viscosity (poise) after:[a] 5 min	10 min	15 min
76	0	15	20	23
	0.93	15	24	35
80	0	17	21	32
	0.93	20	36	49
85	0	18	65	124
	0.93	23	81	160
90	0	32	222	445
	0.93	35	267	532

[a]Coefficient of variation is 10%.

Baking Properties - Temperature Profiles

Temperature profiles were recorded continuously at the positions previously described. Varying levels of chlorine did not create temperature variations greater than ± 4°C at any of the four thermocouple positions. Temperature gradients were established positionally within all the cakes irrespectively of chlorine treatment. The highest temperature was recorded by the edge thermocouple (6.9 cm from the center); the lowest temperature, generally at 2.5 cm from the center. This may be the result of the patterns of batter flow as described by Trimbo et al. (1966).

Figure 4 shows the center temperatures recorded across five levels of chlorine treatment. These center temperature curves show either three or four distinct sections: (1) an initial period of rapid temperature increase until the 8th min of baking corresponding to 83-86°C; (2) a period of less rapid temperature rise to the 17th min or to temperatures of 99-101°C; (3) a short period of intermediate temperature rise; and (4) a period of steady-state temperature after the 21st min with the temperatures approximately 111°C. This final period was not observed in all of the cakes, and its presence was not related to the level of chlorine treatment. Thus, there were no differences in the patterns of heat penetration that could be related to the level of chlorine treatment.

Water Loss Rates

The water loss rates versus time curves are shown in Fig. 5. The values for the rate of water loss as a function of baking time are the averages of three replications. The curves for all cakes show four distinct regions. During the first 4-5 min of baking, the systems begin to heat up, and water loss appears to be simply a function of temperature increase as if it is an isotropic system. At the end of this period, the temperature has

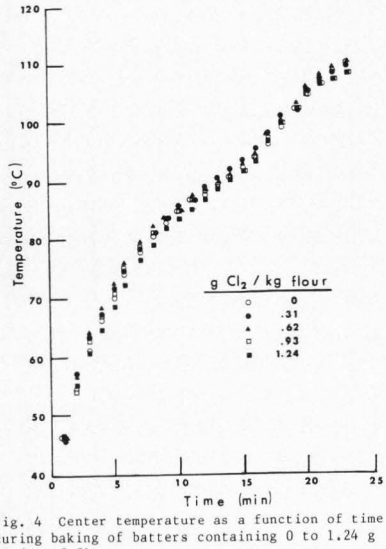

Fig. 4 Center temperature as a function of time during baking of batters containing 0 to 1.24 g Cl_2/kg of flour.

reached approximately 71°C. Changes then begin to take place within the batter that result in increased rates of water loss during the second period, which continues for 5-6 min. There were no observable differences throughout the first two sections of the curve across the level of treatments. The third section of the curve is characterized by a constant or decreased level of water loss. All the cakes entered this period at approximately 11 min into the baking time when the water loss rate is between 0.52 and 0.57 g/min. At levels below 0.93 g/kg, the water loss rate increased gradually during this period. It was not until the commercial level, 0.93 g/kg, that the water loss rate remained constant at 0.53 g/min for a period of 5 min. During this period, the curve of the 1.24 g/kg sample in contrast to the other levels actually showed a decrease in water loss rate. The final period is characterized by an accelerated rate of water loss at all levels of chlorine. Thus, we can see that the effect of the level of chlorine in the water loss characteristics of the cakes during the baking process is more pronounced than the effect on the temperature gradient profiles.

Characteristics of the final cake

Table 1 summarizes the measurements made on the final cake as well as the pH and specific gravity of the batter. The areas of the cross-sectional tracings recorded as an index to cake volume in Table 1 suggest that increasing levels of chlorine treatment improve cake volume to a maximum corresponding to the 0.93 g/kg (commercial level use). The volume decreased at the 1.24 g/kg level, suggesting that the treatment is no longer optimal. The cake shrinkage indicators (diameter) reported in Table 1 show greater shrinkage at the lower levels of chlorine treatment. The minimum shrinkage was associated, again, with the 0.93 g/kg cake. Above this level, shrinkage of the cake again increased. The contour index reflects final shape of the cake. At the first two levels of treatment, the index reflects a sunken appearance. The surface of the 0.62 g/kg cake is relatively flat. At the commercial level of treatment, the cake is well-rounded. Above the commercial level, the contour index is less rounded. Based on the evaluation of these characteristics of the final cakes, the commercial level of treatment provided optimal results.

SEM of the cake crumb

SEM data were collected to determine differences in the cake crumb by evaluating swelling or matrix development in the final cake structure. The same positional effects reported by Gordon et al. (1979) were observed in all the cakes regardless of the level of chlorine treatment. Since these differences were not directly a function of the chlorine, attention was focused on the effect of the chlorine treatment on the structural development at a given position. The micrographs in Figure 6 show samples taken from the center bottom position across the five levels of chlorine treatment. Subjective evaluation of these micrographs is based on differences observed in the starch granules and in the matrix development. It is difficult to quantify these differences. For example, it is impossible to measure the degree of

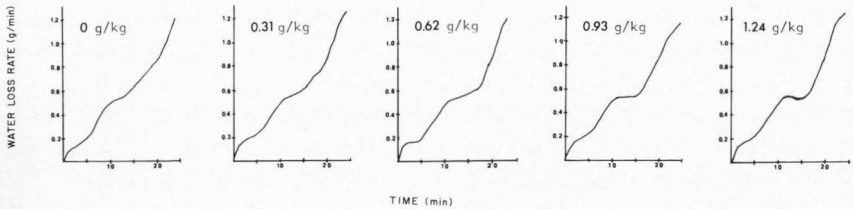

Fig. 5 Water loss rates as a function time for batters containing 0 to 1.24 g Cl_2/kg flour.

granule swelling during gelatinization because of the limited number of granules viewed and the natural size distribution of the granules. As the matrix becomes more developed, the individual granules become less distinguishable. For this reason, less attention will be given to the size of the granules than to the more obvious structural differences. In the untreated sample (Figure 6a), the extragranular material forms clumps on the surface and between the starch granules. The granules themselves are intact, but have an amorphous appearance. At the 0.31 g/kg level of treatment (Figure 6b), there is evidence of the matrix being more fully developed. This material is thought to be made up of a combination of solubilized starch-lipid-protein. This lipid-protein-solubilized starch material begins to form a more continuous network between the granules. The next increment of treatment 0.62 g/kg (Figure 6c) shows further development of the matrix. The granules are still intact but appear less distinct as they become more embedded within the matrix. The matrix material also seems to have a cementing effect. The increased association between granules results in a greater buildup of the structural units reflected in the more three-dimensional appearance of the structure compared to the two lower levels. At the commercial level of the treatment (Figure 6d), the starch granules become less distinct as the matrix becomes more extensive. The formation of the larger building blocks due to the cementing effect of the extragranular material is still evident. The 1.24 g/kg level (Figure 6e) shows yet more extensive covering, making it impossible to identify the embedded granular structures. From this series, a most obvious structural difference at the center bottom position is the increased development of the lipid-protein-solubilized starch matrix with increasing chlorine treatment. This then acts to cement the components into larger building block units which will ultimately influence the final cake structure. The micrograph in Figure 7 shows two SEM photographs taken at the middle position of the untreated and commercial level treatments. The information gained by the higher magnification supports the findings in the lower magnification (Fig. 6). In the untreated sample, the extragranular material appears in clumps among the granules. Structure of the cake must then rely more on granule-to-granule contact. At the commercial level the extragranular material now forms a more continuous layer along the edge of the granule. The granules are more separated but seem embedded in a more solid matrix; therefore, they do not appear to function as individual units but as components of the larger building block units.

Discussion

It appears that the chlorination of soft wheat cake flours may have several effects upon the functionality of these flours when incorporated into a batter system for cake formulation. It appears that particle size needs to be increased to an optimum size in order to give a better structure in the cake; however, it is not yet known if the increased size observed in the dry particles is responsible for the increased association of the components in the final cake. From the preliminary data on flour component chlorine uptake, there is indication that chlorine:sulfur ratio for the protein component is more responsive to increasing levels of chlorination than is the chlorine:potassium ratio in the starch component. If there is indeed preferential uptake of chlorine by the protein component in the chlorinated cake flour, this might explain, in part, the increase in the viscosity and coincides with extensive matrix development when either flour-water slurries or total batter components are heated. This would then account, in part, for the greater viscosity that one sees with the Brabender Amylograph measurements and with the Haake Rotoviscometer. It does not exclude, however, the possibility that chlorine could affect the starch itself by influencing the ability of the amylose to be leached out of the starch granule and to complex with the protein component of the flour. Therefore, the earlier increase in viscosity with chlorination may aid in better structural development during the baking process, resulting in maximum volume and contour, and in less shrinkage of the baked cakes. These indices of good cake structure (maximum contour and minimized shrinkage) are reversed when we exceed the commercial level of chlorine treatment of the flour. At this time, it is not obvious why this reversal should occur. Temperature profiles during the baking process do not seem to be affected by level of chlorination. In other words, at any moment in time during baking, temperatures in the different positions are similar whether the batters are made from treated or untreated flour. Some dramatic differences, however, are seen in the water loss characteristics during the baking process. These might be due to purely physical differences such as the increasing viscosity, which may impair the water movement out of the cake or to differences in crumb pore structure. The water loss characteristics may also reflect differences in starch gelatinization and/or protein denaturation patterns or complexing behavior that result from the response of starch lipid or protein fractions to chlorination and subsequent heating in the batter system. These changes could affect the water and energy requirements needed for these transitions and interactions to take place. However, at levels exceeding the commercial level of chlorine treatment, the rate of water loss still shows a local maximum in which the rate of water loss decreases for a short time period within the temperature range of the starch phase transitions. Why this happens is not well-defined or understood at this time. It might be that the overdevelopment of the matrix results in more of a barrier to the movement of water out of the system. Further experiments will need to be done in order to better evaluate the meaning of the water movement inhibition during the period of starch phase transitions, because prior to and after that period the rates of water loss appear similar.

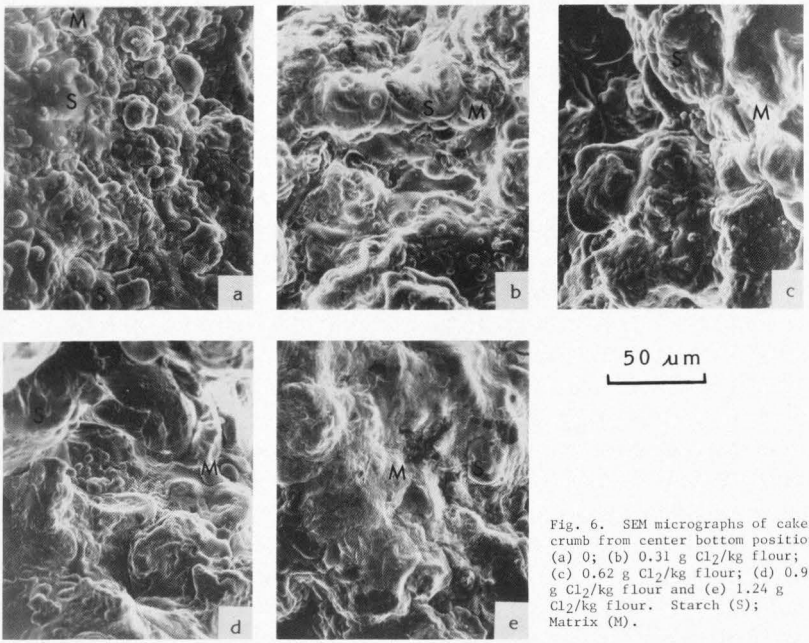

Fig. 6. SEM micrographs of cake crumb from center bottom position: (a) 0; (b) 0.31 g Cl_2/kg flour; (c) 0.62 g Cl_2/kg flour; (d) 0.93 g Cl_2/kg flour and (e) 1.24 g Cl_2/kg flour. Starch (S); Matrix (M).

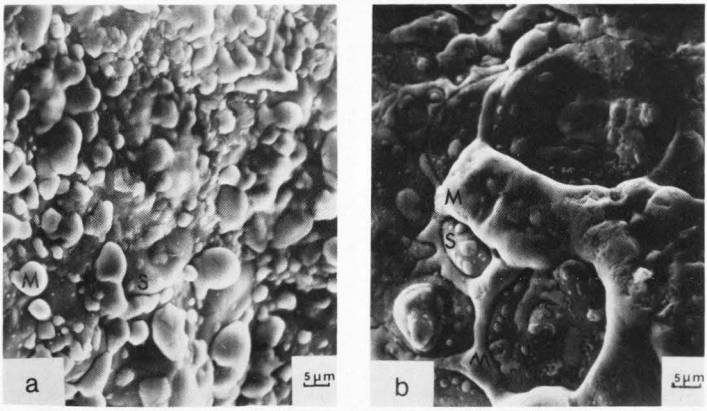

Fig. 7. SEM micrographs of middle position: (a) 0 g Cl_2/kg flour; (b) 0.93 g Cl_2/kg flour. Starch (S); Matrix (M).

Acknowledgements

This study was supported in part by the University of Minnesota Agricultural Experiment Station Projects No. 18-27 and 18-63 (Scientific Journal Article No. 13603). Appreciation is also expressed to General Mills, Inc., Minneapolis, MN 55426.

References

Allen JE (1977). A calorimetric and ultrastructural study of the effect of chlorine bleaching on wheat flour and wheat starch. Ph.D. Thesis. Cornell University, New York.

Gilles KA, Kaelble EF, Youngs VL (1964). X-ray spectrographic analysis of chlorine in bleached flour and its fractions. Cereal Chem. 41, 412-424.

Godsalve EW, Davis EA, Gordon J, Davis HT (1977). Water loss rates and temperature profiles of dry cooked muscles. J. Food Sci. 42, 1038-1045.

Gordon J, Davis EA, Timms EM (1979). Water loss rates and temperature profiles of cakes of different starch content baked in a controlled environment oven. Cereal Chem. 56, 50-57.

Hsu EE, Gordon J, Davis EA (1980). Water loss rates and scanning electron microscopy of model cake systems made with different emulsification systems. J. Food Sci. 45, 1234-1250, 1255.

Huang G, Finn JW, Varriano-Marston E (1982a). Flour chlorination. I. Chlorine location and quantification in air-classified fractions and physicochemical effects on starch. Cereal Chem. 59, 496-500.

Huang G, Finn JW, Varriano-Marston E (1982b). Flour chlorination. II. Effects on water binding. Cereal Chem. 59, 500-506.

Kissell LT, Donelson JR, Clements RL (1979). Functionality in white layer cake of lipids from untreated and chlorinated patent flours. I. Effect of free lipids. Cereal Chem. 56, 11-14.

Kulp K, Tsen CC, Daly CJ (1972). Effect of chlorine on the starch component of soft wheat. Cereal Chem. 49, 194-200.

Seguchi M, Matsuki J (1977). Studies on pan-cake baking. I. Effect of chlorination of flour on pan-cake qualities. Cereal Chem. 54, 287-299.

Nasir, MJ (1976). X-ray analysis without the need for standards. J. Microsc. 108, 79-87.

Sollars WF (1961). Chloride content of cake flours and flour fractions. Cereal Chem. 38, 487-500.

Trimbo HB, Ma Shao-mu, Miller BS (1966). Batter flow and ring formation in cake baking. Bakers Digest 40, (1)40-45.

Tsen CC, Kulp K, Daly CJ (1971). Effects of chlorine on flour proteins, dough properties, and cake quality. Cereal Chem. 48, 247-255.

Whistler RL, Mittag TW, Ingle RR (1966). Mechanism of starch depolymerization with chlorine. Cereal Chem. 43, 362-371.

Whistler RL, Pyler RE (1968). Action of chlorine on wheat flour polysaccharides. Cereal Chem. 45, 183-191.

Youngquist RW, Hughes DH, Smith JD (1969). Effect of chlorine on starch-lipid interactions. (Abstr.) Cereal Sci. Today 14, (3)90.

Discussion with Reviewers

R. Moss: Why do the readings of temperature and water loss rates stop at 23 minutes although the baking time is 25 minutes?

Authors: The design of the oven is such that there is a two minute lag-time during which the water vapor clears the oven and the wet-bulb, dry-bulb temperatures are recorded. The time scale is corrected for this, but the data for the last two minutes of baking cannot be recorded. For details, see Godsalve et al. (1977).

W.J. Wolf: Have you attempted to use TEM in these studies?

Authors: Yes, preliminary studies from unpublished freeze fracture data show that unheated starch granule surfaces from wheat flour that has been treated with 1.24 g/kg are smoother than those of starch granule surfaces from flour that has not been chlorine-treated. Generally speaking, the starch granule cross-sections from untreated and unheated granules appear to show a ridge around the circumference that support the surface granule observation. Also, after heating up to 102°C, the overall degree of swelling is not noticeably different between 0 and 1.24 g/kg chlorine treatment, although some lamellar-type layering seems to be present in the untreated starch granules as they swell. Further work is being done to verify these observations.

FOOD MICROSTRUCTURE, Vol. 2 (1983), pp. 161-163
SEM Inc., AMF O'Hare (Chicago), IL 60666 U.S.A.

STRANDED STRUCTURE DEVELOPMENT IN THERMALLY PRODUCED WHEY PROTEIN CONCENTRATE GEL

T. Beveridge*[1], L. Jones[2] and M. A. Tung[2]

[1]School of Food Science
Macdonald Campus of McGill University
Ste. Anne de Bellevue, Quebec, Canada
H9X 1C0
[2]Department of Food Science
University of British Columbia
Vancouver, British Columbia, Canada

*Present Address:
Agriculture Canada
Research Station
Summerland, British Columbia
V0H 1Z0, CANADA

Abstract

Scanning electron micrographs of thermally induced whey protein concentrate gels were taken. Sample preparation was accomplished by glutaraldehyde fixation, osmium tetroxide post-fixation and critical point dehydration. Stranded or beaded gel structures were observed on the external surface of a gas bubble, suggesting that a "string-of-beads" gel microstructure may result from bubble formation during thermal treatment.

Initial paper received July 22, 1983.
Final manuscript received October 26, 1983.
Direct inquiries to T. Beveridge.
Telephone number: 604-494-7711.

KEY WORDS: Protein Gel, Whey Protein, Structure Development, Bubble, Scanning Electron Microscopy

Introduction

Scanning electron microscopy (SEM) has become a standard technique for the examination of the microstructure of thermally formed protein gels (Kalab and Harwalkar, 1973; Hermansson, 1979; Yasui et. al., 1979). Generally, in critical point dried preparations, these gels have been observed to consist of a network of globular particles of aggregated protein, apparently adhering together. Occasionally, during the SEM examination of egg albumen and whey protein concentrate gels, areas were encountered which appeared as a "string-of-beads" entanglement of strands. Indeed, the appearance of bead strands is not uncommon in the literature (Hermansson, 1979; Yasui et. al., 1979) and it is possible that this forms the normal gel matrix. However, considerable variability in gel microstructure has been observed, and this paper offers a possible explanation for some of this variation.

Methods

Gels (22.8% w/w solids, room temperature) were formed from a commercial whey protein concentrate (WPC: Dairyland Products Inc., Savage, Minnesota, USA) containing 30.5% protein (N x 6.38), 9.5% moisture, 6.0% ash and $<$ 0.5% fat, as determined by standard methods (AOAC, 1975). Heating in a water bath for 30 min. at 90°C in screw-capped test tubes gelled the solutions. WPC gels were scalpel cut to approximately 2 x 2 x 4 mm pieces and fixed overnight in 4% glutaraldehyde in 0.07 M phosphate buffer, pH 7.0, followed by phosphate buffer rinse (0.07 M, pH 7.0, 3 x 10 min.). Osmium tetroxide fixation (1% OsO_4 in 0.07 M phosphate, pH 7, 3 x 10 min.) was followed by ethanol dehydration (50, 70, 80% in distilled deionized water, 5 min. each; 90% 2 x 10 min., 100%, 3 x 10 min.), then transferred to amylacetate (25, 50, 75% in ethanol, 10 min. each; 100%, 1 hr.). Critical point drying using liquid CO_2 completed the process. The dried pieces were fractured and mounted on aluminium stubs with epoxy glue and coated with gold-palladium alloy in a sputter coating device (Technics Inc., 7950 Cluny Court, Springfield, Virginia, USA). A Cambridge Stereoscan scanning

electron microscope operated at 20 kV was used to examine the gels.

Results and Discussion

Figure 1 shows a gas bubble which has been cut through with the scalpel during the initial specimen preparation. The view is on the cut edge of the piece and not the fractured surface and extensive scalpel damage on the cut edge around the gas bubble is obvious. Figure 2 is a magnified image of the inside surface of the gas bubble. The stranded, beaded or filamentous appearance of the gel formed at the bubble surface is evident. The features of figure 2 may be compared to those of figure 3, an image obtained from a fractured surface of gel, free of apparent bubbles. It is clear that the movement and stretching of developing coagulum in the region of a forming and expanding bubble combined with the surface tension forces at the interface can markedly influence gel ultrastructure.

The source of the gas responsible for bubble formation in the gels is unclear, but it may arise from gas occluded during solution preparation, evolution of dissolved gas during heating or steam generation. Also unclear is how numerous the bubbles are and to what extent they develop during gel formation because the WPC solutions are themselves very cloudy, almost opaque. Observations of the formation of thermally induced protein gels of 5-6% egg albumen at pH 9 suggest that bubbles could be quite numerous and extensively developed. In opalescent albumen systems, many small bubbles could be seen forming throughout the gel during heating over 30 min. Larger bubbles formed at the test tube wall and all bubbles disappeared on cooling. The possible physical or chemical effects of gas evolving within thermally gelling protein systems have not been discussed by other workers in this field. Certainly the extent of sulphydryl oxidation in heated protein solutions depends upon the amount and nature of the gas present (Beveridge and Arntfield, 1979). The evolution of gas in the developing structural matrix could also substantially influence the perceived rheological properties of the gels.

References

A.O.A.C. (1975). Official Methods of the Association of Official Analytical Chemists. 12th edition. Association of Official Analytical Chemists. P.O. Box 540, Benjamin Franklin Station, Washington, D.C. 20044, USA.

Beveridge T, Arntfield S. (1979). Heat induced changes in sulphydryl levels in egg white. Can. Inst. Food Sci. Technol. J.; 12: 173-176.

Hermansson AM. (1979). Aggregation and Denaturation Involved in Gel Formation in Functionality and Protein Structure. A. Pour-El (ed.) ACS Symposium Series. American Chemical Society. Washington, D.C.; 92: 81-103.

Kalab M, Harwalkar, VR. (1973). Milk gel structures I. Application of scanning electron microscopy to milk and other food gels. J. Dairy Sci.; 56: 835-842.

Yasui T, Ishioraski M, Wakano H, Samejima K. (1979). Changes in shear modules, ultrastructure and spin-spin relaxation times of water associated with heat induced gelation of myosin. J. Food Sci.; 44: 1201-1204.

Discussion with Reviewers

D. N. Holcomb: Why were such large (2 x 2 x 4 mm) specimens used? Are the authors sure that the fixatives penetrated throughout the specimens?

Authors: The samples were of convenient size for handling. Adequate fixative penetration was not a problem since a uniform yellow color was noted on the cross-section of freshly trimmed, glutaraldehyde fixed specimens and a uniform black-gray color was seen on fractured surfaces of osmium post-fixed specimens. Protein gels of this type seem quite porous and allow rapid fixative penetration.

M. Kalab: Was the whey protein concentrate degassed (e.g., by lowering the pressure) and did this treatment affect the incidence of the gas bubbles?

Authors: The solutions of whey protein concentrate were not degassed. The observations reported here were made during studies relating rheological, chemical and ultrastructural properties of protein gels (Beveridge et. al., J. Agric. Fd. Chem., in press) and were not pursued further. Since it is probable that dissolved gases are a major source of gas for bubble formation, it is likely degassing will affect gas bubble incidence.

M. Kalab: What happened to the protein matrix at the test tube wall where gas bubbles were evident at 90°C but vanished after cooling? Were there any signs of the string-of-beads structure where the bubbles had been or was such a structure observed only around permanent bubbles? What was the consistency of the whey protein concentrate at 90°C before cooling? Was it already a gel (holding the shape of the container) or a highly viscous liquid which actually settled on cooling? (This question is closely associated with the previous one because it is aimed at finding out whether the beaded structures originated at 90°C or during cooling.)

Authors: We cannot answer the first questions since the specimens were scalpel cut from the central portion of the thermally produced gel, specifically to avoid "artifacts" generated by possible interactions between the test tube wall and the gelling protein. At the time of preparation, the possibility of bubbles producing structure within the gel was not considered. The gelled whey protein concentrate at 90°C is sufficiently stiff to hold the container shape on inversion, however, the possibility of flow

(bubble disappearance) on cooling cannot be eliminated. It seems likely that the structures observed here originate at 90°C and are fixed on cooling. Obtaining definitive answers will require experiments designed to study the effects of bubble formation on ultrastructure modification rather than the simple observation reported here.

D.N. Holcomb: Figure 1 has scratches or some similar defect. Perhaps the authors have an unblemished copy or the Figure could be trimmed to elimate the "scratches".
Authors: The defects are "scratches" on the negatives. Since the number of pictures available are limited and cropping this one would eliminate the edge of the bubble, the decision was taken to go "warts and all" rather than lose the image of the bubble.

M. Kalab: The incidence of the permanent gas bubbles in the gel would be easy to demonstrate by freezing the fixed and dehydrated (in absolute ethanol) samples, fracturing them, melting in absolute ethanol, CPD, and SEM. Would you please show a micrograph of a characteristic fracture and indicate the average bubble diameter?
Authors: The resources to do this are not available. Care should be taken when examining a fractured surface for gas bubbles. Since it is likely that the fracture would pass through the bubble, this could occur at any level of the bubble, and with an irregular edge. It may not be obvious that the structure imaged was once on the surface of a bubble.

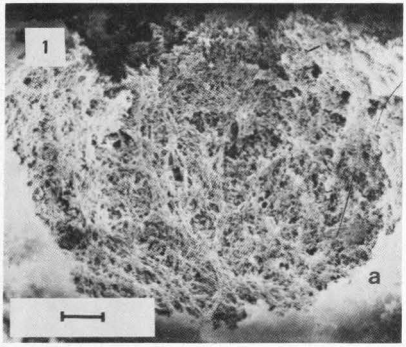

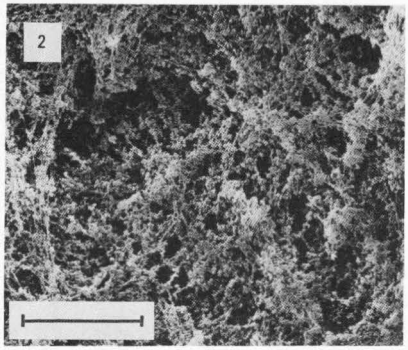

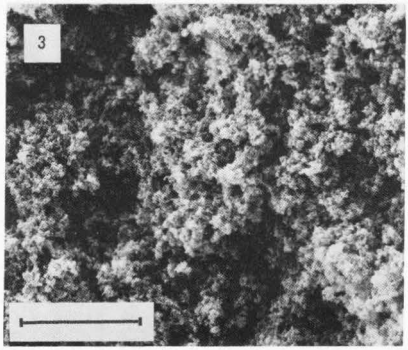

Fig. 1. Scanning electron micrograph of structure on the surface of a gas bubble formed in heat-induced whey protein concentrate gel. a: cut edge of bubble damaged by scalpel. Bar represents 50 microns.
Fig. 2. Detail of the central area of Fig. 1 showing stringed microstructure. Bar represents 50 microns.
Fig. 3. Microstructure of whey protein concentrate gel on fractured surface, remote from gas bubbles. Bar represent 50 microns. Note the magnification of Figs. 2 and 3 are the same.

FOOD MICROSTRUCTURE, Vol. 2 (1983), pp. 165-173
SEM Inc., AMF O'Hare (Chicago), IL 60666 U.S.A.

THE EFFECTS OF COMMERCIAL PROCESSING ON THE STRUCTURE AND MICROCHEMICAL ORGANIZATION OF RAPESEED

S.H. Yiu[1,2], I. Altosaar[1] and R.G. Fulcher[3]

[1]Department of Biochemistry, University of Ottawa, Ottawa, Ontario, K1N 9B4
[2]Present Address: Food Research Institute, Agriculture Canada, Ottawa, Ontario, K1A 0C6
[3]Ottawa Research Station, Agriculture Canada, Ottawa, Ontario, K1A 0C6

Abstract

Rapeseed samples collected from different processing stages were obtained from one commercial crushing plant for the present investigation. The samples included (A) whole seeds, (B) flaked seeds, (C) press cakes, (D) solvent extracted meal, (E) desolventized meal and (F) cooled, desolventized meal. Frozen and/or glycol methacrylate-embedded sections of the samples were examined using the techniques of fluorescence microscopy. Mechanical crushing tended to disrupt cell walls. After cooking and expeller pressing, individual protein bodies fused to form large masses encompassing phytin-containing globoids. Storage lipids also coalesced into larger droplets. Most of the oil was removed after solvent extraction and was absent inside cotyledon cells after desolventization. The final meal product contained primarily hull and cotyledon fragments. The cotyledon fragments consisted of an amorphous protein matrix embedded with phytin globoids and supported by a network of broken cell walls. The structural and microchemical organization of the hull were not much affected by the processing. Phenolic compounds, mucilage, cell wall polysaccharides, chlorophyll, storage proteins and lipids could be detected by various fluorescence microscopic techniques.

Initial paper received August 21, 1983.
Final manuscript received November 2, 1983.
Direct inquiries to S.H. Yiu.
Telephone number: 613-995-3700.

KEY WORDS: Rapeseed, Processing Effects, Structure, Microchemical Organization, Flake, Press Cake, Meal.

Introduction

One of the most important aspects in oilseed and cereal grain processing is quality control. Knowledge of the effects of processing on the structure and chemical composition of the end product is essential for establishing parameters associated with good quality. In rapeseed processing, most of the quality evaluation studies have focussed mainly on the chemical aspects of rapeseed oil and meal (Rutkowski, 1970; Ohlson, 1976; Sosulski and Zadernowski, 1981). The effects of processing on structural changes at the cellular level were also studied by means of electron microscopy (Hofsten, 1974; Stanley et al., 1976; Mills and Chong, 1977; Smith, 1979). Recently, fluorescence microscopic techniques have been adapted to analyze the structural and microchemical organization of cereal grains (Fulcher and Wong, 1980) and rapeseed (Poon et al., 1980; Yiu et al., 1982). Specific and sensitive markers and an improved epi-illuminating system of the microscope coupled with the relative rapid preparation (frozen sections) and staining procedures have made fluorescence microscopy an indispensable analytical tool. These techniques (Yui et al., 1982) not only reveal fine cellular structure but also their chemical constituents. Hence, they are particularly suitable for rapid screening of seed samples and related products.

The present study investigated the effects of processing on the storage reserves of rapeseed and products derived therefrom using fluorescence microscopy. The objectives of the project were to study cellular changes due to cell wall rupture during crushing and the effects of processing on the extractability of some of the chemical constituents including proteins, chlorophyll, oil, mucilage, phytate and phenolic compounds.

Materials and Methods

Rapeseed Samples

Samples of rapeseeds of mixed Canola (of low erucic acid and glucosinolate contents) varieties (*Brassica campestris* L. and *Brassica napus* L.),

flakes, cakes and meals were collected after different stages of processing (Fig. 1) from one commercial crushing plant where the prepress solvent extraction procedure was used. Four batches of such samples were obtained at various occasions between October and November, 1981. More than two separate specimen blocks were prepared from each sample for either frozen or glycol methacrylate-embedded sections. A total of 500 sections from each sample were obtained for fluorescence microscopic analysis.

Frozen Sections

To facilitate frozen sectioning whole seed samples were usually fixed in 3% glutaraldehyde in 0.025M potassium phosphate buffer, pH 7.2, at 4°C for 12 hours prior to freezing. Samples of flaked seeds were not fixed. Fixed or unfixed samples were immersed in a drop of embedding medium for frozen sections (Tissue-Tek II C.T. Compound, Lab-Tek Products, Miles Laboratories, Inc., Naperville, Illinois) on a specimen holder. The holder was immediately frozen in dry ice (solid CO_2) and transferred to a cryostat microtome (S.L.E.E. Co. Ltd., London S.E. 13, England). Sections 4-8 μm in thickness were cut at -15°C to -20°C and placed on glass slides pre-coated with 1% gelatin.

Glycol Methacrylate (GMA)-embedded Sections

Samples other than whole seeds or flakes were first suspended in molten 2% agar in a petri dish. The sample thus embedded in agar was cut into 1-2 mm^3 blocks and subsequently fixed, dehydrated and embedded as described previously (Fulcher and Wong, 1980). Briefly, tissues were fixed in the glutaraldehyde fixative as mentioned in the previous section for 24-48 hours. They were then dehydrated through methyl cellosolve, ethanol, n-propanol and n-butanol and infiltrated with GMA monomer for 3-5 days prior to polymerization at 60°C in gelatine capsules. Sections were cut 1-5 μm thick on an ultramicrotome (Sorvall Inc., Newtown, Connecticut) using glass knives and were affixed to glass slides for subsequent examination.

Microscopic Examinations

Sections were examined with a Zeiss Universal Research Microscope (Carl Zeiss Ltd., Montreal) equipped with both a conventional bright-field illuminating system and a III RS epi-illuminating condenser combined with an HBO 200 W mercury-arc illuminator for fluorescence analysis. The III RS condenser contained three fluorescence filter combinations each with a dichromatic beam splitter and an exciter/barrier filter set with maximum transmission at 365 nm/>418 nm (FC I), 450-490 nm/>520 nm (FC II) and 546 nm/>590 nm (FC III). Photomicrographs were obtained using 35 mm Kodak Tri-X Pan film or Ektachrome 400 Daylight film. Specimens were photographed unstained to demonstrate autofluorescent substances or after one of the following staining procedures.

Staining Procedures

Storage Lipids Major storage lipid reserves were detected using methods described by Fulcher and Wong (1980). Frozen sections were stained with 0.01% (w/v) aqueous Nile Blue A (Eastman Kodak Co., Rochester, N.Y.) for 60 seconds. Stained sections were rinsed and mounted in water under a coverslip and examined microscopically using the FC II filter system.

Storage Proteins GMA-embedded sections were stained with 0.001% (w/v) aqueous 1-anilino-8-naphthalene sulfonic acid (ANS) (Fisher Scientific Co., Fairlawn, N.J.) for 1-2 minutes. ANS imparts intense blue fluorescence to storage protein bodies when viewed with FC I.

Phytin GMA-embedded sections were stained with 0.01% (w/v) aqueous Acriflavine-HCl (Matheson, Coleman and Bell Manufacturing Chemists, Norwood, Ohio), pH 3.1, for 15 minutes. After rinsing and drying, sections were mounted in immersion oil and viewed with FC III.

Cell Wall Carbohydrates and Mucilage GMA-embedded sections were stained either with 0.01% (w/v) aqueous Calcofluor White M2R New (American Cyanamid Co., Bound Brook, N.J.) or 0.01% (w/v) aqueous Congo Red (Fisher Scientific Co., Fairlawn, N.J.) for 1-2 minutes. Stained sections were examined using FC I for Calcofluor White and FC III for Congo Red.

Phenolics Many phenolic compounds emit blue autofluorescence under short wavelength excitation. Unstained frozen or GMA-embedded sections were mounted in non-fluorescent immersion oil and examined microscopically using filter system FC I. To enhance autofluorescence, sections were exposed to ammonia vapour, mounted in oil and examined immediately.

Chlorophyll Chlorophyll emits red fluorescence under long wavelength excitation. Frozen sections were mounted in 95% aqueous glycerol and examined microscopically using filter system FC III.

Results

Rapeseed samples collected for the present study included: (A) whole seeds; (B) flaked seeds; (C) press cakes; (D) solvent extracted meal; (E) desolventized meal; and (F) cooled, desolventized meal. A simplified schema of rapeseed processing depicting stages from which samples were collected for the present study is shown in Figure 1.

Whole Seeds

The whole seed sample collected from each processing batch was used as a control for subsequent studies. The mature rapeseed consists of the hull (seed coat), the endosperm and a large embryo (consisting of a radicle and two conduplicate cotyledons). Figure 2 illustrates the structural organization of a rapeseed. The

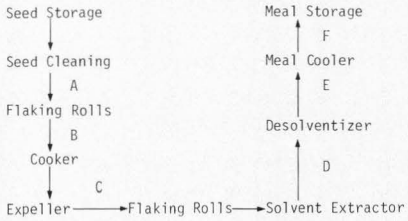

Fig. 1 A simplified schematic flow chart of rapeseed meal processing (Clandinin, 1981) showing stages from which samples (A) whole seeds, (B) flaked seeds, (C) press cakes, (D) solvent extracted meal, (E) desolventized meal and (F) cooled, desolventized meal were collected.

hull consists of an epidermal layer, a subepidermal layer, a thick palisade layer and a pigment layer. All except the palisade layer emit blue autofluorescence under short wavelength excitation indicating the presence of low molecular weight plant phenolic components (Fulcher et al., 1972; Harris and Hartley, 1976). The rapeseed endosperm consists of an aleurone cell layer and a hyaline layer of crushed parenchyma cells. Protein bodies containing phytin globoids and oil droplets are present inside cells of the aleurone layer, the cotyledons and the radicle. A diagrammatic presentation of the above structures is shown in Fig. 3.

Color Micrographs

For convenience the color micrographs are presented in Figs. 4-11, and are discussed in the following paragraphs.

Flaked Seeds

Flaked seeds were collected immediately after the flaking rolls, but before the cooking stage. Microscopic examination of the resulting mixture of hull and cotyledon fragments showed the effect of mechanical pressure on some of the cellular components. Transverse fractures of the cell wall were seen in many cotyledonary cells. At higher magnification and using a combination of two staining procedures (ANS/Calcofluor White), detailed structures of protein bodies and the cell wall were revealed. Due to the fractured cell wall, protein bodies from one cell were seen protruding into the cavity of adjacent cells (Fig. 4). Phytin globoids were clearly visible indicating that the mechanical force had little effect on the structural and chemical organization of the rapeseed storage protein. The structure of oil bodies was also unaffected by the flaking process although oil droplets were no longer confined within individual cells.

Press Cakes

Cooking and expeller pressing (Fig. 1) induced considerable changes to the structural organization of the flaked materials. Most noticeable were the decreased number of oil droplets and the emergence of larger oil bodies within the cell as revealed by the Nile Blue A staining (Fig. 5). Additional fractures of the cell wall were observed when sections were stained with Calcofluor White (Fig. 6) or Congo Red (Fig. not shown) and examined microscopically. Although phytin globoids remained intact inside the protein structure, individual protein bodies were no longer recognizable. Instead, they aggregated to form single masses (Fig. 7). The stainability of the protein masses was reduced indicating that the effect of

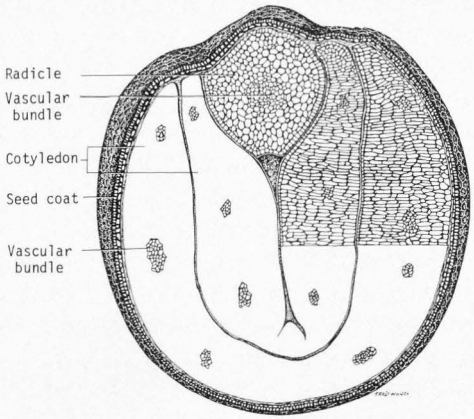

Fig. 2 Line drawing of the structural organization of a whole rapeseed

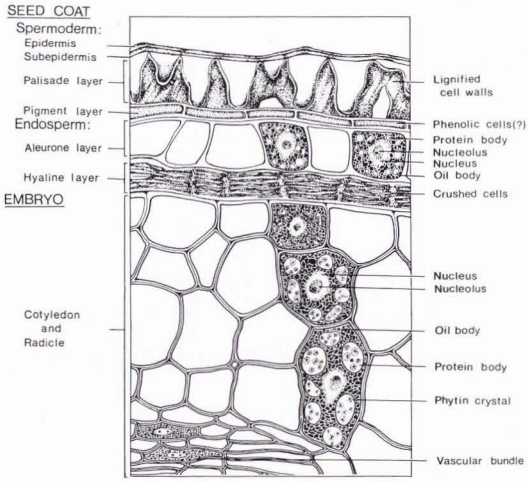

Fig. 3 (Left) Line drawing of the detailed structural and microchemical organizations of rapeseed.

processing might have altered the affinity between certain functional groups of the protein and ANS.

Solvent Extracted Meal

The apparent difference between these samples and those collected from the preceding stages was the colour appearance. While both the flake and oil cake were yellowish-brown in colour, reflecting the original dark seed coat and yellow cotyledon, the dried meal coming out from the solvent extractor was chalky white with black flecks. Examination of the meal under the microscope revealed it to be devoid of oil bodies after staining with Nile Blue A (Fig. not shown). Occasionally, a small amount of residual oil could be seen trapped between the cells. A matrix composed mainly of protein was shown by the ANS staining (Fig. 8) and phytin globoids were still present inside the protein structure.

Desolventized Meal

In contrast to the meal obtained after solvent extraction, the meal coming out from the desolventizers was dark brown in colour. The only oil present in the meal was seen within the aleurone cell layer which remained attached to the hull after flaking (Fig. 9). The structural components of the hull were relatively unchanged with

(Legends for figures on the opposite page)

Fig. 4. Flaked seed section stained with ANS and Calcofluor White demonstrating fractured cell walls (arrows) with a protein body (*) protruding from one cell into another. Photographed using FC I.

Fig. 5 Rapeseed press cake section stained with Nile Blue A showing coalesced oil bodies (arrows). Photographed using FC II.

Fig. 6 Calcofluor White stained rapeseed press cake section demonstrating the presence of channeled cell walls. Photographed using FC I.

Fig. 7 Press cake section stained with ANS and Calcofluor White showing fractured cell walls (arrows) and fused protein body masses (*). Photographed using FC I.

Fig. 8 Solvent extracted rapeseed meal section stained with ANS to show fused protein bodies (*). Photographed using FC I.

Fig. 9 Desolventized rapeseed meal section stained with Nile Blue A showing hull fragments with residual oil bodies (arrows) and cotyledon pieces (C). Photographed using FC II.

Fig. 10 Cooled, desolventized rapeseed meal section stained with Calcofluor White showing a network of broken cell walls. Photographed using FC I.

Fig. 11 Unstained, unprocessed green rapeseed section demonstrating chloroplasts (arrows) within cotyledonary cells (C). Photographed using FC II.

(Scale bars on the micrographs represent μm)

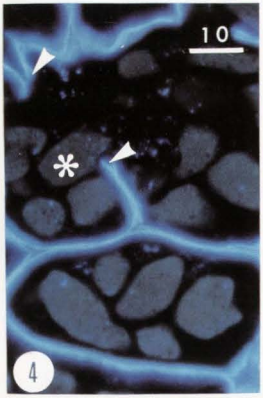
10
4

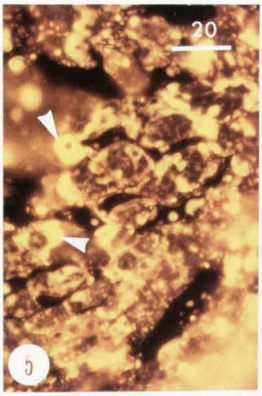
20
5

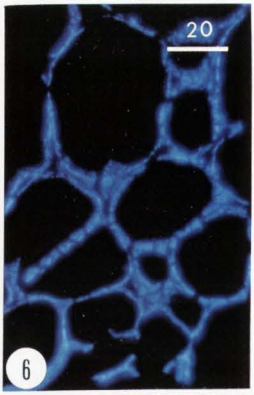
20
6

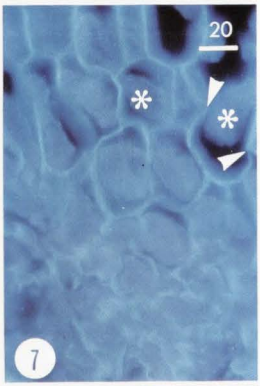
20
7

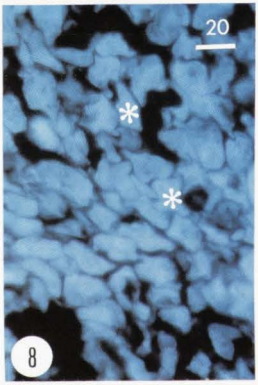
20
8

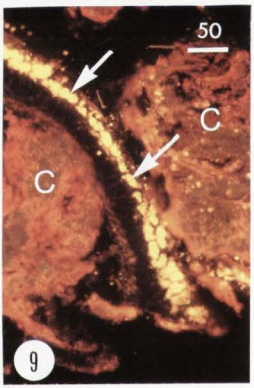
50
C
C
9

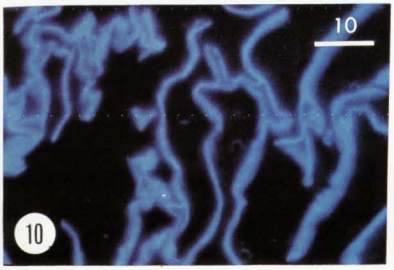
10
10

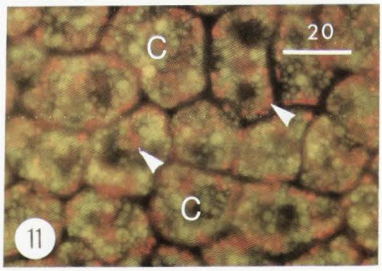
C
20
C
11

protein masses remaining inside cells of the aleurone layer. Storage proteins of the cotyledon were now further compressed to form a homogeneous protein matrix still embedded with intact phytin globoids (Fig. 12). Additional coalescence of protein masses was probably due to the effect of steaming used during desolventization.

Cooled, Desolventized Meal

After solvent stripping and toasting, the meal is cooled and put into storage, ready for marketing. The most obvious difference between this final stored product and the meal coming out from the desolventizers is its texture. The former is finer in quality than the latter. However, under the microscope little difference was observed between the two. The final meal contained fragments, many of which consist of a protein matrix supported by a network of broken cell walls (Fig. 10). Detailed structures were revealed at higher magnification. The fusion of individual protein bodies had left behind vacuoles or an entire empty space within the cell surrounded by the remaining cell wall (Fig. 13). Phytin globoids were clearly visible in the protein matrix after staining with Acriflavine-HCl (Fig. 13).

In general, storage lipids were no longer detected within the cell except in fragments containing parts of the aleurone layer. Most of the seed coat layers and walls of the aleurone cells remained intact after processing. The autofluorescent characteristic (under short wavelength excitation using FC I) of some of the seed coat layers (Fig. 14) remained unchanged indicating the retention of phenolic compounds in

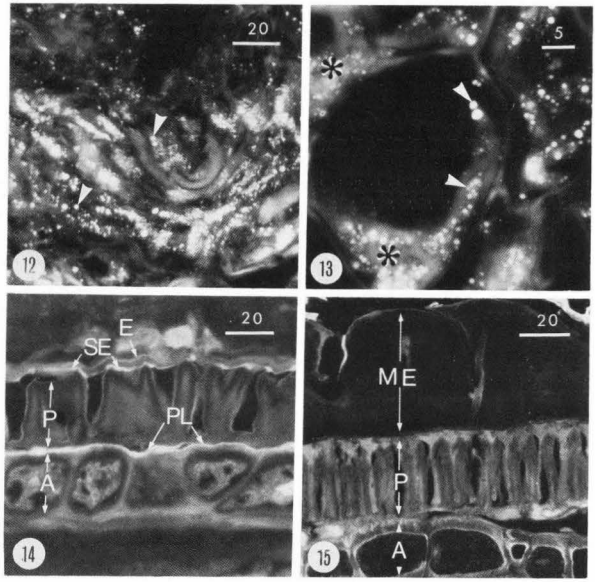

Fig. 12 Desolventized meal section stained with Acriflavine-HCl demonstrating phytin globoids (arrows) within the protein matrix. Photographed using FC III.
Fig. 13 Acriflavine-HCl stained rapeseed meal (cooled and desolventized) section demonstrating fused protein masses (*) embedded with residual phytin globoids (arrows). Photographed using FC III.
Fig. 14 Unstained rapeseed meal (cooled and desolventized) section showing the autofluorescent sub-epidermis (SE) and pigment layer (PL) in addition to the epidermis (E) palisade layer (P) and aleurone layer (A). Photographed using FC I.
Fig. 15 Congo Red stained Canola meal (cooled and desolventized) section showing the mucilagenous epidermis (ME), the palisade layer (P) and aleurone layer (A). Photographed using FC III.
(Scale bars on the micrographs represent μm)

the hull. Occasionally, red autofluorescent bodies could be detected (using FC II or FC III) within cells of the aleurone layer demonstrating the presence of chloroplasts. Normally, chlorophyll is found in cells of the aleurone layer and the cotyledons of green rapeseed (Fig. 11). The absence of chlorophyll in the cotyledon fragments of rapeseed meal suggested that either very few green seeds were processed in these particular batches or that the chlorophyll was removed by processing. Mucilage, which is normally present in the epidermis of some yellow seed coated rapeseed varieties such as Candle, could be detected occasionally by staining the meal with either Calcofluor white or Congo Red (Fig. 15).

Discussion

This study revealed that mechanical processing such as crushing mainly affected the structure of cell walls (Fig. 4). Individual protein and oil bodies remained intact after crushing. However, cooking and expeller pressing did alter the structures of these major storage reserves of rapeseeds. Protein bodies fused to form one single mass (Fig. 7) and oil droplets coalesced to become larger bodies (Fig. 5). The above observations are similar to those found by Smith (1979). Rapeseed oil bodies within the cotyledon were successfully removed by the prepress solvent extraction procedure whereas the denatured protein bodies remained unaffected. Heating rapeseed with minimum moisture content at low to medium temperature (below 110°C) for a short time has little effect on the bioavailability of certain essential amino acids such as lysine (Clandinin, 1981). Even though denaturation of protein takes place during processing, it may increase the nutritive value of the meal by making the protein more readily assimilable. The extent of protein denaturation in the samples used for the present investigation could not be determined by the fluorescence microscope. However, it is known that the temperatures used for processing rapeseed meal would not diminish the nutritive value of the protein (Clandinin, 1981). The present investigation also revealed that phytin still remained associated with the denatured protein mass (Figs. 12 and 13). The negative effect of phytate on the bioavailability of minerals is well documented (McCane et al., 1943; Davies and Nightingale, 1975). Rapeseed phytate was shown to cause zinc deficiency in the rat (Jones, 1979). Improved processing techniques will be required to obtain a rapeseed meal of relatively low phytin content.

The presence of phenolic compounds and lignin in rapeseed hull has been demonstrated by microscopic techniques (Yiu et al., 1982) as well as chemical assays (Theander et al., 1977; Vose, 1974). Phenolic compounds are known to have deleterious effects on the bioavailability of certain essential amino acids such as lysine and methionine as well as the colour and flavour of rapeseed meal (Sosulski, 1979). The present microscopic examinations revealed that the prepress solvent extraction procedures removed few phenolic compounds from rapeseed hull (Fig. 14) and had little effect on modifying its structural (cell wall) components. The persistent components partially account for the high fibre content of rapeseed hull, thus indirectly decreasing the nutritive value and palatability of rapeseed meal. The increasing popularity of the yellow seed coated variety, Candle, might lead to another set of problems. The mucilage content of Candle seed coats (Fig. 15) may induce additional processing cost as well as the risk of fungal infection (Schans et al., 1982) possibly resulting in reduced storage ability of the meal. Chlorophyll was not detected in cells of the cotyledon but was present in some of the intact aleurone cells associated with the hull of green rapeseeds. The presence of chlorophyll in rapeseed oil suggested that this cellular component was extracted by the chemical procedure. The fractured cell walls as seen in figure 4 would have facilitated the process.

In a previous study, it was demonstrated that some rapeseed meal fragments still contained intact cells full of oil droplets even at the final stage of the processing (Yiu et al., 1982). Indeed, a similar phenomenon has been observed in this study. Cells with intact walls encompassing their cellular contents were found among some of the hull and cotyledon fragments. Intact cell walls would undoubtedly reduce the availability of internal nutrients. The ratio of intact cells to broken cells estimated in the meal samples was not high but could be sufficient to cause a lower yield of the oil and a reduced nutritive value of the meal. Hence, efficiency of processing should be checked on a constant basis to establish good quality control of the final product. The fluorescence microscope, with its analytical diversity, has proven to be a convenient tool to serve such a function.

Acknowledgements

We are grateful to Abigail Brumell for her technical assistance, Fred Wong for the line drawings and Dr. H. Poon for his previous contribution to this project. This research was funded in part by a Canola Council of Canada (Canola Utilization Assistance Grant 82-31) and in part by Agriculture Canada research contract OSU80-00280. This presentation is contribution 557 from Food Research Institute and 721 from Ottawa Research Station, Agriculture Canada, in Ottawa.

References

Clandinin DR. (1981). In *"Canola Meal for Livestock and Poultry"*. Canola Council of Canada. Winnipeg, Manitoba. Publication No. 59. p. 5-7.

Davies NT, Nightingale R. (1975). The effects of phytate on intestinal absorption and secretion of zinc, and whole-body retention of Zn, copper, iron and manganese in rats. Br. J. Nutr. 34: 243-258.

Fulcher RG, O'Brien TP, Lee JW. (1972).

Studies on the aleurone layer. 1. Conventional and fluorescence microscopy of the cell wall with emphasis on phenolcarbohydrate complexes in wheat. Aust. J. Biol. Sci. 25: 23-24.

Fulcher RG, Wong SI. (1980). Inside Cereals - A fluorescence microchemical view. In *"Cereals for Food and Beverages"* (G.E. Inglett and L. Munk, eds.). Recent Advances in Chemistry and Technology. Academic Press, New York, p. 1-25.

Harris PJ, Hartley RD. (1976). Detection of bound ferulic acid in cell walls of the Gramineae by ultraviolet fluorescence microscopy. Nat. 259: 508-510.

Hofsten AV. (1974). The ultrastructure of seed of some Brassica species - new source of seed protein. Svensk. Bot. Tidskr. 68: 153-163.

Jones JD. (1979). Rapeseed protein concentrate preparation and evaluation. J. Am. Oil Chem. Soc. 56: 716-721.

McCane RA, Edgecombe CA, Widdonson EM. (1943). Phytic acid and iron absorption. Lancet 2: 126-128.

Mills JT, Chong J. (1977). Ultrastructure and mineral distribution in heat-damaged rapeseed. Can. J. Plant Sci. 57: 21-34.

Ohlson JSR. (1976). Processing effects on oil quality. J. Am. Oil Chem. Soc. 53: 299-301.

Poon NH, Fulcher RG, Altosaar I. (1980). Rapeseed microchemistry. In *"Analytical Chemistry of Rapeseed and its Products"*. Canola Council of Canada, Winnipeg, Manitoba. p. 143-152.

Rutkowski A. (1970). Effect of processing on the chemical composition of rapeseed meal. Proceedings: Intern. Rapeseed Conference, Ste. Adélè, Québec, Canada. (Rapeseed Assoc. of Canada, Pubs., Winnipeg, Manitoba) p. 496-515.

Schans J, Mills JT, Van Caeseele L. (1982). Fluorescence Microscopy of Rapeseeds Invaded by Fungi. Phytopathology 72: 1582-1586.

Smith CG. (1979). Oil Seeds. In *"Food Microscopy"* (Vaughan, J.G., ed.). Acad. Press, London. p. 35-74.

Sosulski F. (1979). Organoleptic and nutritional effects of phenolic compounds on oilseed protein products: A review. J. Am. Oil Chem. Soc. 56: 711-715.

Sosulski F, Zadernowski R. (1981). Fractionation of rapeseed meal into flour and hull components. J. Am. Oil Chem. Soc. 58: 96-98.

Stanley DW, Gill TA, deMan JM, Tung MA. (1976). Microstructure of rapeseed. Can. Inst. Food Sci. Technol. J. 9: 54-60.

Theander O, Aman P, Miksche GG, Yasuda S. (1977). Carbohydrates, polyphenols, and lignin in seed hulls of different colors from turnip rapeseed. J. Agric. Food Chem. 25: 270-273.

Vose JR. (1974). Chemical and physical studies of mustard and rapeseed coats. Cereal Chem. 51: 658-665.

Yiu SH, Poon NH, Fulcher RG, Altosaar I. (1982). The microscopic structure and chemistry of rapeseed and its products. Food Microstructure 1(2): 135-143.

Discussion with Reviewers

D.W. Irving: Prior to freezing, were the fixed samples rinsed in buffer or frozen directly from the fixative?
Authors: The fixed samples were frozen directly from the fixative.

D.W. Irving: Could it be that one of the factors involved in reduced stainability of protein masses with subsequent processing is because the protein is not as "concentrated," i.e. it's spread out over a larger surface area?
Authors: Yes, it could be possible. However, one cannot determine if protein concentration contributes to the cause since it is difficult to measure protein quantity microscopically.

D.W. Irving: Relating to presence of phenolic compounds in the seed coat, would it be possible or feasible to mill the rapeseed to remove the seed coat prior to oil processing?
Authors: Yes, it is feasible to dehull the seed prior to processing. However, the step is usually omitted because it subsequently lowers the yields of both oil and protein.

J.T. Mills: Could the transverse fractures of the cell wall seen in the flake samples be artifacts induced by sectioning?
Authors: No, they could not be because the sample was embedded in glycol methacrylate and the pattern of damage was not consistent throughout the entire section.

J.T. Mills: How do you know that the transversed fractures of the cell wall seen in the press cake sample are not pits?
Authors: It is possible that these are pits. However, pits tend to be more uniform in organization. We are currently investigating the detailed structure of rapeseed cell wall.

FOOD MICROSTRUCTURE, Vol. 2 (1983), pp. 175-181
SEM Inc., AMF O'Hare (Chicago), IL 60666 U.S.A.

MICROSTRUCTURE OF WINGED BEANS

K. SAIO, Y. NAKANO* AND S. UEMOTO**
National Food Research Institute,
Ministry of Agriculture, Forestry and Fisheries,
Tsukuba, Ibaraki 305, Japan

*Present address: Central Research Laboratory, Ajinomoto Co. Ltd.,
Kawasaki, Kanagawa 210, Japan

**Kyushu University, Hakozaki, Fukuoka-city 812, Japan

Abstract

Microstructures of seven plant introductions of winged beans (*Psophocarpus tetragonolobus*) produced in Okinawa, Japan were investigated. In cotyledonary cells of winged beans, protein bodies plus numerous lipid bodies were distributed in a cytoplasmic network. Starch granules were often found in some introductions but rarely in others. All seven introductions had very thick cell walls. The high protein, fat and hemicellulose contents of winged beans are consistent with the numerous protein bodies, lipid bodies and thick cell walls in the mature cotyledonary cells. The cell walls contained a number of depressions or cavities 1 to 2 μm deep which frequently occurred opposite complementary pits in adjacent cells (presumably pit-pairs). Plasmodesmata traverse the cell walls in the pit-pairs. In order to determine changes during development, cultivar UPS-32 cultivated at Fukuoka-city was used. In cotyledonary cells at 30 days after flowering, cell walls which had pit-pairs with plasmodesmata, developing amyloplasts with starch granules, vacuoles with dense flocculent materials, tubular rough endoplasmic reticulum, mitochondria etc., were observed but no protein bodies or lipid bodies were apparent. Protein bodies and lipid bodies were, however, found at 45 days after flowering. Cotyledonary cells at 45 days contained many starch granules but mature seeds contained few, if any.

Initial paper received January 3, 1983.
Final manuscript received September 17, 1983.
Direct inquiries to K. Saio.
Telephone number: 02975-6-8051.

Key Words: winged bean, Psophocarpus tetragonolobus, cotyledonary cell, protein body, lipid body, cell wall, pit-pairs, plasmodesmata, maturation, electron microscopy

Introduction

Winged beans (*Psophocarpus tetragonolobus*) are indigenous to Papua New Guinea and Southeast Asia but are attracting attention elsewhere as a potential food resource because of their high protein and fat contents. In their tropical and subtropical regions of origin, they are cultivated in domestic gardens and are consumed in immature stages as a vegetable for table use. Not only the seeds but also the pods, leaves, flowers, stems and tubers of winged beans are edible. Research on food use of mature seeds is still under investigation and a few trials to make foods have been reported (1, 4, 8). It is known that the hard structure of the beans is unfavourable for food processing (7) but there are few reports on the ultrastructure of this potentially important legume (10).

Materials and Methods

In the first experiment, we examined mature seeds of seven plant introductions (PIs) which were introduced and cultivated by the Okinawa Branch, Tropical Agriculture Research Center. The Center designated the PIs 001, 002 and so on in the order in which they were introduced. The beans used were of the 1978 crop. Their characteristics are listed in Table 1.

Table 1:
Characteristics of winged beans introduced and cultivated by the Okinawa Branch, Tropical Agriculture Research Center

Plant introduction (PI)	Country of origin	Cultivar (strain)	Beginning of flowering	Average time of maturation
001	Indonesia	local	Oct. 30	middle of Feb.
002	Indonesia	No.902	Nov. 17	beg. of Mar.
003	Indonesia	No.909	Nov. 9	beg. of Mar.
004	Indonesia	No.1126a	Oct. 15	middle of Jan.
007	Nigeria	TPT-2	Oct.29	middle of Feb.
012	Papua New Guinea	UPS-122	Oct. 26	end of Dec.
013	Okinawa	local	Nov. 1	beg. of Feb.

Data from Takada (9)

In the second experiment, cv. UPS-32 introduced from Papua New Guinea and cultivated in 1979 at

Fukuoka-city, Japan, was used to determine changes during development. Samples at 30, 45 and 58 days after flowering (DAF) were studied. Seed was sown in the greenhouse on July 15 and began to flower on October 14. Maturation was assumed at the time of complete browning and drying of the pods.

Soybeans used for comparative analysis of carbohydrate fractions were of the IOM type (grown in Indiana, Ohio and Michigan) imported from the United States.

Preparation of microscopic specimens

Small pieces of cotyledonary tissue were cut out with a razor blade, fixed with 5% glutaraldehyde solution and then with 1% osmium tetroxide solution (both in phosphate buffer containing 5% sucrose, pH 6.7), dehydrated with a graded acetone series (40 to 100%) and embedded in Epon resin.

For the light microscope (LM) the block prepared as described above was sliced to about 1 µm thickness with an LKB Ultratome and affixed on a glass slide. Protein was stained with 0.5% solution of Coomassie Brilliant Blue in 7% acetic acid and 50% methanol and then decolorized with 7% acetic acid and 50% methanol. Lipids were stained with a saturated solution of Sudan Black B in 50% ethanol and polysaccharides were detected with Schiff's reagent after oxidation with 0.5% periodic acid solution.

For the transmission electron microscope (TEM, JEM 100-B or JEM EX-1200), the same block used for LM was ultrathin-sliced and stained with saturated uranyl acetate solution and then saturated lead acetate solution in ethanol which was filtered just before staining.

Analysis of chemical components

PI 003 (Table 1) was used for chemical analysis. Moisture content was measured by drying at 105°C for 4 hours. Crude protein was determined by the Kjeldahl method (N x 6.25) and crude fat was measured by Soxhlet extraction with ethyl ether for 16 hours, drying in vacuum at 50°C and weighing. Ash was determined by heating in a muffle furnace at 550°C overnight. Crude fiber was measured after hydrolysis with 25% HCl and then with 25% NaOH, each for 3 hours.

The fractionation of polysaccharides was as follows (6): The beans were ground and extracted with n-hexane. The defatted powder was extracted with cold water and centrifuged. The residue from the centrifugation was extracted with boiling water and again centrifuged. The residue was dried and weighed (A). A was treated with sodium hypochlorite solution (100 µl of acetic acid and 750 mg of sodium chlorate were added to 50 ml of water at 75°C), filtered and washed through a glass filter, dried and weighed (B). B was treated with 10% NaOH solution for 18 to 24 hours with stirring, centrifuged, washed, dried and weighed (C). C was ashed at 900°C and weighed (D). Lignin was calculated as A - B, hemicellulose as B - C and cellulose as C - D. To compare with the values for winged beans, polysaccharides in soybeans were fractionated by the same method.

Results

Figure 1 shows LM-images of sections of mature seeds of seven PIs stained with Coomassie Brilliant Blue. The cotyledonary cells of all 7 PIs contained many protein bodies. On the other hand, the cell sections of PI 003 contained 2 to 4 protein bodies that were 6 to 8 µm in diameter plus many protein bodies that were only 2 to 3 µm in diameter; the protein bodies were nearly circular in shape. In PIs 001, 004, 007 and 013 numerous protein bodies, which were 3 to 4 µm in diameter, filled each cell and their shapes were slightly distorted. In PIs 002 and 012, the number and shape of protein bodies were rather similar to PI 003.

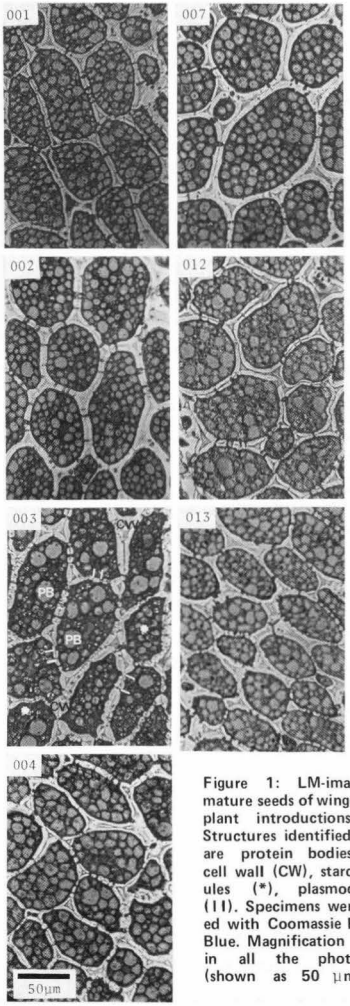

Figure 1: LM-images of mature seeds of winged bean plant introductions (PIs). Structures identified in 003 are protein bodies (PB), cell wall (CW), starch granules (*), plasmodesmata (||). Specimens were stained with Coomassie Brilliant Blue. Magnification is same in all the photographs (shown as 50 µm bar.)

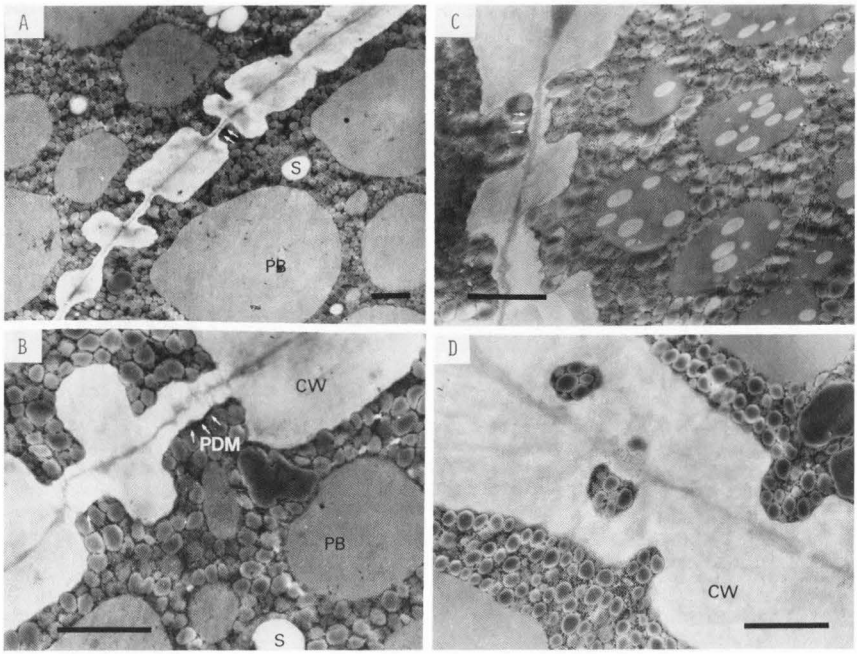

Figure 2: TEM-images of winged bean PI 003 (A,B) and PI 007 (C,D). Micrographs show protein bodies (PB), cell walls (CW), starch granules (S), lipid bodies (LB) and plasmodesmata (PDM, white arrows). Photograph C shows electron translucent inclusions in protein bodies. Bar in each photograph represents 2 µm.

Sudan Black B stained the cytoplasmic network and periodic acid-Schiff reagent stained the cell walls and starch granules. In PI 003 each cell section contained 10 to 20 starch granules which were 1 to 2 µm in diameter, whereas the other PIs contained hardly any starch granules. All PIs had cell walls 1 to 10 µm thick which included many depressions or cavities.

Figure 2 shows TEM-images of PIs 003 and 007 which were previously observed to be different under LM. The cytoplasmic portion stained with Sudan Black B contained numerous lipid bodies which were 0.4 to 0.7 µm in diameter. Protein bodies generally had no inclusions but in some cells they contained ovoid structures of low electron density (Fig. 2-C). There appeared to be a cell-to-cell variation in the distribution of these inclusions. The cell walls contained a number of depressions or cavities 1 to 2 µm deep which frequently occurred opposite complementary pits in adjacent cells (Figs. 2-A and 2-B). These paired depressions or cavities presumably are pit-pairs (3). The pit-pairs were filled with cytoplasm and the cell walls in these regions were less than 1 µm thick. Plasmodesmata traverse the cell walls in the pit-pairs (Figs. 2-A, 2-B and 2-C). Figure 2-D is an example of pits that do not oppose each other in the walls of two neighboring cells.

Table 2 summarizes the chemical composition of PI 003 and the content of polysaccharides fractionated from it. The high contents of crude protein and fat support the abundant occurrence of protein bodies and lipid bodies, respectively. The high content of

Table 2; Chemical composition of winged bean seeds (PI 003) and polysaccharide data for soybeans[a]

	Winged beans (%)	Soybeans (%)
moisture	10.43	
crude protein	34.89	
crude fat	17.70	
ash	3.86	
crude fiber	7.65	
total carbohydrate	27.42	
lignin	3.2	1.3
hemicellulose	25.3	8.2
cellulose	9.4	7.5

a: all values on dry basis except moisture

polysaccharides in winged beans corresponds to their thick cell wall structure but hemicellulose was extraordinarily dominant, when compared with that in soybeans.

LM-images of cotyledonary cells of winged beans of cv. UPS-32 cultivated at Fukuoka-city harvested at 30, 45, and 58 DAF are shown in Figure 3. At 30 DAF, cells were still less than 50 μm in diameter; they contained several vacuoles and small starch granules but no protein bodies. Nuclei stained with periodic acid-Schiff reagent were often observed and some were seen undergoing cell division. At 45 DAF cell size and thickness of cell walls had developed to the same extent as those at 58 DAF (mature seed), being about 100 μm in diameter and 1 to 10 μm thick, respectively. Pit-pairs were clearly recognized even under the LM. The cotyledonary cells at 45 DAF contained numerous starch granules and protein bodies of different sizes (1 to 30 μm). At 58 DAF starch granules were hardly to be found and protein bodies of nearly uniform size (5 to 10 μm) filled the cells.

Figures 4 and 5 show TEM-images of cotyledonary cells of winged beans harvested at 30 and 45 DAF, respectively. In Fig. 4-A are shown cell walls which have pit-pairs with plasmodesmata, amyloplasts with starch granules and several vacuoles. Dense flocculent materials were dispersed in most of the vacuoles but appeared coagulated in some cells as shown in Fig. 4-D. In Fig. 4-B (enlarged portion of Fig. 4A) the cytoplasm contained numerous ribosomes, tubular rough endoplasmic reticulum, dictyosomes (arrows) and dense bodies (*). Numerous mitochondria (arrows) were found (Fig. 4-C). The developing amyloplast in Fig. 4-E exhibited thylacoids (arrows). In the 45 DAF sample (Fig. 5-A), protein bodies and lipid bodies were already observed but many starch granules still remained. Plasmodesmata were observed through the center of a pit-pair as shown in Fig. 5-B.

Discussion

As far as the seven introductions of mature winged beans used were concerned, the microstructures of their cotyledonary cells were rather similar. Using the same samples, Yanagi et al. (11) found that the proteins of winged beans consisted of fractions of about 3S and 6 to 7S (main storage protein) by ultracentrifugal analysis and that no significant differences between introductions existed except for differences in the 3S fraction. The numerous protein bodies and lipid bodies in the mature cotyledonary cells are consistent with the high protein and fat contents of the seeds. The protein content of winged beans was comparable to that of soybeans but hemicellulose of winged beans was much higher than for soybeans as shown in Table 2. The plasmodesmata were characteristically found between pit-pairs which had pores connecting adjacent cells. They were observed in mature seeds but were also found at 30 and 45 DAF in cv. UPS-32 used to determine changes during development. It is also noteworthy that starch granules increased at 45 DAF and decreased again at 58 DAF, compared to the changes in starch content of ripening soybeans. In the latter period of maturation protein bodies appeared to become more uniform in size and starch granules rapidly decreased. The slight difference in microstructure of PI 003 might be connected with variations in maturation.

The maturity of winged beans seems to vary with cultivation conditions. As reported by Data and Pratt (2), winged beans of PI 007 which were sown in September and flowered from early December to the end of the following March reached maximum pod size at 20 to 22 DAF, maximum pod fresh weight at about 25 DAF, maximum seed size at about 30 DAF and maximum seed fresh weight at about 45 DAF. Pods, pedicels and seeds were completely dried after 60 DAF. On the other

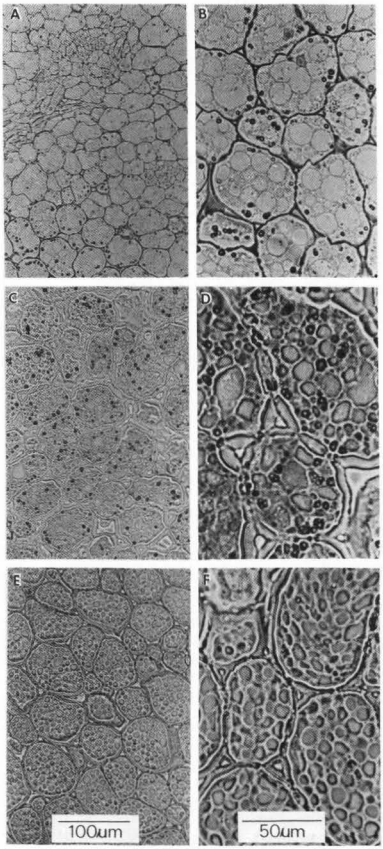

Figure 3: LM-images of cv. UPS-32 harvested at 30 (A, B), 45 (C,D), and 58 (E,F) DAF. The photographs were taken after staining with periodic acid-Schiff reagent.

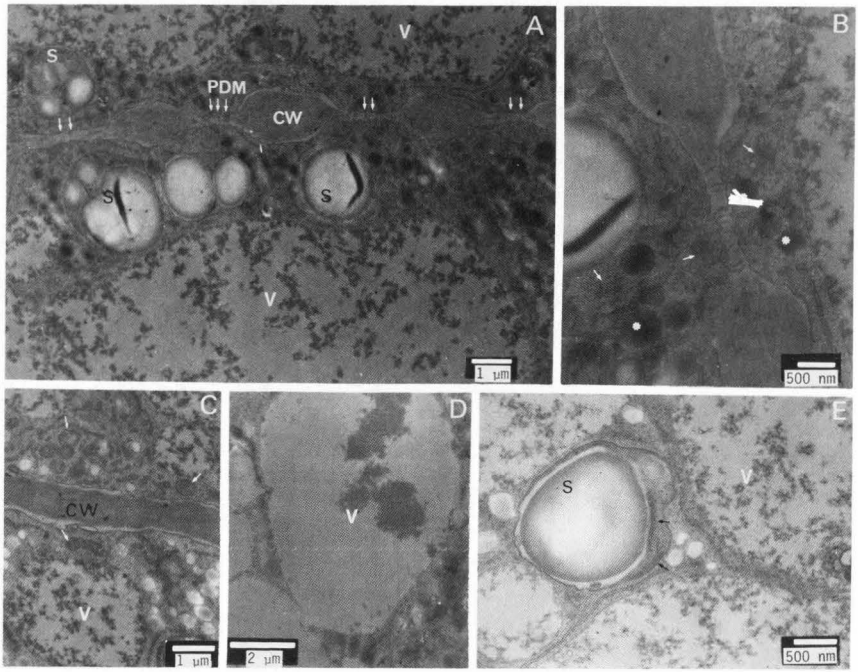

Figure 4: TEM-images of cv. UPS-32 harvested at 30 DAF. A shows pit-pairs with plasmodesmata (PDM, white arrows), cell wall (CW), starch granules (S) and vacuoles (V). B is a higher magnification of a part of A, showing a pit-pair with PDM in the center, dense bodies (*), dictyosomes (white arrows), starch granules and vacuoles. C shows vacuoles and a number of mitochondria (white arrows) and electron translucent bodies. D shows vacuoles in which dense flocculent materials are coagulated, being different from other vacuoles (A, B, C and E). E shows a developing amyloplast in which a starch granule and thylacoids (black arrows) are observed. All micrographs show tubular rough endoplasmic reticulum surrounding vacuoles.

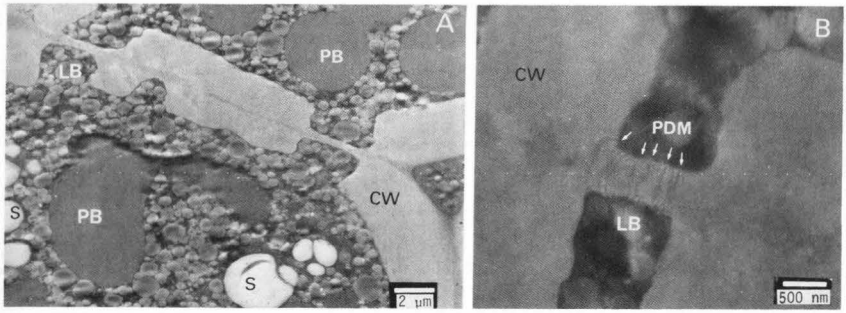

Figure 5: TEM-images of cv. UPS-32 harvested at 45 DAF. A shows pit-pairs of cell wall (CW), protein bodies (PB) and starch (S). Cytoplasm is filled with lipid bodies (LB). B shows a pit-pair with plasmodesmata (PDM).

hand, Kadam et al. (5) collected the pods of 40, 50, 60 and 70 day old plants and completely matured pods of 80 to 85 day old plants. Takada (9) reported that the cultivars in Okinawa that were sown on May 11 flowered from early October to November (120 to 150 days) and matured at 70 to 90 DAF. However, the ones sown on August 17 flowered from early December to the following March (60 to 90 days) and matured at 60 to 100 DAF. Data and Pratt (2) emphasized that winged beans (probably green pods for table use) must be harvested no later than 20 DAF for fresh use because after 20 DAF fiber development increases and tissues become too tough. Kadam et al. (5) showed that the cooking time of the seeds increased gradually until plants were 70 days old and rapidly increased at maturity (80 to 85 days). Cv. UPS-32 which was cultivated at Fukuoka-city in a temperate zone and under the extremely long day for these beans was sown on July 15, flowered from October 14 (about 90 days) and matured at 58 DAF. These seeds at 45 DAF had tough cell walls.

TEM-images of cv. UPS-32 at 30 DAF (Fig. 4) show a morphological change of cellular constituents which may be involved in the formation of protein bodies, lipid bodies and starch granules in cotyledonary cells. However, we do not refer to this question and a systematic fine structural investigation of these constituents during development will be reported in our progressing work.

Acknowledgement

The authors sincerely thank Dr. H. Takada of the Tropical Agriculture Research Center for his kind gift of the winged bean samples.

References

1. Claydon A. (1981). The winged bean as a commercial vegetable food, in: 2nd International Seminar of Winged Beans, W. Herath (ed.), International Dambala (Wing Bean) Inst., Colombo, Sri Lanka (in press).

2. Data E S, Pratt H K. (1980). Patterns of pod growth, development and respiration in the winged bean (*Psophocarpus tetragonolobus*), Trop. Agric. (Trinidad) **57**, 309-317.

3. Esau K. (1960). Anatomy of seed plants, John Wiley and Sons, New York, 32-35.

4. Gandjar I. (1978). Fermentation of the winged bean seeds, The Winged Bean **1**, 330-334.

5. Kadam S S, Kute L S, Lawande K M and Salunkhe D K. (1982). Changes in chemical composition of winged beans (*Psophocarpus tetragonolobus L.*) during seed development, J. Food Sci. **47**, 2051-2057.

6. Kainuma K, Sasaki T. (1982). Food Analysis, Korin Press, Tokyo, 230.

7. Omachi M, Ishak E, Homma S and Fujimaki M. (1983). Manufacturing of tofu from winged bean and the effect of presoaking the bean on cooking. Nippon Shokuhin Kogyo Gakkaishi **30**, 216-220.

8. Shurtleff W R. Household preparation of winged bean tempeh, tofu, milk, miso and sprouts, The Winged Bean, Philippine Council for Agriculture, Los Banos, 335-339.

9. Takada H. (1977). Introduction of new crop, winged beans. Nettai Noken Shuho **31**, 58-63.

10. Varriano-Marston E, Beleia A and Lai C C. (1983). Structural characteristics and fatty acid composition of *Psophocarpus tetragonolobus* seeds, Ann. Bot. **51**, 631-640.

11. Yanagi S, Yoshida N and Saio K. (1983). Generality and diversity of winged bean (*Psophocarpus tetragonolobus*) protein in eight various lines. Agric. Biol. Chem. **47**, 2267-2272.

Discussion with Reviewers

C. Bair: Would you care to speculate on the nature of the low electron dense inclusions you observed in the protein bodies of winged beans? (Fig. 2C). In my investigations of soybeans I frequently found inclusions similar to those reported here. The inclusions not only varied in size and distribution, but also in electron density. There appeared to be a cell-to-cell (or tissue-to-tissue) variation in the distribution of these inclusions. Most of the inclusions were electron translucent, but some contained electron dense or scattered electron dense materials. X-ray microprobe analysis of these electron dense inclusions revealed a high level of phosphorus, and was believed to be the storage site of phytate.

Authors: In these experiments, we found the low electron dense inclusions but not electron dense ones in the protein bodies. But Saio et al. (1977) have observed electron dense inclusions in the protein bodies of sunflower and they were rich in phosphorus as determined by X-ray microprobe analysis. We agree with your opinion that they may be storage sites for phytate.

C. Bair: How do you explain the difference in the electron density of the lipid bodies shown in Figs. 2 and 5? Those in Fig. 2 are electron dense while those observed in Fig. 5 are electron translucent.

Authors: We have also observed differences in the degree of electron density of lipid bodies. Whenever we used lead nitrate in alkaline pH for electron staining, lipid bodies became electron translucent. Lead acetate used in these experiments made lipid bodies of soybean very electron dense, while those of winged bean were partly translucent (we did the two experiments the same way and at the same time). Saio et al. (1980). have also found that electron density decreased after storage of the seeds, using soybeans. We are not sure that it was caused by differences of quality of lipids.

C. Bair: Fig. 4B shows a considerable amount of electron dense materials scattered throughout the cytoplasm. Upon closer examination, they appear to be in close association with or originating from the rough endoplasmic reticulum. Could this be spherosomal or lipid body development? Numerous other researchers working with various tissues have reported that spherosomes originate from enlarged fragments of the endoplasmic reticulum.

Authors: We are now investigating the fine structural changes of winged beans during development in more detail, using UPS-45 or -99 harvested every 5 days. Consequently, we do not have any comments to make about spherosome development at this time.

C. A. Newell: Since winged beans are quite similar in seed composition to the soybean, how does the microstructure of developing cotyledons in the winged bean compare with those of soybeans? And how does the winged bean compare with other legume seeds in which such studies have been done?

Authors: We have not yet examined the microstructure of developing soybean cotyledons but plan to do so in the future and are also interested in comparative studies on other legumes. In developing seeds of *Vicia faba*, Harris (1979) and Adler and Müntz (1983) reported on development of endoplasmic reticulum or protein bodies. And Baumgartner et al. (1980) described localization of reserve protein in endoplasmic reticulum of *Phaseolus vulgaris*. Bergfeld et al. (1980) also reported on formation of protein bodies in *Sinapis alba L*. Concerning soybeans, Bils and Howell (1963) worked on developing soybean cotyledons and recently Thorne (1981) reported on the morphology and ultrastructure of soybean seed tissues and N. Kaizuma (Univ. of Iwate, Japan) presented papers at the annual meetings of the Japanese Association of Breeding in 1981, 1982 and 1983 on genetical studies on protein body development in soybean cotyledon cells (Kaizuma and Kasai 1981; Sato et al. 1982; Kaizuma and Sato 1983; Kamatsuda et al. 1983).

C. A. Newell: The authors have pointed out the thickness of the cell walls in winged bean cotyledons. How do these compare with other legume seeds? If winged bean cotyledonary cells do have much thicker walls than hitherto found for legumes generally, is there any particular adaptive significance to this characteristic?

Authors: In the regions lacking pit-pairs, the cell walls of winged beans are 5 to 10 times thicker than those found in soybeans and several Phaseolus species that we have examined. Some varieties of lupine (*Lupinus mutabilis*) seeds, however, also have very thick cell walls (unpublished data). We are not aware of any particular adaptive significance for thick cell walls in winged beans.

Additional References

Adler K, Muntz K. (1983). Origin and development of protein bodies in cotyledons of *Vicia faba*: Proposal for a uniform mechanism, Planta **157**, 401-410.

Baumgartner B, Tokuyasu K T and Chrispeels M J. (1980). Immunocytochemical localization of reserve protein in the endoplasmic reticulum of developing bean (*Phaseolus vulgaris*) cotyledons, Planta **150**, 419-425.

Bergfeld R, Kuhnl T and Schopfer P. (1980). Formation of protein storage bodies during embryogenesis in cotyledons of *Sinapis alba* L, Planta **148**, 146-156.

Bils R F, Howell R W. (1963). Biochemical and cytological changes in developing soybean cotyledons, Crop Sci. **3**, 304-308.

Bils R F, Howell R W. (1960). Biochemistry and cytology of developing soybean cotyledons, Proceedings of the Plant Physiology Meeting xviii.

Harris N. (1979). Endoplasmic reticulum in developing seeds of *Vicia faba*: A high voltage electron microscope study, Planta **146**, 63-69.

Kaizuma N, Kasai A. (1981). On the morphology of protein body and spherosome in soybean cotyledon cell, Japan. J. Breed. **31**, suppl. 1, 222-223.

Kaizuma N, Sato Y. (1983). Genetical studies on protein body development in soybean cotyledon cells, protein molecule species contained in nucleo-globules and incorporation of T^3 - leucine into them, Japan. J. Breed. **33**, suppl. 1, 320-321.

Kamatsuda T, Kaizuma N and Kitamura K. (1983). Genetical studies on protein body development in soybean cotyledon cells: Electrophoretic protein analysis of the globular body isolated from cotyledon cells in early maturating stage, Japan. J. Breed. **33**, suppl. 2, 16-17.

Saio K, Gallant D and Petit L. (1977). Electron microscope research on sunflower protein bodies, Cereal Chem. **54**, 1171-1181.

Saio K, Baba K. (1980). Microscopic observation on soybean structural changes in storage, Nippon Shokuhin Kogyo Gakkaishi **27**, 343-347.

Sato Y, Kaizuma N and Kitamura K. (1982). Genetical studies on protein body development in soybean cotyledon cells: Isolation and characterization of RNA-body, Japan. J. Breed. **32**, suppl. 1, 94-95.

Thorne J H. (1981). Morphology and ultrastructure of maternal seed tissues of soybean in relation to the import of photosynthate, Plant Physiol. **67**, 1016-1025.

FOOD MICROSTRUCTURE, Vol. 2 (1983), pp. 183-188
SEM Inc., AMF O'Hare (Chicago), IL 60666 U.S.A.

ß-GLUCANS IN THE CARYOPSIS OF *SORGHUM BICOLOR* (L.) MOENCH

C.F. Earp[1], C.A. Doherty[1], R.G. Fulcher[2] and L.W. Rooney[1]

[1]Cereal Quality Lab, Department of Soil and Crop Sciences, Texas A&M University, College Station, Texas 77843-2474; [2]Agriculture Canada Research Station, Cereal Section - ORS, Ottawa, Ontario CANADA K1A 0C6

Abstract

Fluorescence microscopy was used to determine the location of ß-glucans in sorghum. Sections from three genetically different sorghum cultivars were stained with Calcofluor or Congo Red, fluorochromes which have been reported to react with ß-glucans. Autofluorescence, indicative of ferulic acid in other cereals, was observed in untreated sections. When stained sections were treated with endo-ß-glucanase, fluorescence was reduced or entirely eliminated in pericarp, aleurone and endosperm cell walls. ß-Glucans were isolated from the endosperm of three sorghum cultivars. When reacted with the two dyes, Calcofluor or Congo Red, precipitates formed immediately, a reaction which is similar to that produced by mixed linkage ß-glucans from other cereals.

Initial paper received August 29, 1983.
Final manuscript received November 10, 1983.
Direct inquiries to C.F. Earp.
Telephone number: 409-845-2925.

KEY WORDS: Fluorescence microscopy, ß-glucans, Sorghum bicolor, cell walls, fluorochromes, autofluorescence

Introduction

ß-Glucans are high molecular weight polymers comprised primarily of ß 1,3 and 1,4 linked glucopyranosyl units. The presence of mixed linkage 1,3 and 1,4 ß-glucans has been reported in the endosperm of barley (Anderson et al 1978; Wood et al 1977), oats (Wood et al 1977; Wood and Fulcher 1978), wheat (Fulcher and Wong 1980) and sorghum (Woolard et al 1976, 1977). During the brewing process, the presence of high levels of barley ß-glucans can cause viscosity problems in the wort or beer (Ducroo and Delecourt 1972). In South Africa, sorghum beer is a major industry, making sorghum ß-glucans of particular interest. In the preparation of the African food tô (a porridge-like product), differences in stickiness have been documented by Da et al (1982). It is possible that the stickiness characteristic may be due in part to ß-glucans.

Calcofluor White M2R New, an optical brightener, was used by Hughes and McCully (1975) as a stain for cell walls of higher plants. Wood and Fulcher (1978) reported that the optical brightener Calcofluor White M2R New caused intense fluorescence in barley endosperm cell walls, a major component of which is a mixed linkage ß1,3:1,4 glucan. A similar fluorescence in the endosperm cell walls occurred when sections were stained with Congo Red. Wood and Fulcher (1978) characterized a relatively specific reaction in which both Congo Red and Calcofluor precipitated mixed linkage ß-glucan from oats and barley. In further studies of this reaction, Wood (1980a) reported that the strongest reaction occurred with polysaccharides containing "contiguous (1→4) ß-linked D-glucopyranosyl units, such as cereal ß-D-glucans, xyloglucan and substituted celluloses." Wood (1980b) demonstrated a difference in precipitation curves of the oat and barley ß-glucan which he believed to be due to differences in molecular weight of the two ß-glucans.

Work at Carlsberg Research Center by Gibbons (1981) and Aastrup et al (1981) has taken the basic research of Wood and Fulcher and applied this information to an industrial setting. Half kernels of barley are mounted in a modeling clay template, stained with Calcofluor and viewed in the Malt Modification Analyser developed at Carlsberg (Munck et al 1978). As cell wall

breakdown occurs, fluorescence is lost and the degree of modification in the endosperm can be expressed as % loss of fluorescence in the cell walls. The modified kernels are compared to a standard set of modified kernels.

The purpose of the work presented here was to locate and identify sorghum mixed-linkage β-glucans whose occurrence has previously been reported (Woolard et al 1976, 1977). Because the first step in germination is the breakdown of cell walls, cell wall structure of the pericarp and endosperm is important in germination studies. Therefore, identification of cell wall components could lead to a better understanding of the germination or malting process. This type of information can also aid in the comparison of sorghum kernel structure to that of other cereals. Fluorescence microscopy was used in this study to determine the location of β-glucans in sorghum. Sections were stained with either Calcofluor or Congo Red, two fluorochromes which have been reported to be specific for mixed linkage β-glucans. Fluorescence microscopy has also been used in a number of other studies to locate a wide range of specific compounds in cereals (Fulcher 1982; Fulcher and Wong 1980; Gibbons 1981) and oilseeds (Yiu et al 1982). Many phenolic compounds, such as ferulic acid, fluoresce in the blue region of the spectrum. This autofluorescence is produced when the compound is subjected to ultraviolet light and is not caused by any stain or fluorochrome. Ferulic acid has been identified as a cell wall component in wheat (Fulcher et al 1972; Fausch et al 1963) barley and oats (Fulcher and Wong, 1980), and other Gramineae family members (Harris and Hartley, 1976). Earp et al (1983) documented autofluorescence in sorghum. HPLC analysis of cell wall extracts according to the method of Hahn et al (1983), also suggested that ferulic and coumaric acids were the major phenolic acids in the cell walls of the three sorghum cultivars.

Materials and Methods

Samples

Three sorghum cultivars were selected to typify differences in genetic diversity. The genetics of the three varieties as currently understood are presented below.

BTx3197 ($RRyyb_1b_1B_2B_2SS$) a thick, white pericarp and no pigmented testa.

Early Hegari ($RRyyB_1B_1B_2B_2ss$) a thick, white pericarp and a pigmented testa.

ATx623 X SC0103-12 ($RRYyB_1B_1b_1B_2B_2SS$) a thick, brown pericarp sorghum (genetically red) with a pigmented testa and a dominant spreader.

All samples were grown at Halfway, Texas in the Texas Agricultural Experiment Station Nursery in 1980.

Fixation and Embedding

Mature sorghum kernels were cut in halves or quarters with a sharp xylene cleaned razor blade. The half kernels were fixed in 3% glutaraldehyde in a 0.025 M phosphate buffer (pH-6.8) for 48 hr at 4°C. Fixed specimens were dehydrated and then embedded in glycol methacrylate according to the procedure of Feder and O'Brien (1968).

Fluorescence Microscopy

Glycol methacrylate sections of ~1 µm were treated with Calcofluor (Biofluor, Calbiochem-Behring Corp., La Jolla, CA.) (0.01% w/v) in distilled water for 1 min or with Congo Red (0.1% w/v) in distilled water for 5 min. Excess stain was removed by washing with distilled water. Sections were air-dried, mounted in immersion oil and viewed with a Zeiss Universal Research Microscope equipped with a IIIRS epi-illuminator system and a 100W mercury arc lamp. Untreated sections and those stained with Calcofluor were examined with an exciter filter and a barrier filter combination (FC I) with maximum transmissions of 365 and > 418 nm, respectively. The exciter and barrier filters combination III (FC III) with maximum transmissions of 546nm and > 590 nm respectively were used in viewing fluorescence produced by Congo Red interactions.

Enzyme Treatment of Sections

Endo-1,3(4) β-D-glucanase from Bacillus subtilis was provided by the Department of Plant Science, University of Manitoba. The enzyme showed no activity towards starch, carboxymethyl cellulose, arabinoxylan or xylan. Only trace enzyme activity with laminaran was observed. When assayed with lichenin, β-glucanase activity was measured as 108 units/ml with 1 unit = 1 µmole equivalent glucose released per minute under assay conditions. The enzyme was diluted 1:10 for microscopic use. Sections were treated with β-glucanase overnight at room temperature.

β-Glucan Isolation

Sorghum varieties were pearled using a Udy decorticating mill (Udy Corp., Fort Collins, CO) until no further pericarp removal could be achieved. Then, the pearled grain was scraped with a razor blade to remove any remaining pericarp fragments. The pearled grain was ground (through a 1mm screen) with a Udy laboratory mill (Udy Corp., Fort Collins, CO) prior to analysis. Sorghum "gum" was isolated from 5 g of ground, pearled grain using the procedure of Wood et al (1977). The gum was dissolved in 10 ml of distilled water. β-Glucans were precipitated with Congo Red or Calcofluor using the procedure of Wood and Fulcher (1978).

Results

The observations of cell walls were the same for all three sorghum cultivars. Discussion will be for sorghum in general. Untreated sections exhibited a bright blue autofluorescence in the pericarp, aleurone and endosperm cell walls. (Figs. 1, 2 and 3). In other cereals, this autofluorescence has reportedly been due to ferulic acid (Fulcher et al 1972; Fulcher & Wong 1980). In work conducted in this laboratory, ferulic acid has been shown to be the major phenolic compound in isolated cell walls from these three sorghum cultivars (Earp et al 1983). No autofluorescence was observed in the pigmented testa (Fig. 2). In Calcofluor-treated sections, an intense bluish-white fluorescence could be seen in the pericarp cell walls (Fig. 4)

and in the endosperm cell walls. In the aleurone cell walls (Fig. 5) and in the scutellar parenchyma cell walls (Fig. 6), a thin band of bluish-white fluorescence surrounded the cytoplasm. The bright blue autofluorescence can also be seen between the Calcofluor bands.

Since the blue colors produced by autofluorescence and Calcofluor staining are very similar, Congo Red, which fluoresces red, can be used to differentiate between the ferulate produced fluorescence and that produced by mixed linkage ß-glucans. When sections were treated with Congo Red, a bright red fluorescence could be seen in the cell walls of the pericarp (Fig. 7), aleurone (Fig. 8) and the endosperm (Figs. 8 and 9). Starch granules appeared red due to nonspecific staining but were not fluorescent as seen in the cell walls (Figs. 7-9). Congo Red is a histological stain that has been used for staining starch (Gurr, 1960). Starch granules in the thick mesocarp can be clearly seen (Fig. 7). Intense red fluorescence was also observed in the endocarp (cross and tube) cell walls (Fig. 7). After treatment with the ß-glucanase enzyme, little or no fluorescence could be detected in the pericarp (Fig. 10), aleurone (Fig. 11) or endosperm (Fig. 12) cell walls. Figures 7 and 8 were taken of the variety without a testa (BTx3197) while Figures 10 and 11 were taken of cultivars with a testa. The testa layer appeared fluorescent after ß-glucanase treatment. The source of this fluorescence has not been determined.

After following the ß-glucan isolation procedure of Wood et al (1977), the resulting precipitate was dissolved in distilled water. When Calcofluor was added to the solution, a gel-like substance immediately began to drop out of solution. This precipitate was off-white in color. When Congo Red was added to the solution, a red precipitate was formed. This precipitation reaction has been described by Wood and Fulcher (1978) for both oat and barley ß-glucans.

Discussion

In order to understand the effects of various processing techniques on the sorghum kernel, information concerning cell wall structure is needed. ß-Glucans were first isolated and identified by Woolard et al (1976, 1977) who were interested in cell wall structure as related to sorghum germination in the production of South African beer. The use of fluorescence microscopy in this study has enabled one to identify the location of ß-glucans in the sorghum kernel. Glennie et al (1983) examined cell walls of germinated sorghum grain with scanning electron and transmission electron microscopy. The authors observed extensive modification in the aleurone cell walls but no visible changes in the endosperm cell walls. In order for the sorghum endosperm to be modified during germination, some change in the cell wall structure must occur. It will be of interest to use the technique described in this paper to study germinated sorghum and to determine the fate of ß-glucans during germination.

Sorghum is processed by a number of other methods to improve its nutrient availability when used as a livestock feed. Mechanical grinding improves feed efficiency markedly. This would be due to the physical action of grinding, breaking down cell wall structure, thus exposing starch and protein to enzyme attack during digestion (Hale and Theurer, 1972). Reconstitution is a process by which water is added to grain to raise the moisture level to 25 to 30%. The grain is then stored in an air-limited environment, usually for 21 days. Reconstitution is controlled germination and would be similar to the malting process in brewing. When sorghum is ground after reconstitution, feed efficiency has been reported to increase 16 to 22% over ground dry grain (Riggs and McGinty, 1970). In a microscopic study by Sullins and Rooney (1971), it was reported that reconstitution affects the kernel at the subcellular level causing a general disruption of the endosperm, particularly the peripheral endosperm. It was postulated that the disorganization may be due to enzymatic activity similar to that seen during malting where ß-glucanase initiates cell wall degradation. Fluorescence microscopy using the Calcofluor and Congo Red fluorochromes would be a useful tool in determining what changes occur in cell wall structure during the processing of cereals for feed and food products.

Acknowledgements

The authors wish to thank Dr. G.M. Ballance, Department of Plant Science, University of Manitoba, for providing us with the purified endo-1,3(4) ß-D-glucanase for the ß-glucan enzyme study. This project was partially supported by the INTSORMIL Title XII Sorghum and Millet Research Program, supported in part by Grant AID/DSAN/XII/G-0149 from the Agency for International Development in Washington, D.C., 20253. Contribution No. 725 from Ottawa Research Station.

References

AASTRUP S, GIBBONS GC, MUNCK L. (1981). A rapid method for estimating the degree of modification in barley malt by measurement of cell wall breakdown. Carlsberg Res. Commun., 46, 77-86.

ANDERSON MA, COOK JA, STONE BA. (1978). Enzymatic determination of 1,3:1,4-ß-glucans in barley grain and other cereals. J. Inst. Brew., 84, 233-239.

DA S, AKINGBALA JO, ROONEY LW, SCHEURING JF, MILLER FR. (1982). Evaluation of Tô quality in a sorghum breeding program. Pages 11-23: Proceedings of the International Symposium on Sorghum Grain Quality. ICRISAT. Patancheru, A.P. India.

DUCROO P, DELECOURT R. (1972). Enzymatic hydrolysis of barley ß-glucans. Wallerstein Lab. Com., 35, 219-228.

EARP CF, DOHERTY CA, ROONEY LW. (1983). Fluorescence microscopy of the pericarp, aleurone layer and endosperm cell walls of three sorghum cultivars. Cereal Chem., 60, 408-410.

FAUSCH H, KUNDIG W, NEUKOM J. (1963). Ferulic acid as a component of a glycoprotein from wheat flour. Nature, 199, 287.
FEDER N, O'BRIEN TP. (1968). Plant microtechniques: some principles and new methods. Amer. J. Bot., 55, 123-142.
FULCHER RG. (1982). Fluorescence microscopy of cereals. Food Microstructure, 1(2), 167-175.
FULCHER RG, O'BRIEN TP, LEE JW. (1972). Studies on the aleurone layer. I. Conventional and fluorescence microscopy of the cell wall with emphasis on phenol carbohydrate complexes in wheat. Aust. J. Biol. Sci., 25, 23-34.
FULCHER RG, WONG SI. (1980). Inside cereals - a fluorescence microchemical view. in: Cereals for Food and Beverages - Recent Progress in Cereal Chemistry and Technology. Inglett, G.E. and Munck, L. (eds.). Academic Press. New York. 1-26.
GIBBONS, GC. (1981). Visualization of α-amylase movement and cell wall breakdown during barley malting - practical application of current research. ASBC Journal. 39, 55-59.
GLENNIE CW, HARRIS J, LIEBENBERG NVDW. (1983). Endosperm modification in germinating sorghum grain. Cereal Chem., 60, 27-31.
GURR E. (1960). Encyclopaedia of Microscopic Stains. Leonard Hill Books, Ltd. London. p. 140.
HAHN DH, FAUBION JM, ROONEY LW. (1983). Sorghum phenolic acids, their HPLC separation and their relation to fungal resistance. Cereal Chem., 60, 25-259.
HALE WH, THEURER CB. (1972). Feed preparation and processing. in: Digestive Physiology and Nutrition of Ruminants. Vol. III. Church, D.C. (ed.). Oregon State University, Corvallis, OR. Ch. 4.
HARRIS P.J., HARTLEY R.D. 1976. Detection of bound ferulic acid in cell walls of the Gramineae by ultraviolet fluorescence microscopy. Nature, 259, 508-510.
HUGHES J, McCULLY ME. (1975). The use of an optical brightener in the study of plant structure. Stain Technology, 50, 319-329.
MUNCK L, FEIL C, GIBBONS GC. (1978). Swedish patent application No. 7811307-3. (Copy available from L. Munck, Dept. Biotechnology, Carlsberg Res. Ctr., Gamle Carlsberg Vej 10, DK-2500 Valby, Copenhagen, Denmark)
RIGGS JK, McGINTY DD. (1970). Early harvested and reconstituted sorghum grain for cattle. J. Animal Sci., 31, 991-995.
SULLINS RD, ROONEY LW. (1971). Physical changes in the kernel during reconstitution of sorghum grain. Cereal Chem., 48, 567-575.
WOOD PJ, PATON D, SIDDIQUI IR. (1977). Determination of β-glucans in oats and barley. Cereal Chem., 53, 524-533.
WOOD PJ, FULCHER RG. (1978). Interaction of some dyes with cereal β-glucans. Cereal Chem., 55, 952-966.
WOOD, PJ. (1980a). Specificity in the interaction of direct dyes with polysaccharides. Carbohydrate Res., 85, 271-287.
WOOD, PJ. (1980b). The interaction of direct dyes with water-soluble substituted celluloses and cereal β-glucans. Ind. Eng. Chem. Prod. Res. Dev., 19, 19-23.
WOOLARD GR, RATHBONE EB, NOVELLIE L. (1976). A hemicellulosic β-D-glucan from the endosperm of sorghum grain. Carbohydrate Res., 51, 249-252.
WOOLARD GR, RATHBONE EB, NOVELLIE L, OHLSSON JT. (1977). Structural studies on the water-soluble gums from the endosperm of sorghum grain. Carbohydrate Res., 53, 101-108.
YIU SH, POON H, FULCHER RG, ALTOSAAR I. (1982). The Microscopic structure and chemistry of rapeseed and its products. Food Microstructure, 1(2), 135-143.

Figure Captions

Fig. 1-12. Al - aleurone layer; CF - Calcofluor fluorescence; CW - cell wall; E - endosperm; EN - endocarp (cross and tube cells); EP - epicarp; M - mesocarp; SG - starch granule; SP-scutellar parenchyma; T - testa. Cultivar is indicated in parenthesis. FC = filter combination.

Scale bar numbers indicate μm.

Fig. 1. Untreated section showing intense autofluorescence in pericarp, aleurone and endosperm cell walls (BTx3197). Photographed using FC I.

Fig. 2. Untreated section showing autofluorescence in pericarp, aleurone and endosperm cell walls (ATx623 X SC0103-12). Photographed using FC I.

Fig. 3. Aleurone cells with intense autofluorescence in cell walls (Early Hegari). Photographed using FC I.

Fig. 4. Calcofluor (Biofluor) stained section showing bluish-white fluorescence produced in the mesocarp cell walls BTx3197). Photographed using FC I.

Fig. 5. Calcofluor (Biofluor) stained section showing bluish-white fluorescence in the aleurone cell wall (BTx3197). Darker blue autofluorescence can be seen between the two bands of Calcofluor-produced fluorescence. Photographed using FC I.

Fig. 6. Calcofluor produced fluorescent bands in scutellar parenchyma cell walls (Early Hegari). Photographed using FC I.

Fig. 7. Congo Red staining of the pericarp cell walls (BTx3197). Photographed using FC III.

Fig. 8. Congo Red staining showing fluorescence of aleurone and endosperm cell walls. Starch granules stain red but are not fluorescent (BTx3197). Photographed using FC III.

Fig. 9. Congo Red staining showing fluoresence of endosperm cell walls (BTx3197). Photographed using FC III.

Fig. 10. After treatment with β-glucanase, the section shows little or no fluorescence in the pericarp or aleurone cell walls (ATx623 X SC0103-12). Photographed using FC III.

Fig. 11. After treatment with β-glucanase, little or no fluorescence can be seen in the aleurone cell walls (Early Hegari). Photographed using FC III.

Fig. 12. After treatment with β-glucanase, little fluorescence remains in the endosperm cell walls (Early Hegari). Photographed using FC III.

β-Glucans in Caryopsis of Sorghum Bicolor (L.) Moench

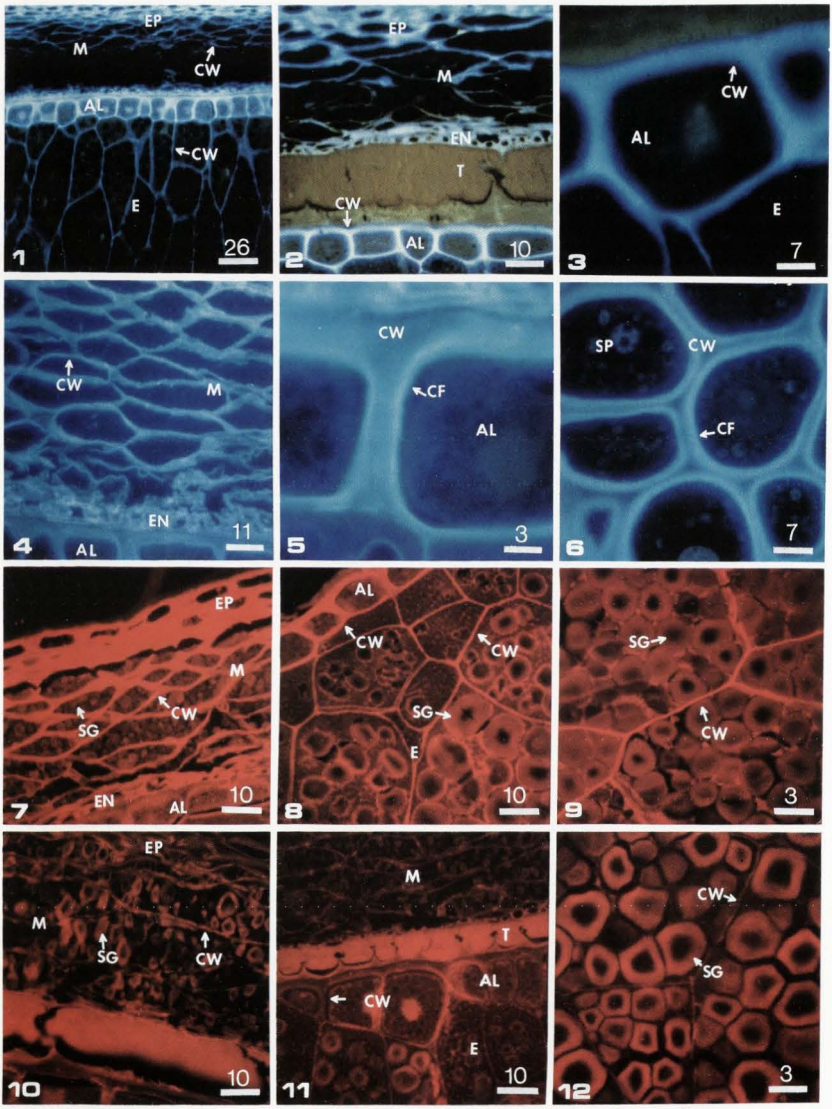

Discussion With Reviewers

E.A. Davis: The Congo Red stain appears to be brighter around the outer edges of the starch granules. Is that due to the 3-dimensional character of starch and therefore uneven focussing in the microscope?
Authors: We feel that is merely optical staining of the starch granules.
C.W. Glennie: Were the Calcofluor and Congo Red techniques tried on malted sorghum?
Authors: Not yet. We already have some germinated sorghum embedded and will be looking at it next.
C.W. Glennie: Autofluorescence, presumably due to ferulic acid is found in all endosperm cell walls (Earp et al 1983). During malting studies, I have found that the amount of endosperm cell wall decreased but the amount of ferulic did not. Did the authors find any interference from ferulic acid when the cell walls were treated with glucanase before Calcofluor treatment?
Authors: We did not see any interference from ferulic acid when the cell walls were treated with β-glucanase. The autofluorescence was still present after the β-glucanase treatment.

MILK, DAIRY PRODUCTS

STRUCTURE AND PROPERTIES OF THE PARTICULATE CONSTITUENTS OF HUMAN MILK. A REVIEW.
Rüegg M, Blanc B. 1982. Food Microstructure 1(1), 25-47. [Federal Dairy Res. Inst., CH-3097 Liebefeld, Switzerland].

Milk contains different types of colloidal or coarsely dispersed particles, such as casein micelles, membrane fragments, fat globules, and cells. The fat globules are composed of sub-populations of differently sized particles. In contrast to cow's milk, the overall average diameter (d_{vs}) increases with advancing lactation from about 1.8 µm in colostrum to 4.0 µm in mature milk. Membrane materials originating from the milk fat globule membrane, plasma membrane, secretory vesicles, and other sources can be found in milk serum. These particles have also been called lipoprotein particles. Their size ranges from about 10 to 400 nm. New results concerning the structure of human milk casein particles show that their average size is considerably smaller than in cow's milk and that their average diameter tends to increase with advancing lactation. The d_{vs} values in human milk range from about 11 to 55 nm and in cow's milk from approximately 90 to 100 nm. The structure of the acidified or renneted human milk differs significantly from that of equally treated cow's milk. In human milk there is no coagulation at all or the coagulum appears much looser than in bovine milk. The different types of cells in human milk have diameters in the range of about 8 to 40 µm. A sharp decrease in the total cell number from about 3×10^6/mL in colostrum to 10^4 - 10^5/mL in mature milk can usually be observed. The relative amount of each type of cell varies in the course of lactation. The epithelial cells, typically 15 to 20 µm in diameter, become the predominant type after 2 to 3 months.

DETECTION OF BUTTERMILK SOLIDS IN MEAT BINDERS BY ELECTRON MICROSCOPY
Kalab M, Comer F. 1982. Food Microstructure 1(1), 49-54. [Food Res. Inst., Res. Branch, Agric. Canada, Ottawa, Ontario, Canada K1A 0C6].

Nonfat dry milk and buttermilk (BM) solids used as ingredients in meat binders can be differentiated by TEM. The meat binders are suspended in water and coarser ingredients such as wheat and mustard flours are separated from the milk solids by low-speed centrifugation (415 g for 30 min). The milk solids thus purified are concentrated by ultracentrifugation (8×10^4 g for 90 min) and the resulting pellets are embedded in a resin, thin-sectioned, stained, and examined by TEM. BM solids are revealed by the presence of fat globule membrane fragments. In the absence of BM solids only casein micelles are found in the pellets. Sensitivity of this technique is 1 part of BM solids in 20 parts of milk solids, that is 5% of BM (w/w).

PHYSICAL PROPERTIES AND MICROSTRUCTURE OF CREAM CHEESE
Obashi T, Nagai S, Masaoka K, Haga S, Yamauchi K, Olson NF. 1983. Nippon Shokuhin Kogyo Gakkaishi 30(5), 303-307. [Fac. Agric., Miyazaki Univ., Miyazaki-shi, Miyazaki-ken, 880, Japan].

Some cream cheese commercially manufactured from fresh cream, whole milk, and skim milk powder were examined for quality characteristics such as general composition, physical properties, and microstructure (SEM). The results obtained were summarized as follows: (1) Average yield of final products was 400 kg/1000 kg of cheese milk. (2) The mean composition of all 21 samples under study were 0.92, 55.68, 33.32, 8.55, and 1.08% in acidity, moisture, fat, protein, and ash, respectively. (3) Elastic modulus and adhesiveness of the cream cheese were estimated using 11 and 10 samples, respectively. The former averaged 15.46×10^6 dyne/cm^2, and the latter averaged 1.21×10^3 dyne/cm^2, indicating that these physical properties were liable to variation compared with chemical composition. (4) SEM for examining the microstructure of these cream cheeses revealed that remarkable structural changes occurred during cheese making: A part of the fat globules was in contact with casein micelle aggregates forming amorphous clumps, while residues of fat globule fragments were fused one with each other and produced large clusters everywhere.

INFLUENCE OF HOMOGENIZATION OF CONCENTRATED MILKS ON THE STRUCTURE AND PROPERTIES OF RENNET CURDS
Green ML, Marshall RJ, Glover FA. 1983. Journal of Dairy Research 50, 341-348. [Nat. Inst. for Res. in Dairying, Shinfield, Reading RG2 9AT, U.K.].

Whole milk was concentrated by ultrafiltration in a plant causing some homogenization of the fat. Comparisons were made with milk concentrated in a plant causing little homogenization and with milk homogenized conventionally. None of the processes appreciably affected the casein micelle size distribution. On rennet treatment of homogenized milk, casein micelle aggregation occurred more slowly, the protein network in the curd was less coarse and the rate of whey loss was reduced, compared with non-homogenized milk at the same concentration. In using concentrated milks for cheesemaking, homogenization improved the composition of Cheddar cheese because of increased fat and moisture retention, but curd fusion was poorer. Some aspects of the texture of the mature cheeses were improved, but the free fatty acids levels were higher. Values for the firmness of curds, formed from milks processed in different ways, did not relate to the extent of aggregation of the casein micelles. It is suggested that the complete cheesemaking process is driven by the tendency of the casein to aggregate.

ELECTRON MICROSCOPIC LOCALIZATION OF SOLVENT-EXTRACTABLE FAT IN AGGLOMERATED SPRAY-DRIED WHOLE MILK POWDER PARTICLES
Buchheim W. 1982. Food Microstructure 1(2), 233-238. [Inst. f. Chemie & Physik, Bundesanstalt f. Milchforschung, D-2300 Kiel, Federal Republic of Germany].

An agglomerated spray-dried whole milk powder has been studied by electron microscopy before and after extracting approximately 10% of total fat with petroleum ether at 25°C for 1 h. The powder samples were suspended in polyethylene glycol, cryofixed and further prepared by the freeze-fracturing technique. These studies demonstrate that the solvent-extractable fat (the so-called 'free fat') consists partly of surface fat and partly of fat extracted from fat globules within the powder particles. The spatial distribution of such solvent-accessible fat globules appeared to be rather uneven, i.e., whereas certain limited volumes within a powder particle showed an almost complete extraction, others remained unaffected. There were no indications that fat globules near the periphery of the powder particles were more accessible for the solvent than those in the interior of the particles. The results of this study generally confirm the model by Buma for the distribution of 'free fat' in dried milk.

MICROSTRUCTURE OF YOGHURT STABILIZED WITH MILK PROTEINS
Modler HW, Kalab M. 1983. Journal of Dairy Science 66(3), 430-437. [Food Res. Inst., Agric. Canada, Ottawa, Ontario, Canada K1A 0C6].

Skim milk yogurts were stabilized with a variety of casein- and whey protein-based ingredients. Experimental yogurts contained 1.5% added protein and were compared to a reference yogurt prepared with 0.5% gelatin (225 Bloom strength).

SEM and TEM revealed extensive fusion of casein micelles in yogurts prepared with additional casein. Yogurts prepared with skim milk powder and milk protein concentrate were composed of casein micelle chains held together by short links. Sodium caseinate induced formation of large and excessively fused micelles.

Yogurts prepared with 3 types of commercial whey protein concentrate were similar in structure but differed distinctively from casein-based yogurts in that casein micelles were individual in nature with intermicellar spaces spanned with flocculated protein.

LIGHT AND ELECTRON MICROSCOPY OF CELLS IN PIG COLOSTRUM, MILK AND INVOLUTION SECRETION
Lee CS, Cauley IMc, Hartmann PE. 1983. Acta Anatomica 116(2), 126-135. [Dept. Vet. Preclin. Sci., Univ. of Melbourne, Parkville, Victoria, Australia].

Cells in pig colostrum, milk, and involution secretion were identified using LM and EM. Cell types identified were neutrophils, macrophages, epithelial cells, eosinophils, and lymphocytes. The neutrophils predominated in colostrum and involution secretion, whereas in milk it was the epithelial

cells. Macrophages and lymphocytes were present throughout lactation and so too were eosinophils which were always present in lower concentrations. Both neutrophils and macrophages were seen with phagocytic vacuoles containing either lipid, casein, or cellular debris. The possible roles played by the phagocytic and lymphoid cells in the protection of the mammary gland of the sow and the gut of the neonate from pathogenic microorganisms is discussed.

COMPOSITION AND MICROSTRUCTURE OF SOFT BRINE CHEESE MADE FROM INSTANT WHOLE MILK POWDER

Omar MM, Buchheim W. 1983. Food Microstructure 2(1), 43-50. [Dept. Food Sci., Univ. of Zagazig, Zagazig, Egypt].

Comparative studies were made on the composition, microstructure, and sensory attributes of soft brine cheese made from instant whole milk powder and from raw milk. The chemical analysis of young and ripened (1 and 2 months) cheeses revealed similarity except for a higher salt content in the cheese made from reconstituted milk at the end of ripening. EM studies showed distinct differences in the structure of the protein matrices in the ripened cheese samples, i.e. a very homogeneous structure in the cheese made from raw milk compared with a slightly aggregated state of the protein in the cheese made from reconstituted milk. Sensory evaluation resulted in an overall acceptable quality of the cheese made from reconstituted milk except for a higher saltiness.

DEVELOPMENT OF MICROSTRUCTURE IN SET-STYLE NONFAT YOGHURT - A REVIEW

Kalab M, Allan-Wojtas P, Phipps-Todd BE. 1983. Food Microstructure 2(1), 51-66. [Food Res. Inst., Agriculture Canada, Ottawa, Ontario, Canada K1A 0C6].

The development of microstructure in natural set-style nonfat yoghurt was studied by SEM and TEM. In addition to the results of thin-sectioning and conventional SEM described in the literature, this review illustrates gelation of milk with micrographs obtained by rotary shadowing of casein micelles and their clusters. The existence of void spaces occupied by lactic acid bacteria in yoghurt was confirmed by cold-stage SEM of uncoated specimens. The microstructure of yoghurt is affected by the preheat treatment of milk, bacterial starter cultures, total solids content, and the presence of thickening agents. The microstructure was found to be related to firmness and susceptibility to syneresis. Suggestions on the preparation of yoghurt samples for EM have been included in this review.

ELECTRON MICROSCOPY OF MILK AND MILK PRODUCTS: PROBLEMS AND POSSIBILITIES

Schmidt DG. 1982. Food Microstructure 1(2), 151-165. [Netherlands Inst. for Dairy Res., P.O. Box 20, 6710 BA Ede, The Netherlands].

Milk and dairy products have frequently been studied by TEM and SEM. The specimen preparation procedure may considerably influence the final result, and formation of artefacts is frequently observed. In this respect, formation of ice crystals during cryofixation is a well-known phenomenon. But dehydration, to an extent such as is required for embedding procedures, also appears to be harmful to dairy products. Micrographs of thin sections of plastic-embedded samples of casein submicelles show threadlike material, whereas in freeze-etched specimens only spherical particles are found. Similar observations are made when samples of cheese and of concentrated milk are investigated. It is therefore concluded that the use of organic solvents for dehydration purposes is to be avoided when studying the fine structure of casein. High-voltage EM has not yet found any application to speak of in dairy research, but may become of interest in the study of the three-dimensional networks in milk gels by using thick sections. As yet electron microprobe analysis has found only little adoption in dairy research, viz. in energy-dispersive X-ray microanalysis of the Ca and P contents of casein micelles, and of the composition of crystalline inclusions in cheese.

PARACRYSTALLINE ARRAYS OF MILK FAT GLOBULE MEMBRANE-ASSOCIATED PROTEINS AS REVEALED BY FREEZE-FRACTURE

Buchheim W. 1982. Naturwissenschaften 69, 505. [Inst. f. Chemie & Physik, Bundesanstalt f. Milchforschung, D-2300 Kiel, Federal Republic of Germany].

A high degree of macromolecular order was visualized in the proteinaceous, 10-50 nm wide inner coat separating the milk fat globule membrane from the triglyceride core. Such paracrystalline structures are frequently present in bovine milk fat globules but are distributed rarely in human and caprine milk fat globules.

FOODS OF PLANT ORIGIN

WATER ABSORPTION OF SOYBEAN SEEDS AND ASSOCIATED CAUSAL FACTORS

Calero E, West SH, Hinson K. 1981. Crop Science 21, 926-933. [Inst. Food & Agric. Sci., Univ. of Florida, Gainesville, FL 32611, U.S.A.].

Twelve cultivars, introductions, and breeding lines, and seven progenies from different crosses were used to study the rate of water absorption at 100% relative humidity and 24°C for 8 days and under standard germinating conditions for 8 and 24 h. Seed coats of selected samples of seed from the water absorption studies were observed using SEM.

A negative correlation between seed size and the percentage of water uptake was found in some materials, but this relationship did not hold for all. A range of water uptake rates was observed. Furthermore, the shape and size of pores present in the seed coat were different for the various materials. Small seeds had a higher percentage by weight of seed coat and large, rounded pores, whereas large and medium seeds had a lower percentage of seed coat with smaller, elongated pores. Waxy material was embedded in different densities into the epidermis. Ecuador 2, Bragg, Ss-Da-010 and the progenies from Bragg x (Cobb x PI86490) F4 appear to imbibe water slowly. Small elongated pores and a high density of waxy material embedded in the epidermis were associated with low absorption.

FUNGAL PENETRATION OF SOYBEAN SEED THROUGH PORES

Hill HJ, West SH. 1982. Crop Science 22, 602-605. [Inst. Food & Agric. Sci., Univ. of Florida, Gainesville, FL 32611, U.S.A.].

Mycelia of seed-borne fungi have been postulated to enter the seed coat of soybean [Glycine max (L.) Merr.] through seed coat defects and the hilum region. The objective of this study was to determine if fungal mycelia could also enter the seed via the naturally occurring pores on the seed coat surface. Using SEM, naturally occurring pores on the surface of the seed coat were observed as providing a means of entry into the seed. These pores were found to penetrate deeply into the palisade layer providing passage into the hourglass layer. Fungal hyphae were observed to extend into these pores. These pores, therefore, can provide a means of fungal entry without the presence of visible seed coat defects.

THE MICROSCOPIC STRUCTURE AND CHEMISTRY OF RAPESEED AND ITS PRODUCTS

Yiu SH, Poon H, Fulcher RG, Altosaar I. 1982. Food Microstructure 1(2), 135-143. [Food Res. Inst., Agric. Canada, Ottawa, Ontario, Canada K1A 0C6].

The location and distribution of some of the storage constituents in the structures of rapeseed and its products were investigated. Hand-cut or glycol methacrylate-embedded sections were stained with dyes or fluorochromes of known specificities and examined using fluorescence, bright-field, and/or polarizing microscopy. Results obtained from the study were based upon observations of characteristics of the various stainings, birefringence, induced fluorescence, and autofluorescence. The effects of enzymatic hydrolysis, solvents, and processing on the cellular structures and their affinity for certain dyes/fluorochromes were also investigated. Major and minor storage constituents were tentatively located in the structure of rapeseed. Lipids and proteins were stored within separate cellular organelles which were distributed throughout the aleurone layer of the endosperm and cells of the embryo. These two accounted for the major portions of rapeseed storage reserves. Phytin crystals were detected inside the protein bodies of the embryonic cells. Most of the rapeseed polysaccharides were present as structural (cell-wall) carbohydrates of which amyloid was one of the major components. The seed coat of rapeseed is a complex structure containing structural carbohydrates, mucilage, and lignin. The testa of the yellow seed-coated cultivar, Candle, was structurally and chemically different from that of other rapeseed varieties.

[A HISTOLOGICAL STUDY OF BERRY SETTING IN 'MUSCAT OF ALEXANDRIA' GRAPES] [In Japanese]

Okamoto G, Imai S. 1982. Journal of the Japanese Society for Horticultural Science 50(4), 436-444. [Coll. Agric., Univ. of Okayama, Okayama 700, Japan].

Fluorescence microscopy revealed that in most florets, pollen tubes reached 3 to 4 ovules out of 4 in the ovary on the first day after pollination. Division of the primary endosperm nucleus, which occurs in the fertilized embryo sac, began 2 or 3 days after anthesis.

FURTHER STUDIES ON AGGREGATION AND INSOLUBILIZATION OF SOYBEAN 11S GLOBULIN WITH HUMIDITY DURING STORAGE
Hoshi Y, Yamauchi F. 1983. Agricultural and Biological Chemistry 47(7), 1473-1479. [Dept. Food Chem., Fac. Agric., Tohoku Univ., Sendai 980, Japan].

When lyophilized soybean 11S globulin was stored at 50°C and a relative humidity of 96%, the redispersibility of the protein, as measured over a 1 h period, was drastically decreased after 4 h. When the redispersing time was prolonged to 24 h, 11S globulins stored for up to 12 h redispersed similarly to the control, but became insoluble after 24-h storage. A gel filtration study showed that the stored 11S globulin had already polymerized mainly through disulfide bonds after 12 h of storage.

SEM showed that a globular structure of the control 11S globulin changed to an aggregated structure during storage. Polymerized subunits linked with disulfide bridges were observed using gel filtration in the presence of sodium dodecyl sulfate (SDS) and SDS-polyacrylamide gel electrophoresis: the number of the polymerized subunits increased during storage. The 11S globulin, however, did not polymerize as much with humidity as it polymerized by heat denaturation at 100°C (ionic strength 0.5 and protein concentration 0.5%).

STRUCTURAL CHARACTERISTICS AND FATTY ACID COMPOSITION OF PSOPHOCARPUS TETRAGONOLOBUS SEEDS
Varriano-Marston E, Beleia A, Lai CC. 1983. Annals of Botany 51, 631-640. [Dept. Grain Science, Kansas State Univ., Manhattan, KS 66506, U.S.A.].

Winged bean (Psophocarpus tetragonolobus) seed coat in the hilar region consists of a double layer of sclereids, tracheid bar, and spongy parenchyma cells. This is contrasted to the seed coat structure on either side of the hilar region, which has a single layer of sclereids, columnar cells, and crushed parenchyma cells.

Cotyledonary cells are large (50 to 100 µm in diameter) and have cell walls 2.4 to 4.7 µm thick with pit-pair structures. Protein bodies and lipid bodies are the main structural components of the cytoplasm while only a small number of starch granules are present in each cell. The major portion of the lipid can be removed by non-polar solvents and contains oleic and linoleic acids as the predominant unsaturated fatty acids. High levels of behenic acid were present in both "free" and "bound" lipids. LM, TEM, and SEM supported the findings. [Copyright 1983 by Annals of Botany Company].

[EFFECT OF TEMPERATURE ON THE INTERNAL MORPHOLOGY AND DEVELOPMENT OF LEAVES IN CHINESE CABBAGE (BRASSICA CAMPESTRIS L.)] [In Japanese]
Ootake Y. 1982. Journal of the Japanese Society for Horticultural Science 51(3), 329-337. [Aichi-ken Agric. Res. Center Anjo Branch, Ikeura, Anjo, Aichi 446, Japan].

The process of leaf development in relation to temperature was investigated morphogenetically to clarify the mechanism of the "small head" formation in Chinese cabbage. Seedlings of 'Nozaki-Kohai No. 3' were grown in a phytotron kept at day-night temperatures of 25 to 30°C (high), 18 to 23°C (medium), and 10 to 15°C (low). For histological observations, leaves and shoot apices collected at 7-day intervals were fixed and sectioned by the paraffin microtechnique.

In leaf 5 (numbered from the base) the thickness of the midrib was greatest at medium temperature and smallest at the high temperature. Cell numbers and dimensions in other tissues were also temperature-dependent.

[HISTOLOGICAL OBSERVATIONS ON THE CHILLING INJURY OF CUCUMBER FRUIT DURING COLD STORAGE] [In Japanese]
Rhee JK, Iwata M. 1982. Journal of the Japanese Society for Horticultural Science 51(2), 231-236. [Fac. Agric., Univ. of Tokyo, Bunkyoku, Tokyo 113, Japan].

Histological changes were observed during the development of external symptoms of chilling injury in cucumbers (cv. Tokiwa Shin No. 2) stored at 4°C. Main external symptoms were pitting and whitish leakage on the cucumber surface. At more advanced stages, epidermal cells collapsed with more than 7 to 8 layers of parenchymal cells under the epidermis, and the whitish leakage derived from cellular collapse by oozing to the fruit surface through stomata and also into intercellular space.

[HISTOLOGICAL OBSERVATIONS ON THE CHILLING INJURY OF TARO TUBERS DURING COLD STORAGE] [In Japanese]
Rhee JK, Iwata M. 1982. Journal of the Japanese Society for Horticultural Science 51(3), 362-368. [Fac. Agric., Univ. of Tokyo, Bunkyoku Tokyo 113, Japan].

Histological observations were carried out on taro (Colocasia esculenta Schott cv. Dotare) tubers during the development of internal browning due to chilling injury at 4°C. An attempt was also made to histologically detect phenolic substances and polyphenol oxidase associated with internal browning. It was found that tannin cells were scattered in epidermal and vascular tissues, and also in the inner parenchyma tissue. The shape of tannin cells was generally elliptical, but those in the vascular tissues were rectangular. Slight browning occurred in some tannin cells and surrounding parenchyma cells in each tissue already before the onset of internal browning. Although phenolic substances in taro tubers were detected mainly in tannin cells, some of them were also found in secretory canals. Polyphenol oxidase was detected in the parenchyma cells, tannin cells, and secretory canals.

[THE RELATIONSHIPS OF PLANT HORMONES, SUGARS AND NITROGEN TO THE EARLY DEVELOPMENT OF RADISH ROOT] [In Japanese]
Hayata Y, Suzuki Y. 1982. Journal of the Japanese Society for Horticultural Science 51(1), 56-61. [Inst. Agric. & Forestry, Univ. of Tsukuba, Sakura, Niihari-gun, Ibaraki 305, Japan].

Changes in the contents of plant hormones, sugars, and nitrogen in radish (Raphanus sativus L. radicula group) were investigated during the early development of the root.

Auxin (I) and cytokinin (II) activities in the leaves decreased gradually with root development. The sugar contents also decreased up to the 16th day after sowing, but varied little afterwards. In the hypocotyl, however, an increase in II activity was observed 21 days after sowing, when the primary cortex began to slough off. Thereafter, the dry weight of hypocotyl increased rapidly. The I activity increased remarkably with thickening of the root on the 29th day after sowing. The reducing and total sugar contents decreased up to the 21st day after sowing but increased afterwards with thickening of the root.

STUDIES OF THE UNIFORMITY OF ELEMENTAL COMPOSITION IN DIFFERENT AREAS OF GLOBOID CRYSTALS IN PROTEIN BODIES OF CUCURBITA MAXIMA AND RICINUS COMMUNIS SEEDS
Lott JNA. 1983. Scanning Electron Microsc./1983/II: 923-928 (SEM Inc., AMF O'Hare, IL 60666, U.S.A). [Biol. Dept., McMaster Univ., 1280 Main St. W., Hamilton, Ontario, Canada L8S 4K1].

Seed protein bodies usually contain electron-dense inclusions called globoid crystals which are thought to be rich in phytin. In past studies, energy dispersive X-ray analysis (EDX) was used to study protein body-to-protein body, cell-to-cell, and tissue-to-tissue differences in the elemental composition of globoid crystals. The studies reported here used an STEM for EDX analysis of many areas within individual globoid crystals. Studies of globoid crystals from C. maxima cotyledons showed that a given globoid crystal was of relatively uniform composition throughout although there were differences in composition from cell to cell. Some globoid crystals from R. communis endosperm showed measurable internal differences in Ca content.

PROTEIN BODIES IN DORMANT, IMBIBED AND GERMINATED SUNFLOWER COTYLEDONS
Allen RD, Arnott HJ. 1982. Food Microstructure 1(1), 63-73. [Dept. Biol., Univ. of Texas at Arlington, Arlington, TX 76019, U.S.A.].

SEM was used to observe the morphology and structure of protein bodies in dormant and imbibed sunflower cotyledons and to document the morphological changes in protein bodies during germination and seedling growth. In order to clearly visualize dormant seed structure, anhydrous fixation techniques were employed. Definite differences in cellular structure are seen in comparisons of dry and imbibed seed tissues. As germination proceeds, protein bodies lose their smooth spherical shape and become indented and pitted. Protein body coalescence and fusion precedes the formation of a central protein vacuole. As protein is hydrolyzed, protein vacuole density decreases, and its surface becomes granular, then fibrous, in appearance. Removal of protein from the protein vacuole appears to proceed more rapidly in cells closest to the embryonic axis. The protein vacuole becomes the main cell vacuole as remaining storage protein is hydrolyzed. The cotyledon cells undergo a gradual change in function from a quiescent storage stage, through a major exporting phase and to their final function of photosynthesis.

STUDIES ON BLACKENING OF PEPPER (PIPER NIGRUM, LINN) DURING DEHYDRATION

Mangalakumari CK, Sreedharan VP, Mathew AG. 1983. Journal of Food Science 48(2), 604-606. [Reg. Res. Lab. (CSIR), Trivandrum 695 019, Kerala, India].

Histochemical studies carried out in fresh pepper berries at different stages of maturity showed that phenolic compounds distributed throughout the berries at a very young stage were confined to the epicarp and mesocarp alone at full maturity. The blackening that occurs in pepper on drying or on injury also showed a similar distribution pattern. Flavanols were not found in the young stage but appeared in the innermost cells of mesocarp covering endocarp after fertilization. Spores of Glomerella cingulata, present even in healthy pepper berries, were found to be the source of phenolase enzyme taking part in the blackening. Phenols in pepper were enzymatically oxidized and gave rise to black color when the cells were disturbed by dehydration or maceration. The results are illustrated with LM and SEM micrographs.

ULTRASTRUCTURAL STUDY OF THE DEVELOPMENT OF OIL CELLS IN THE MESOCARP OF AVOCADO FRUIT

Platt-Aloia KA, Gross JW, Thomson WW. 1983. Botanical Gazette 144(1), 49-55. [Dept. Botany & Plant Sci., Univ. of California, Riverside, CA 92521, U.S.A.].

The development of idioblastic oil cells in the mesocarp of avocado fruit was studied by EM. Observations concentrated on the formation of the complex cell wall and on the process of oil accumulation. The cell wall of the mature oil cells has 3 distinct layers: an external primary wall, a suberin lamella, and an interior tertiary wall. No significant oil accumulation was observed until after the suberin layer was deposited and tertiary wall formation had begun. Formation of an extensive network of smooth tubular endoplasmic reticulum was observed concomitant with the initial accumulation of oil in the cytoplasm. In the latter stages of tertiary wall formation, the primary site of oil accumulation shifted from the cytoplasm to the vacuoles. By the time the deposition of the tertiary wall was complete, most of the cell volume was occupied by a massive oil droplet; the cytoplasm, which was devoid of membranes, was displaced to the cell periphery.

EFFECT OF ASCORBATE ON AN ISOLATED MITOCHONDRIAL FRACTION DURING AGEING OF SWEDE (BRASSICA NAPUS VAR. NAPOBRASSICA)

Slinde E, Baardseth P, Kryvi H. 1983. Food Chemistry 11(2), 117-125. [Norwegian Food Res. Inst., PB 50, N-1432 Aas-NLH, Norway].

The average sedimentation coefficient (S-value) of swede mitochrondria was 8300±400 S in a hypotonic 0.25 M sucrose buffer (pH 7.4), when malate dehydrogenase was used as the marker enzyme. A differential centrifugation procedure giving optimal recovery of the mitochondria has been worked out. TEM of the isolated mitochrondrial fraction shows well preserved, but somewhat swollen, mitochondria. The fraction contained approximately 4% plastoglobuli and/or peroxisomes. The respiratory control ratio (RCR; state 3: state 4 respiration) was found to be 3/2 ± 0.6. Ascorbic acid (I) equilibrated with the respiratory chain and both the endogenous and I-stimulated respiration increased throughout the storage year. I contributed to the non-enzymatic cytochrome c reducing activity in plant extracts.

THE CAUSE OF REDUCED COOKING RATE IN PHASEOLUS VULGARIS FOLLOWING ADVERSE STORAGE CONDITIONS

Jones PMB, Boulter D. 1983. Journal of Food Science 48 (2), 623-626, 649. [Dept. Bot., Univ. of Durham, Science Labs., South Road, Durham, DH1 3LE, U.K.].

The interrelationship between reduced cell separation rate, reduced inhibition value, and reduced pectin solubility was investigated with reference to reduced cooking rate in Phaseolus vulgaris also termed the hardbean phenomenon. It was found that reduced imbibition value and reduced pectin solubility can both cause a reduction in the rate of cell separation during cooking of beans and hence an increase in their cooking time and that these 2 factors act synergistically. Accompanying symptoms are solute leakage during soaking due to membrane breakdown, phytin catabolism, and pectin demethylation, all of which are key factors in the development of hardbean.

CEREALS

GRAIN STRUCTURE AND END-USE PROPERTIES

Pomeranz Y. 1982. Food Microstructure 1(2), 107-124. [U.S Dept. of Agric., Agric. Res. Service, North Central Reg. U.S. Grain Marketing Res. Center, Manhattan, KS 66502 U.S.A.].

Practical implications of grain structure relate t every step from grain development and production throug marketing to processing, utilization, and consumption. Th structure and adherence of the hulls may contribute t protection of grain during germination and malting and pro tection against insect infestations. Germ retention durin threshing and separation during processing depend on th germ structure and location in the kernel. The subaleuron and central endosperm layers differ in cell size, shape, an structure and in composition, especially with regard t protein contents and quality. The main factors in grai hardness are the intrinsic hardness of the main components the strength of interaction within the cell, and the inter action of individual cells to produce overall grain struc ture.

Endosperm structure and hardness are related to whea conditioning, to breakage in milling, and to the structur and composition of the milled flour particles. Milling qual ity is governed by morphological characteristics of th wheat kernel and its mechano-physical properties and by th methods of grinding and separation. Reducing changes i texture and structure during drying of maize and rice ar important in minimizing breakage during handling, storage and transportation, dust formation, and infestation. Differ ences in grain structure are expressed in differences i composition, gradients of components in grain tissues, an end-use properties. Those differences have important nutri tional implications. New microscopic methods to determin grain structure, composition, and end-use properties hav the potential of contributing to improved nutritional quali ty and utilization of cereals by modifying-restructurin grain morphology through classical plant breeding and genet ic engineering.

SCANNING ELECTRON MICROSCOPY OF THE PERICARP AND TESTA O SEVERAL SORGHUM VARIETIES

Earp CF, Kooney LW. 1982. Food Microstructure 1(2), 125-134 [Cereal Quality Lab., Dept. Soil & Crop Sci., Texas A & Univ., College Station, TX 77843, U.S.A.].

Pericarp thickness (determined by Z gene) varies great ly among sorghum varieties ranging from very thin (8 µm) t very thick (160 µm). Pericarp thickness also varies withi an individual kernel. The areas below the style and near th hilum are the thickest with the sides of the kernel bein thinnest. SEM was used to document differences in pericar thickness and to explain milling differences. Varieties wit a thick pericarp had starch granules in the mesocarp cel layers. Sorghums with a thin pericarp did not have starc granules in the mesocarp except near the hilum and styla area. U.S. sorghum varieties studied had a testa thicknes of 16 to 40 µm (side of the kernel) but recently four Mali sorghums from a recent collection had very thin testae of to 16 µm. The Sudanese sorghum Shawaya had a testa rangin in thickness from 28 to 40 µm.

CARBOHYDRATE MAKE-UP OF MINOR MILLETS

Muralikrishna G, Paramahans SV, Tharanathan RN. 198 Starch/Stärke 34(12), 397-401. [Disc. Biochem. & Appli Nutr., Central Food Technol. Res. Inst., Mysore-57001 India].

Starchy and nonstarchy carbohydrates of samai, sanw and panivaragu have been isolated and characterized. Star isolated exhibited single-stage swelling, moderate solubil ty in water, but a very high solubility in dimethoxy sul oxide, and non-ionic character similar to several starch from Leguminoseae. Treatment with mild alkali resulted the separation of large-hexagonal and small-spherical gra ules. Considerable retrogradation of the linear amylo fraction was observed. Hemicellulose A was shown to be non-cellulosic glucan, whereas hemicellulose B was compos of hexoses, pentoses, and uronic acids in varying propo tions. The alkali-insoluble residues were exclusively co posed of glucose and thus constituted the fibre fraction.

ECHANISM OF POPCORN POPPING

oseney RC, Zeleznak K, Abdelrahman A. 1983. Journal of ereal Science 1(1), 43-52. [Dept. Grain Sci. & Ind., Kansas tate Univ., Manhattan, KS 66506, U.S.A.].

During the popping of popcorn the pericarp acts as a ressure vessel. It was found that the initial break in the ericarp affects popped volume more radically than do any ubsequent breaks. Popping occurs at about 177°C, which is quivalent to a pressure of 135 psi inside the kernel. Most f the water in the kernel is superheated at the moment of opping and provides the driving force for expanding the ernel once the pericarp ruptures. At temperatures below 77°C the proportion of kernels that have popped declines arkedly. SEM was used to document changes occurring in the ernel as a result of popping. In the translucent endosperm he superheated water appears to vaporize into the hilum, xpanding the starch to a thin film. In the opaque endosperm arge voids are produced and the starch granules remain irefringent. The voids around the starch provide an alterative site into which the superheated water vaporizes. hus, the starch granules are not expanded and retain their irefringence.

Copyright 1983 Academic Press Inc. (London) Limited.]

TUDIES ON THE SPECIFICITY OF INTERACTION OF CEREAL CELL ALL COMPONENTS WITH CONGO RED AND CALCOFLUOR. SPECIFIC ETECTION AND HISTOCHEMISTRY OF (1→3),(1→4) β-D-GLUCAN

ood PJ, Fulcher RG, Stone BA. 1983. Journal of Cereal cience 1(2), 95-110. [Food Res. Inst., Agric. Canada, Ottawa, Ontario, Canada K1A 0C6].

The (1→3),(1→4)-β-D-glucan (I) of oats (Avena sativa) induces major changes in the absorption and fluorescence pectra of the dyes Congo Red and Calcofluor, and is stained ntensely by these dyes. The interactions are not observed ollowing degradation of the polysaccharide by a specific β-glucan endohydrolase from Bacillus subtilis (EC.3.2.1.73) II). Spectral changes in the dyes, and staining as assessed y fluorescence microscopy, were observed with various cell reparations and polysaccharide fractions from oats, barley Hordeum vulgare), and wheat (Triticum aestivum), but were bolished following treatment with II, thereby establishing he specificity of the dye binding. Components other than I, uch as arabinoxylan, neither stained nor showed interaction n solution. The specificity of the dye-polysaccharide ineraction enabled the location of I to be identified as eing in the endosperm cell walls and inner walls of aleurone cells in oats, barley, and wheat.

Copyright 1983 Academic Press Inc. (London) Limited.]

YE INTERACTIONS - A BASIS FOR SPECIFIC DETECTION AND ISTOCHEMISTRY OF POLYSACCHARIDES

ood PJ, Fulcher RG. 1983. The Journal of Histochemistry and ytochemistry 31(6), 823-826. [Food Res. Inst., Agriculture anada, Ottawa, Ontario, Canada K1A 0C6].

Specific histochemical staining can be related to specific interactions of dyes and polysaccharides in solution. pecificity evidently depends upon polysaccharide conformaion and the need for a close "fit" between polysaccharide nd ligand. As a consequence, microscopic identification of ereal β-(1→4)(1→3)-D-glucan and β-(1→3)-D-glucan is possibe, and is demonstrated using Congo Red, Calcofluor, and niline Blue staining.

Copyright 1983 by the Histochemical Society, Inc.]

RODUCTION OF FLAT BREAD BY EXTRUSION COOKING USING DIFFERNT WHEAT/RYE RATIOS, PROTEIN ENRICHMENT AND GRAIN WITH POOR AKING ABILITY

ntila J, Seiler K, Seibel W, Linko P. 1983. Journal of Food ngineering 2(3), 189-210. [Tech. Res. Centre of Finland, ood Res. Lab., SF-02150 Espoo 15, Finland].

Flat-breadlike products were continuously produced on a reusot-Loire twin-screw extrusion-cooker using wheat and ye flours of different qualities, their mixtures and unmiled whole grain as raw materials. Feed rate and feed moisure contents were used as process variables. Soy protein, heat gluten, sodium caseinate, and milk powder were used as rotein sources in enrichment experiments. The effects of aw materials, ingredients, and process variables on specfic volume, degree of expansion, water content, breaking orce, sensory quality, and some other product characterisics on energy consumption were determined and are discused. Acceptable flat bread could be produced by extrusion ooking even from relatively poor quality raw materials. The esults are supported by numerous SEM micrographs.

PATTERNS OF MODIFICATION IN MALTING BARLEY

Briggs DE, MacDonald J. 1983. Journal of The Institute of Brewing 89(4), 260-273. [Dept. Biochem., Univ. of Birmingham, P.P. Box 363, Birmingham B15 2TT, U.K.].

The modified regions of the starch endosperms of malted grains were fragile and, in thin sections (LM), the cell walls in these regions did not stain readily with Congo Red or Trypan Blue, although SEM demonstrated some cell-wall material remained. Initially the enzymes causing modification came from the scutellum, but later more came from the aleurone layer. Patterns of modification in different grains differed significantly, but usually resembled those recorded previously except that often modification had advanced further by the nucellar sheaf cells.

In grains treated with gibberellic acid (I), modification advanced faster, particularly beneath the aleurone layer, after 2 days germination. In tumbled or commercially abraded grains malted with (I), modification was even more rapid, but in more than 99% of the grains the same patterns of modification occurred. Two-way modification was a rare event.

Decorticated grains modified exceptionally quickly and, when treated with (I), massive subaleurone modification occurred.

The cell walls of the tissues that resisted modification fluoresced strongly in uv light, in contrast to those of the starchy endosperm.

FLUORESCENCE MICROSCOPY OF CEREALS

Fulcher RG. 1982. Food Microstructure 1(2), 167-175. [Ottawa Res. Station, Agric. Canada, Ottawa, Ontario, Canada K1A 0C6].

The fluorescence microscope is one of the most sensitive instruments available for morphological and microchemical analysis of biological material, and especially of cereal grains. Recent innovations in illuminating systems, fluorescence chemistry, and specimen preparation have combined to provide significant improvements over conventional bright-field microscopy in both specificity and sensitivity. A variety of relatively specific fluorescent markers has been devised for routine and high resolution detection of all major cereal components. Several examples of useful fluorescent markers are described, including appropriate methods for specimen preparation, fluorescence analysis, and photography.

FREEZE-ETCH OF EMULSIFIED CAKE BATTERS DURING BAKING

Cloke JD, Gordon J, Davis EA. 1982. Food Microstructure 1 (2), 177-187. [Dept. Food Sci. & Nutr., Univ. of Minnesota, 1334 Eckles Ave., St. Paul, MN 55108, U.S.A.].

Cryofixation and freeze-etching techniques were used to study the structure of cake batters made from a lean cake formulation before heating and after heating to temperatures up to 100-102°C. Batters were prepared without added emulsifiers and with saturated and unsaturated monoglycerides (I) replacing 5 and 10% of the oil. Unsaturated I were more effective than saturated I in dispersing oil droplets through the batter. Saturated I formed liquid crystals during baking. The temperature at which starch granules began to swell was slightly higher for saturated I-containing cakes. The batter matrix between starch granules was more clearly defined in unsaturated I-containing cakes.

COMPUTERIZED IMAGE ANALYSIS OF SURFACE BROWNING OF PIZZA SHELLS

Unklesbay K, Unklesbay N, Keller J, Grandcolas J. 1983. Journal of Food Science 48(4), 1119-1123. [Dept. Electric Engineering, Univ. of Missouri, Columbia, MO 65211, U.S.A.].

An objective measurement using computerized image analysis technique was developed for determining the level of brownness on the bottom of surface of pizzas. Infrared heat processing (327/332°C) was investigated for both wheat and soy-fortified, wheat pizza shells. Moisture, fat, total and unavailable lysine were determined by chemical analysis. A linear function was developed which shows promise for predicting the available lysine content for soy-fortified shells. This function utilizes information taken from the image of the bottom of the pizza. This technique could be useful in cases where a rapid, nondestructive test for available lysine in baked dough is needed.

ULTRASTRUCTURE STUDIES OF PASTA. A REVIEW
Resmini P, Pagani MA. 1983. Food Microstructure 2(1), 1-12. [Istituto ind. agrarie, Univ. degli studi, Via Celoria 2, 20133 Milan, Italy].

Freeze-fracturing can be used effectively to study pasta microstructure both in the dry and cooked state. After a water-glycerol soaking, conventional raw wheat pasta shows an uncoagulated protein matrix in which the starch granules are uniformly dispersed. Starch granules appear unswollen with a spherulitic structure. Extensive protein denaturation and starch swelling may occur during processing when a temperature higher than 60°C is attained in drying. Extensive structural transformations take place in cooking. A fibrillar protein network which envelops gelatinized starch is the typical structure observed in cooked durum wheat spaghetti. In soft wheat products, however, there is a less extensive protein framework with more diffuse starch particles.

Pasta cooking quality is determined by a physical competition between protein coagulation into a continuous network (I) and starch swelling with spherulite scattering (II) during cooking. If the former (I) prevails, starch particles are trapped in the network alveoli promoting firmness in cooked pasta. However, if the latter (II) prevails, the protein coagulates in discrete masses lacking a continuous framework and pasta is soft and usually sticky. High temperature-low moisture (HT-LM) drying partially overcomes this competition by producing a coagulated protein framework in dry pasta without starch swelling.

HT-LM treatment induces protein-starch interactions and conformational changes in the fine structure of the starch granules during cooking. Linear and branched chain-like fibrils appear in the core of the granules and particle groupings in the outer area. A better understanding of the role of controlled starch modification which optimizes pasta processing permits better use of nonconventional raw materials in pasta preparation.

ENDOSPERM DEGRADATION IN BARLEY KERNELS THAT SYNTHESIZE α-AMYLASE IN THE ABSENCE OF EMBRYOS AND EXOGENOUS GIBBERELLIC ACID
MacGregor AW, Nicholls PB, Dushnicky L. 1983. Food Microstructure 2(1), 13-22. [Canad. Grain Comm., Grain Res. Lab., 1404-303 Main Street, Winnipeg, Manitoba, Canada R3C 3G8].

During germination at 16°C, whole seeds and distal half-seeds of Klages barley and two types of Clipper barley (Types A and B) were analyzed for α-amylase. Structural changes in the endosperms of these seeds and half-seeds were examined by SEM. In Clipper B half-seeds, α-amylase activity increased significantly, there was a detectable amount of starch granule hydrolysis and endosperm structure was markedly degraded. No starch hydrolysis and only trace amounts of α-amylase and endosperm degradation were detected in Clipper A and Klages half-seeds. There was significant α-amylase synthesis, starch hydrolysis, and endosperm degradation in germinated whole seeds of all 3 barley cultivars. Changes were most pronounced in Clipper B. Starch degradation appeared to start in areas of the endosperm close to the embryo.

SOME RECENT ADVANCES IN CEREAL PRODUCTS AS DIETARY FIBERS IN HUMAN NUTRITION
Inglet GE. 1982. Nippon Shokuhin Kogyo Gakkaishi 29(1), 55-61. [Northern Reg. Res. Center, Agric. Res. Service, U.S. Dept. Agric., Peoria, IL 61604, U.S.A.].

A review with SEM micrographs of milled corn bran particles retrieved from feces.

THE MICROSTRUCTURE OF POLISHED, MILLED AND AIR CLASSIFIED RICE AND RICE BRAN
Saio K, Noguchi A. 1983. Nippon Shokuhin Kogyo Gakkaishi 30(6), 331-338. [Nat. Food Res. Inst., Min. Agric., Forestry & Fisheries, 2-1-2 Kannondai, Yatabe, Tsukuba, Ibaraki, 305, Japan].

The microstructure of polished rice and its milled and air classified fractions was studied by SEM. The cells of rice endosperm, showing long rectangular column shapes, were distributed radially from the centre to the outer layer. Sonication of rice bran in the presence of n-hexane and successive milling and air classification appeared promising in producing a protein-rich flour.

STARCH

ALKALI GELATINIZATION OF STARCHES
Maher GG. 1983. Starch/Stärke 35(7), 226-234. [Northern Reg. Res. Center, Agric. Res. Service, U.S. Dept. Agric., Peoria, IL 61604, U.S.A.].

Grain starches, chemically or genetically modified grain starches, tuber starches, and some from other botanical sources were treated at room temperature in media containing a constant amount of water and NaOH. Appearances and viscosities of the mixtures were noted during a 7-day quiescent period. The point of complete gelatinization of the starch was deducible from the viscosity changes, as well as from visual observations. Although there were some noticeable differences between the starches, an NaOH-to-starch ratio of 3.5 to 3.8 meq./g should assure complete gelatinization within several hours or less. This alkali-to-starch ratio is compared to previous ratios expressed in the literature. A slight dependency of the ratio upon the starch concentration is indicated. The birefringence endpoint temperacure ranges of the starches were determined, and other implications from the experiments within the 21 materials are discussed.

PHYSICO-CHEMICAL PROPERTIES OF BLACK PEPPER STARCH
Bhat UK, Tharanathan RN. 1983. Starch/Stärke 35(6), 189-192. [Discipline Biochem. & Applied Nutr., Central Food Technol. Res. Inst., Mysore-570013, India].

Unusually small-sized (2-2.5 μm) starch granules were isolated from black pepper (Piper nigrum) in 25-38% yield. The granules having an amylose content of 18% were non-ionic in nature and exhibited low solubility and low swelling power in water, but high solubility in dimethoxy sulfoxide. The amylogram peak viscosity of the starch was about 530 B.U. with a very little setback (~550 B.U.) on cooling, indicating a stable linear molecule very strongly associated with amylopectin. X-ray diffraction patterns revealed the starch granules to be of the A-type.

IN VITRO DIGESTIBILITY OF NATIVE STARCH GRANULES OF SAMAI AND SANWA
Tharanathan RN, Paramahans SV, Tareen JAK. 1983. Starch/Stärke 35(7), 235-236. [Discipline Biochem. & Appl. Nutr., Central Food Technol. Res. Inst., Mysore-570013, India].

SEM revealed a range of enzyme degradation patterns in the title starch granules digested in vitro with glucoamylase and salivary α-amylase.

LIGHT MICROSCOPY PREPARATION TECHNIQUES FOR STARCH AND LIPID CONTAINING SNACK FOODS
Flint FO. 1982. Food Microstructure 1(2), 145-150. [Procter Dept. Food Sci., Univ. of Leeds, Leeds LS2 9JT, U.K.].

Many processed foods lack the structural integrity associated with biological tissue so that the conventional methods of preparation and staining used in LM may introduce misleading artifacts.

Taking as examples of starch-based processed foods, potato chips (UK potato crisp) and three distinct potato snack foods, methods for preparing and demonstrating the constituents present in cryosections of whole and masticated products are discussed. To show constituents in their true relative locations, vapor staining and polarized light are used. Iodine vapor staining indicates the extent of starch gelatinisation in the dry snack and it is also used to show the structural changes that occur on mastication. Osmium tetroxide vapor colours the liquid fat and polarized light indicates the presence of crystalline fats and intact starch granules.

[GELATINIZATION OF STARCH IN DRIED AZUKI ANN GRANULES] [In Japanese]
Ogawa T, Abe S, Kugimiya M. 1983. Nippon Shokuhin Kogyo Gakkaishi 30(6), 323-330. [Hiroshima Food Res. Inst., 12-70, Hijiyama-honmachi, Minami-ku, Hiroshima-shi, 730, Japan].

Gelatinization of starch in dried plain Azuki Ann granules, which were prepared from azuki bean (Phaseolus chrysanthos), during heating in the presence of water, was studied by measuring the swelling power, solubility, susceptibility to enzyme degradation, and loss of birefringence, and compared with gelatinization of several starches including azuki bean starch. The swelling power, solubility, and susceptibility to enzyme degradation of starch in Ann granules were extremely low.

VERSUCHE ZUR AUFKLÄRUNG DER STRUKTUR VON CITRATSTÄRKEN. 2. MITTEILUNG. STRUKTURMODELLE EINZELNER CITRONENSÄUREESTER DER AMYLOSE UND DES AMYLOPEKTINS [Attempts to explain the structure of citrate starches. 2. Structural models of individual citric acid esters or amylose and amylopectin]
Bleier J, Klaushofer H. 1983. Starch/Stärke 35(1), 12-15. [Univ. Bodenkultur, Inst. f. Lebensmitteltechnol., Peter-Jordan-Str. 82, A-1190 Vienna, Austria].

Starting from a cluster model of the amylopectin (scale 1:10^7) made from threads of wool and an amylose model built from parts of a molecule kit, some sterically possible citric acid esters of starch are shown in 2 dimensions, and the question of the existence of tri-esters of citrate starches is discussed.

THE STARCH OF PUERARIA TUBEROSA - COMPARISON WITH MAIZE STARCH
Soni PL, Agarwal A. 1983. Starch/Stärke 35(1), 4-7. [Forest Res. Inst. & Coll., Govt. of India, P. O. New Forest, Dehra Dun-248006, India].

Pueraria tuberosa starch was isolated from the tuber and purified. SEM of the starch showed polygonal shaped granules which were almost of the same particle size as those of maize starch. P. tuberosa has lower amylose content, almost the same gelatinization temperature range and water binding capacity, and a higher swelling and solubility compared to maize starch. Paste viscosity characteristics show high peak viscosity but also indicate fragile nature of granules in comparison to maize starch.

STUDIES ON STARCHES FROM NIGERIAN SORGHUM
Stark JR, Aisien AO, Palmer GH. 1983. Starch/Stärke 35(3), 73-76. [Dept. Brewing & Biol. Sci., Heriot-Watt Univ., Chambers St., Edinburgh EH1 1HX, Scotland, U.K.].

Two varieties of white Nigerian sorghum have been examined for total lipid, protein, and carbohydrate content. The levels of sucrose, raffinose, fructose, and glucose in the ungerminated grain were measured and the starches have been isolated and purified. Amylose-to-amylopectin ratios, solubility properties, gelatinization temperatures, and the size distribution of the granules were analyzed. Fractionation and chemical analyses of the large and small granules have revealed that the amylose-to-amylopectin ratios of both types of granules were similar.

CORRELATION OF MICROSCOPIC STRUCTURE OF CORN STARCH GRANULES WITH RHEOLOGICAL PROPERTIES OF COOKED PASTES
Christianson DD, Baker FL, Loffredo AR, Bagley EB. 1982. Food Microstructure 1(1), 13-24. [Northern Reg. Res. Center, Agric. Service, U.S. Dept. Agric., Peoria, IL 61604, U.S.A.].

The progressive geometric changes that occur in swelling of corn starch granules during heating throughout the range of gelatinization (63-72°C) and at higher temperatures when substantial amounts of soluble starch are released from the granule were observed by SEM. Corn starch granules begin to swell radially, then undergo radial contraction and random tangential expansion. They form complex geometrical structures at the midpoint range (67-70°C) unlike the more uniform single-dimensional tangential swelling that occurs with lenticular granules of wheat starch. At higher temperatures, when starch begins to solubilize, corn starch granules lose their distinct ridges and appear to melt into thin flat discs. These progressive configurational changes are reflected in the rheological properties of more concentrated starch dispersions cooked for 75 min. At the early stages of gelatinization (63-65°C) the granules are relatively rigid and at high enough concentration show dilatant behavior (viscosity increasing with shear rate). At these temperatures, granules remain rigid and maintain their birefringence but are mechanically sheared by stirring during cooking. Once the granules undergo extensive swelling, develop ridges, and lose their birefringence (67-70°C), they are soft enough to exhibit shear thinning behavior (viscosity decreasing with shear rate). The extent of shear thinning depends on concentration because viscosity and shear stress increase with concentration and the granules become more susceptible to deformation. At high enough concentrations (and associated stresses), the ridges are not as clearly defined as they are at lower concentrations. Granules become more flat and flexible when cooked above 75°C.

FLOW, MIXING AND RESIDENCE TIME DISTRIBUTION OF MAIZE STARCH WITHIN A TWIN-SCREW EXTRUDER WITH A LONGITUDINALLY-SPLIT BARREL
Colonna P, Melcion JP, Vergnes B, Mercier C. 1983. Journal of Cereal Science 1(2), 115-125. [Inst. Nat. Rech. Agronom., Centre Rech. Agro-Alim., Chemin de la Geraudiere, F-44072, Nantes-Cedex, France].

A longitudinally-split barrel was used to study the internal modification of maize starch during extrusion-cooking in a Creusot-Loire BC-72 twin-screw extruder. After steady state conditions were obtained, the extruder barrel was dismantled and samples were taken at points along the screws in order to study (LM and SEM) changes in starch granular structure and macromolecular levels in the different phase transition zones.

Mass transport is the predominant process in the extruder before the reverse flight section where communition is the major event. In the reverse flight zone, starch granules are progressively sheared and melted. Shear along the barrel surface causes rapid cooking, with the formation of a glassy phase. The results show that the combined effect of shear, together with heat and pressure, are mainly responsible for starch modifications. The residence time distribution is a function of extruder size.

PHYSICOCHEMICAL CHANGES IN CORN STARCH AS A FUNCTION OF EXTRUSION VARIABLES
Owusu-Ansah J, van de Voort FR, Stanley DW. 1983. Cereal Chemistry 60(4), 319-324. [Dept. Food Sci., Univ. of Guelph, Guelph, Ontario, Canada N1G 2W1].

The effect of primary extrusion variables, that is temperature, feed moisture, and screw speed, on the gelatinization, water absorption index, water solubility, and cooked viscosity of cornstarch was studied. All the physicochemical characteristics measured except water solubility were significant in their 1st or 2nd order terms. The responses measured were linearly and quadratically related to the variables and accounted for more than 90% of the total variation. Water solubility was not quadratically related to the extrusion variables but increased with increasing temperature and moisture content. The overall physicochemical results indicated some hydrolytic breakdown of starch during extrusion. SEM and X-ray diffractometry were used in examining the milled extrudates.

BARLEY STARCH. VII. NEW BARLEY STARCHES WITH FRAGMENTED GRANULES
DeHaas BW, Goering KJ. 1983. Cereal Chemistry 60(4), 327-329. [Dept. Plant and Soil Sci., Montana State Univ., Bozeman, MT 59717, U.S.A.].

Franubet and Wafranubet are new barley varieties characterized by small, fragmented starch granules. Pasting characteristics and other properties of the starches were compared with those of Betzes and Nubet starches. The Franubet and Wafranubet starches are more resistant to attack by α-amylase than are barley starches with normal granule configuration. Both starches show normal swelling power, but waxy starches such as that from Wafranubet usually have higher swelling values.

CHANGES IN THE STARCH FRACTION DURING EXTRUSION-COOKING OF CORN
Gomez MH, Aguilera JM. 1983. Journal of Food Science 48(2), 378-381. [Food Protein R & D Center, Texas A & M Univ., College Station, TX 77843, U.S.A.].

Whole ground corn was extruded at 23.7, 18.5, 15.4, 13.9, and 7.6% moisture contents (EMC). Decreasing EMC resulted in increases in water solubility index (WSI), enzyme susceptibility (ES), degree of gelatinization and blue values, while water absorption index and water-insoluble carbohydrates decreased. ES and WSI of several blends prepared by combining raw (R), gelatinized (G), and dextrinized (D) corn were compared to those of extruded products. Corn extrudates had properties similar to blends containing G and D corn only. The relative proportion of D corn increased from about 10 to 60%, as EMC decreased. "Dextrinization" appears to become the predominant mechanism of starch degradation during low-moisture, high-shear extrusion. Viscoamylographs, SEM, and LM support these findings.

MEAT

THE FUNCTIONALITY OF SOY PROTEIN CONCENTRATE IN CANNED LUNCHEON MEAT

Schmidt GR, Means WJ, Herriot DF, Miller BF. 1983. Lebensmittel-Wissenschaft und -Technologie 16(1), 55-58. [Dept. Anim. Sci., Colorado State Univ., Fort Collins, CO 80523, U.S.A.].

The objective of this work was to determine the functional properties of STA-PRO 3200 soy protein concentrate (SPC) in a water and pork backfat emulsion that is subsequently blended into a canned luncheon meat formulation. Batches of luncheon meat were formulated with either 4, 2, or 0% SPC, 2 or 1% NaCl, 0.5% sodium tripolyphosphate, 20% water, 30% pork backfat, 15% pork (50% lean), and 30% pork (90% lean). Fat emulsion was prepared by chopping SPC, water, and pork backfat to 12°C. Lean pork was ground through a 4.8 mm plate and fat pork was ground through a 3.2 mm plate, combined, and premixed with the salt and phosphate for 3 min in a vacuum mixer. The fat emulsion was then added to the mixer and vacuum-mixed for an additional 3 min. The product was canned in 301x401 cans and either pasteurized in 76.5°C water to an end point of $F^5_{65.6}$ = 15 or sterilized in steam at 115.6°C to an end point F_0 = 6.0. Addition of 4% SPC significantly reduced the amount of moisture released during pasteurization and sterilization. Addition of 4% SPC also reduced the amount of fat and moisture cookout in the pasteurized product by 31% and in the sterilized product by 33%. There was no effect of salt level. The pasteurized product had significantly less cookout than the sterilized product.

ON THE MECHANISM OF WATER HOLDING IN MEAT: THE SWELLING AND SHRINKING OF MYOFIBRILS

Offer G, Trinick J. 1983. Meat Science 8, 245-281. [Muscle Biol. Div., Agric. Res. Council, Meat Res. Inst., Langford, Bristol BS18 7DY, U.K.].

Water holding in meat has, in the past, been rather poorly understood and has not been explained at all in structural terms. A unifying hypothesis for this phenomenon is that gains or losses of water in meat are due simply to swelling or shrinking of the myofibrils caused by expansion or shrinking of the filament lattice.

Myofibrils have been observed by phase contrast microscopy, and are seen to swell quickly to about twice their original volume in salt solutions resembling those used in meat processing. Such swelling is highly co-operative. Pyrophosphate (I) reduces very substantially the NaCl concentration required for maximum swelling. In the absence of I, swelling is accompanied by extraction of the middle of the A-band; in its presence, the A-band is completely extracted, beginning from its end.

The authors suppose that Cl^- ions bind to the filaments and increase the electrostatic repulsive force between them. A crucial factor in swelling is likely to be the removal at a critical salt concentration of one or more transverse structural constraints in the myofibril (probably cross-bridges, the M-line or the Z-line) allowing the filament lattice to expand. The authors also point out that water losses in rigor, in the PSE condition, and on cooking may well result directly from shrinkage of the filament lattice. [Copyright 1983 by Applied Science Publishers Ltd., England].

MACROSCOPIC WRINKLING OF MUSCLE FIBRES, A SOURCE OF ERROR IN OBJECTIVE ASSESSMENT OF MEAT TOUGHNESS

Rowe RWD. 1982. Meat Science 6, 149-158. [CSIRO Div. Food Res., Meat Res. Lab., P.O. Box 12, Cannon Hill, Queensland, 4170 Australia].

Post-rigor shortening of muscle resulting in macroscopic fibre wrinkling was studied in muscle samples which entered rigor restrained in a stretched condition and were subsequently freed. The amount of wrinkling varied with the initial degree of stretch pre rigor and with the muscle treatment post rigor, depending on such variables as (1) whether or not the muscle was heated and (2) if heated, at what stage the restraint was removed. The consequences of fibre wrinkling relative to the objective testing of meat toughness are discussed.

FUNCTIONALITY OF MUSCLE CONSTITUENTS IN THE PROCESSING OF COMMINUTED MEAT PRODUCTS

Acton JC, Ziegler GR, Burge DL Jr. 1983. Critical Reviews in Food Science and Nutrition 18(2), 99-121. [Dept. Food Sci., Clemson Univ., Clemson, SC 29631, U.S.A.].

Comminuted meat systems represent a complex matrix of constituent interactions where physical and chemical properties of constituents determine the ultimate stability of the product. The functionality of the myofibrillar proteins varies with extent of extractability, and ionic and pH conditions. Primary functional responses of water binding (protein-water interaction), fat holding and emulsification (protein-lipid interaction), and gelation (protein-protein interaction) are also temperature-dependent in the course of processing sequences encountered during comminution and heat processing. Basic concepts and results of applied studies have been critically reviewed to emphasize the interaction effects of the myofibrillar proteins as the predominant constituent controlling the extent of formation and behaviour of the comminuted meat matrix. SEM and TEM; 79 references.

CHARACTERISTICS OF PRE-RIGOR PRESSURIZED VERSUS CONVENTIONALLY PROCESSED BEEF COOKED BY MICROWAVES AND BY BROILING

Riffero LM, Holmes ZA. 1983. Journal of Food Science 48(2), 346-350, 374. [Dept. Foods & Nutr., Oregon State Univ., Corvallis, OR 97331, U.S.A.].

Paired beef semitendinosus portions (86 g) processed either conventionally or by pre-rigor pressure were broiled or microwave cooked. Pre-rigor pressure-treated cooked beef portions were higher ($P<0.05$) than untreated portions in total moisture, pH, exterior color a+ values and subjective tenderness and ease of fiber separation scores than did the untreated portions. Total moisture, drip cooking loss, interior a+ (redness) color value, and exterior L (lightness) and b+ (yellowness) color values were significantly higher in the microwaved beef portions as compared to the broiled portions. Neither juiciness nor flavor of samples were influenced ($P<0.05$) by treatment or by cooking method. SEM indicated differences in microstructure due to cooking and pressure treatment.

USE OF VACUUM DURING FORMATION OF MEAT EMULSIONS

Tantikarnjathep K, Sebranek JG, Topel DG, Rust RE. 1983. Journal of Food Science 48(4), 1039-1041, 1052. [Dept. Animal Sci., Iowa State Univ., Ames, IA 50011, U.S.A.].

Meat emulsion formation under vacuum was studied in a model system and in a sausage emulsion. Sarcoplasmic and myofibrillar extracts from beef and pork infraspinatus muscle were used to compare emulsification of vegetable oil with or without vacuum. Vacuum treatment permitted more oil to be emulsified by all protein extracts. The proportional increase was greater for water-soluble than for salt-soluble extracts. Sausage emulsion was evaluated using frankfurters prepared in a vacuum chopper with or without vacuum. Product stability was improved by application of vacuum only for the entire chopping procedure. Cured color development was more rapid and more complete in the vacuum treatment. Without vacuum chopping, frankfurters showed more obvious cavitation and less density, confirming presence of air within the emulsion.

EFFECTS OF LOW FREQUENCY ULTRASOUND ON PROPERTIES OF RESTRUCTURED BEEF ROLLS

Vimini RJ, Kemp JD, Fox JD. 1983. Journal of Food Science 48(5), 1572-1573. [Food Sci. Section, Dept. Animal Sci., Univ. of Kentucky, Lexington, KY 40546, U.S.A.].

The effects of low frequency ultrasound on exudate yield, breaking strength, cooking yield, water-holding capacity, color, and muscle microstructure were investigated by exposing pieces of lean muscle to slow tumbling and low frequency ultrasonic waves. Results indicated that beef rolls exposed to low frequency ultrasound without added salt were superior in breaking strength and cooking yield to those tumbled with neither ultrasound nor salt and were comparable in breaking strength, cooking yield, and water-holding capacity to those tumbled with salt and no ultrasound exposure. Furthermore, the beef rolls exposed to ultrasound and no salt were superior in color to those to which salt was added. Low frequency ultrasound caused muscle fiber disruption and separation of up to approximately 1 cm in depth in muscle microstructure in the pieces of lean muscle.

EINFRIEREN UND AUFTAUEN VON FLEISCH: EINFLÜSSE AUF MUSKELGEWEBE UND TAUSAFTBILDUNG [Freezing and thawing of meat: Effects on the muscle tissue and development of thaw juice] Hamm R, Gottesmann P, Kijowski J. 1982. Fleischwirtschaft 62(6), 983-991. [Inst. f. Chem. & Phys., Bundesanstalt f. Fleischforschung, E.-C.-Baumann-Str. 20, D-8650 Kulmbach, Federal Republic of Germany].

A review on the effects of freezing and thawing rates on muscle structure (TEM and line drawings), effects of osmotic pressure, protein denaturation, and damage to membranes during freezing, and on methods capable to distinguish fresh meat from thawed frozen meat.

VISUALIZATION OF FREEZE-DRIED AND SHADOWED MYOSIN MOLECULES IMMOBILIZED ON ELECTRON MICROSCOPIC FILMS
Walzthöny D, Bähler M, Wallimann T, Eppenberger HM, Moor H. 1983. European Journal of Cell Biology 30(2), 177-181. [Inst. f. Zellbiol., ETH-Hönggerberg, CH-8093 Zurich, Switzerland].

The standard mica replication technique has produced myosin molecules which were heterogeneous in appearance in terms of shadowing, decoration, contrast, and background. Therefore, an alternative technique for the visualization of myosin molecules was developed: Myosin molecules are sprayed directly onto glow-discharged or silicium monoxide-coated carbon film grids, omitting glycerol. After washing several times with distilled water, rapid freezing, and freeze-drying, the immobilized myosin molecules are visualized by shadow-casting at low temperature and at varying angles. After backing with carbon, the in situ shadowed molecules are observed by EM. This technique has several advantages over the standard method in that it yields more reproducible results. It is potentially useful for investigating interactions of myosin-binding proteins with myosin and for visualizing unshadowed myosin in the STEM.

RAPID FREEZING OF UNPRETREATED TISSUES FOR FREEZE-FRACTURE ELECTRON MICROSCOPY
Severs NJ, Green CR. 1983. Biology of the Cell 47(2), 193-204. [Dept. Card. Med., Cardiothor. Inst., Univ. of London, 2 Beaumont St., London WIN 2DX, U.K.].

A technique for freezing unfixed uncryoprotected tissues from a condition close to that existing in vivo is described. Using a pre-aligned specimen holder clamp system, the tissue is mounted before its excision from a living tissue. Freezing is completed within 2 sec of excision of the sample by manual plunging of the specimen sandwich into liquid propane. Specific conditions were applied to optimise freezing by this method and are essential for its effectiveness. A freeze-fracture survey of various tissues prepared by this technique demonstrates the quality of cryopreservation routinely obtainable. Examination of the directly frozen material reveals some differences in membrane structure compared with pretreated specimens, emphasizing the importance of avoiding pretreatment in freeze-fracture studies. The simplicity of this approach, coupled with its effectiveness, should encourage its adoption as a routine laboratory procedure for those attempting the freeze-fracture examination of directly frozen biological specimens.

[A REVIEW OF THE ABNORMAL CONDITIONS OF FISH MEAT: JELLIED MEAT AND YAKE-NIKU, SPONTANEOUSLY DONE MEAT] [In Japanese] Konagaya S. 1982. Nippon Shokuhin Kogyo Gakkaishi 29(6), 379-388. [Preserv. Div., Tokai Reg. Fish. Res. Lab., 5-5 Kachidoki, chuo-ku, Tokyo, 104, Japan].

Micrographs of various defects in the fish meat are presented.

[EFFECTS OF MAIN REGULATORY PROTEINS ON THE HEAT-INDUCED GEL FORMABILITY OF MYOSIN B] [In Japanese]
Haga S, Ohashi T. 1982. Nippon Shokuhin Kogyo Gakkaishi 29(12), 700-705. [Fac. Agric., Miyazaki Univ., Miyazaki-shi, 880, Japan].

The heat-induced gel formabilities of myosin B (natural actomyosin) and washed actomyosin (which was prepared by removing main regulatory proteins, i.e., tropomyosin and troponin, from natural actomyosin) were investigated. Differences between rheological properties of both proteins were reflected by the microstructure and solubility of the gels. It was concluded that both regulatory proteins had no effect on the heat-induced gel formability of myosin B.

MYOFIBRILS OF COOKED MEAT ARE A CONTINUUM OF GAP FILAMENTS
Locker RH, Wild DCJ. 1982. Meat Science 7, 189-196. [Meat Ind. Res. Inst. of New Zealand (Inc.), P.O. Box 617, Hamilton, New Zealand].

When cooked meat is subjected to high degrees of stretch, it becomes apparent in high magnification electron micrographs that A-filaments have ceased to exist. The A-band is filled with a coagulum of actomyosin. Fragmentation of this coagulum during stretch reveals an array of fine filaments (identified as gap filaments). This result is obtained irrespective of rigor temperature, state of contraction or degree of cooking. If the meat is first aged, the gap filaments surviving in the I-band are too weak to open up the A-band. The results show that myofibrils in cooked meat are entirely dependent on heat-stable gap filaments for structural continuity and tensile strength. Theories of meat tenderness must be revised accordingly. [Copyright 1982 by Applied Science Publishers Ltd., England].

YIELD POINT IN RAW BEEF MUSCLE. THE EFFECTS OF AGEING, RIGOR TEMPERATURE AND STRETCH
Locker RH, Wild DJC. 1982. Meat Science 7, 93-107. [Meat Ind. Res. Inst. of New Zealand, P.O. Box 617, Hamilton, New Zealand].

The yield point of raw sternomandibularis muscle of the ox decreased markedly with ageing. This parameter is the most sensitive and selective indicator of ageing since, unlike shear measurements on cooked meat, it is not complicated by heat denaturation or the contribution of the collagen net.

Rigor at 2°C with consequent cold shortening has little effect on yield point, but rigor at 37°C diminishes yield values relative to the 15°C controls. Muscle stretched by 40-60% during rigor show higher yield points.

Yield was also studied in other muscles. Unaged strips of bull sternomandibularis, or steer psoas and rectus abdominis tended to break rather than yield, but after ageing usually yielded at the same low loads as aged ox sternomandibularis.

The histological changes due to yielding varied widely, but stretched, rather than broken, I-bands were the dominant feature. Our interpretation of the electron micrographs is that in rigor muscle, actin filaments fracture while gap filaments stretch, but in aged muscle both sets of filaments fail simultaneously at low loads. [Copyright 1982 by Applied Science Publishers Ltd., England].

MUSCLE FIBRE DEFORMATION: RIGOR EXTENSIBILITY OF RAW BOVINE MUSCLE
Rowe RWD. 1982. Meat Science 6, 199-209. [CSIRO Div. Food Res., Meat Res. Lab., P.O. Box 12, Cannon Hill, Queensland, 4170 Australia].

Muscle which entered rigor restrained in a stretched condition shortened when freed, resulting in 3 types of wrinkling: (1) fibre wrinkling, (2) myofibril wrinkling, and (3) myofilament wrinkling. The structural consequences of stretching muscle whilst it was in rigor were studied by light and electron microscopy. Rigor extension of contracted or stretched samples in excess of that required to straighten any wrinkles resulted in three types of damage to a high proportion of the sarcomeres. (1) Breaks occurred in the I bands, but not the clean breaks associated with post-rigor muscle. (2) Breaks occurred in the A bands on either side of the M line. (3) Z lines were pulled apart.

AN ALTERNATIVE TO CRITICAL POINT DRYING FOR PREPARING MEAT EMULSIONS FOR SCANNING ELECTRON MICROSCOPY
Basgall EJ, Bechtel PJ, McKeith FK. 1983. Food Microstructure 2(1), 23-26. [Depts. Animal Sci. & Food Sci., Muscle Biol. Lab., Univ. of Illinois, 1503 South Maryland Drive, Urbana, IL 61801, U.S.A.].

A rapid sample drying technique is described which is useful for the simultaneous preparation of large numbers of samples as an alternative to critical point drying. The cryofractured face of meat emulsions was visualized after applying this technique. The fine structure of lipids and proteins was found to be well preserved in comparison to other reports which used critical point dried meat emulsions. Lipid was readily discerned from the protein matrix by selective fixation of the components in duplicate samples. Stereo imaging was useful in enhancing the texture of the cryofractured surface and as an aid in differentiating the protein matrix from the fat component of meat emulsions.

THE COOKING OF SINGLE MYOFIBRES, SMALL MYOFIBRE BUNDLES AND MUSCLE STRIPS FROM BEEF M. PSOAS AND M. STERNOMANDIBULARIS MUSCLES AT VARYING HEATING RATES AND TEMPERATURES
Bendall JR, Restall DJ. 1983. Meat Science **8**, 93-117. [ARC, Meat Res. Inst., Langford, Bristol BS18 7DY, U.K.].

When single myofibres are heated in an aqueous medium up to temperatures of 90°C at pH 5.5, they do not shorten but instead decrease in diameter. This decrease begins slowly at 40°C and reaches a maximal rate and extent at 60°C, when the myofibre volume has decreased to 50% of the initial volume and about 60% of the cell water has been expelled. The myofibres behave similarly when the pH of the medium is raised to 6.8, but the loss of cell water is considerably less (about 42%).

When small myofibre bundles are heated from 10 to 60°C, they behave similarly to single myofibres by decreasing, in diameter only, from 40 to about 60°C. At the latter temperature their volume has decreased to 60% of the initial value and about 48% of the bundle water has been expelled. Above 64°C the bundles shorten, the shortening reaching about 30% of the initial length at 90°C. This shortening, combined with the diameter decrease, leads to a volume decrease to 43% of the initial value and to a loss of about 68% of the cell water. [Copyright 1982 by Applied Science Publishers Ltd., England].

RATE OF FREEZING EFFECT ON THE COLOUR OF FROZEN BEEF LIVER
Zaritzky NE, Añon MC, Calvelo A. 1982. Meat Science **7**, 299-312. [Centro Invest. Desarollo Criotec. Alim. - UNLP-CONICET-CIC, Fac. Ciencias Exactas 47 y 115, La Plata (1900), Argentina].

One problem that arises when freezing liver in plate freezers is the whitish colour acquired by the liver surface when subjected to high freezing rates. The purpose of this paper aims to establish optimum operating conditions for freezing beef liver pieces in a minimum time while maintaining the acceptable colour on the surface.

Samples were subjected to different freezing rates and minimum surface freezing time was established in order to obtain an acceptable colour. This was quantified in terms of lightness using a surface colorimeter. Histological analysis of the samples showed that the size of the ice crystals formed on the contact surface with the coolant is the factor that determines the changes in colour as a result of diffused light reflection phenomena.

On the basis of mathematical heat transfer models with simultaneous change of phase, the minimum characteristic surface freezing time was related to the process operating variables (initial temperature of the liver, coolant temperature, interfacial heat transfer resistance, thickness of the piece), and the optimum freezing conditions were determined, reducing total processing times to a minimum. [Copyright 1982 by Applied Science Publishers Ltd., England].

EFFECT OF HIGH HYDROSTATIC PRESSURE ON MEAT MICROSTRUCTURE
Elgasim EA, Kennick WH. 1982. Food Microstructure 1(1), 75-82. [Clark Meat Sci. Lab., Oregon State Univ., Corvallis, OR 97331, U.S.A.].

Bovine longissimus muscle was prerigor pressure treated at 103.5 MNm^{-2} at 37°C for 2 min and immediately sampled, fixed, and examined by LM, SEM, and TEM. Parameters like pH, Warner-Bratzler shear force values, and sarcomere length were measured and related to the microscopic observations. Pressure treated samples have shorter sarcomere length and lower pH and W-B values. Physical changes include separation of sarcolemmal and endomysial sheath, contraction bands, disruption of myofibrillar structure, and increased interfibrillar and intermyofibrillar spaces. At the subcellular levels, disappearance of glycogen granules, appearance of swollen mitochondria, sarcoplasmic reticulum, and in some cases ruptured mitochondria were observed. These morphological changes in mitochondria and sarcoplasmic reticulum should furnish the additional Ca^{2+} to account for the pressure-induced contraction. The interactions between the chemical and physical effects should account for the tenderizing effect of pressure treatment.

ELECTRON MICROSCOPIC INVESTIGATION OF PSEUDOMONAS FRAGI ATCC 4973 ON INTACT AND SARCOPLASM-DEPLETED BOVINE LONGISSIMUS DORSI MUSCLE AT 21°C
Lee Wing P, Yada RY, Skura BJ. 1983. Journal of Food Science 48(2), 475-478, 500. [Dept. Food Sci., Univ. of Brit. Columbia, Ste. 248-2357 Main Mall, Vancouver, British Columbia, Canada V6T 2A2].

SEM and TEM were used to investigate formation and role of glycocalyx material involved in adhesion of Pseudomonas fragi to intact and sarcoplasm-depleted beef surfaces. Depletion of sarcoplasm did not decrease attachment of P. fragi to bovine muscle. P. fragi caused a rapid increase in pH of only intact muscle. Examination of inoculated muscle (washed and intact) by SEM after 1, 2, 3, or 5 day incubation periods revealed a pebbling effect on the bacterium surface as well as a coiling of glycocalyx material. TEM showed 2 types of polymeric material: one was adherent to the bacterial surface while the other was amorphous. The amorphous type probably corresponded to the coiled glycocalyx revealed by SEM. Close association between glycocalyx and bleb-like evaginations on P. fragi reinforces previous hypotheses concerning their role and functions in attachment and meat spoilage.

FREEZE-INDUCED FIBRE FORMATION IN PROTEIN EXTRACTS FROM RESIDUES OF MECHANICALLY SEPARATED POULTRY
Lawrence RA, Jelen P. 1982. Food Microstructure 1(1), 91-97. [Dept. Food Sci., Univ. of Alberta, Edmonton, Alberta, Canada T6G 2P5].

Coagulated protein obtained by alkali extraction and acid precipitation from bone-containing residues discarded after mechanical separation of chicken was textured by freezing in semi-infinite cylinders followed by heat-setting in a microwave oven. Macrophotography was used to illustrate textural differences resulting from pH variations (4.5-6.0) in the precipitated protein, and changes in the ambient temperature used for freezing (-5 to-32°C). Well-identified, permanent fibres were formed by the process under all conditions studied. The thickness of the fibres decreased and their radial orientation increased with increasing pH and decreasing ambient temperature of freezing. Cross-linkages between parallel fibres of the main fibre structure were observed primarily as a function of pH, high pH samples showing the highest tendency for formation of these cross-links.

INSTRUMENTAL AND SENSORY ANALYSIS OF THE ACTION OF CATHEPTIC ENZYMES ON FLAKED AND FORMED BEEF
Cohen SH, Segars RA, Cardello A, Smith J, Robbins FM. 1982. Food Microstructure 1(1), 99-105. [Sci. & Advanced Technol. Lab., U.S. Army Natick R & D Labs., Natick, MA 01760, U.S.A.].

Texture profile analysis, Instron punch and die testing, laser diffraction measurements, and SEM were used to evaluate the effects of cathepsic enzymes on flaked and formed beef. Although salt (NaCl) and sodium tripolyphosphate (TPP) have often been used to improve the textural quality of flaked and formed beef, the cathepsic enzymes used in this study were shown to be as effective as NaCl/TPP, and in many cases more effective, in improving the textural characteristics of this product. Instron punch and die and SEM analyses showed that the enzyme and NaCl/TPP samples were quite similar; however, laser diffraction measurements of sarcomere lengths were significantly lower for the enzyme-treated samples. Also, various textural parameters including the amount of connective tissue were significantly improved by the cathepsic enzyme treatment.

IMAGE ANALYSIS OF MORPHOLOGICAL CHANGES IN WIENER BATTERS DURING CHOPPING AND COOKING
Kempton AG, Trupp S. 1983. Food Microstructure 2(1), 27-42. [Dept. Biol., Univ. of Waterloo, Waterloo, Ontario, Canada N2L 3G1].

Histological changes in wiener batters during chopping and cooking have often been illustrated with "representative" fields. The practice of selecting representative fields ignores variation and leads to word descriptions that cannot be correlated with numeric scores for functional or sensory tests. If wieners are regarded as a multi-component system, objectivity can be achieved by selecting many fields for each sample according to a rigid sampling plan. Image analysis quantified parameters of both the fat and protein components. The reduction in size of fat globules during chopping of a commercial formulation, for example, was a function of area and aggregate perimeter of several hundred globules compiled by a computer. There was no relationship between wiener firmness and any feature of the microstructure; but even at a low magnification of 30x, several statistically different factors were exposed during this survey which require further study.

FATS AND OILS

THE FREEZE FRACTURE ULTRASTRUCTURE OF PEANUT OIL AND OTHER NATURAL AND SYNTHETIC TRIACYLGLYCEROL DROPLETS
Rigler MW, Roth IL, Kritchevsky D, Patton JS. 1983. Journal of the American Oil Chemists Society 60(7), 1291-1298. [Dept. Microbiol., Univ. of Georgia, Athens, GA 30602, U.S.A.].

The freeze fracture morphology of some emulsified natural and synthetic triacylglycerol oils was examined. Emulsions were frozen by 2 methods, immersion in liquid melted Freon 22 (rate ~100 K/sec) or by a jet of liquified propane (rate ~10,000 K/sec). Emulsion droplets appeared spherical regardless of freezing method. Droplets frozen with propane appeared featureless in cross-fracture and demonstrated smooth cores regardless of oil type. Those frozen by immersion possessed core exhibiting lamellae embedded in an amorphous matrix. Pure unsaturated oils such as triolein appeared structureless regardless of freezing rate, whereas natural oils exhibited characteristic morphologies which were partially related to their saturated fatty acid content. Immersion-frozen peanut oil possessed, in addition to interior lamination, distinct surface laminations regardless of droplet size, emulsion preparation technique, or buffer pH. The laminations were 100 Å thick and extended 3-15 layers deep into the droplet and were caused by long chain C_{20}, C_{22}, and C_{24} fatty acids. Six kinds of peanut oil were examined and their droplet surface laminations could be grouped into 3 structural classes. There was no correlation between structural features of the peanut oils and their atherogenicity. The type of surface lamination that a peanut oil exhibited appeared to be related to its ratio of oleic to linoleic acid. The cryoprotectant glycerol was soluble in olive oil to <0.1% and produced no morphological alterations of the droplet.

ELECTRON MICROSCOPY OF LIPID-PROTEIN MONOLAYERS
Cornell DG, Carroll RJ. 1983. Colloids and Surfaces 6, 385-393. [Eastern Reg. Res. Center, Agric. Res. Service, U.S. Dept. Agric., 600 E. Mermaid Lane, Philadelphia, PA 19118, U.S.A.].

Mixtures of phospholipids with β-lactoglobulin (I) were spread from acidic chloroform : methanol onto the surface of a film balance, then transferred to freshly cleaved mica at 15 mN/m for examination under an EM. Dipalmitoylphosphatidylcholine and dipalmitoylphosphatidic acid did not mix with I and were visible as separate phases in the electron micrographs of the transferred films. Mixed monolayers containing either unsaturated lipids or dimyristoylphosphatidylcholine mixed with I gave completely homogeneous micrographs with no evidence of phase separation. The results suggest that phase separation occurs in monolayers of phospholipid-I when the films are prepared under conditions where the pure lipid exhibits liquid condensed behavior at the air-water interface. Homogeneous lipid-protein films apparently result when the monolayers are prepared under conditions where the lipid exhibits expanded behavior. [Copyright 1983 by Elsevier Science Publishers B. V.]

MICROSCOPY IN THE STUDY OF FATS AND EMULSIONS
Peman JM. 1982. Food Microstructure 1(2), 209-222. [Dept. Food Sci., Univ. of Guelph, Guelph, Ontario, Canada N1G 2W1].

Plastic fats consist of a three-dimensional network structure of crystals in which oil is trapped. This crystal network is held together by weak attractive forces, the nature of which is not definitely established. Crystal size is dependent on temperature history and is subject to polymorphic transitions which greatly affect the microstructure of the system. The microstructure of fats has been investigated by using polarized LM, EM, and X-ray diffraction analysis. Recently, a permeametric method has been developed which enables the determination of the specific surface area of the crystals in a fat. This method is a useful complement of the microscopic techniques. SEM has not been widely used in studying fat crystal structures. The use of microscopy in the study of microstructure of emulsions presents even greater problems than in the fat field. Emulsifiers may form liquid crystalline mesophases which may be studied by polarized light microscopy and X-ray diffraction analysis.

SOME EFFECTS OF LIPIDS ON THE STRUCTURE OF FOODS
Larsson K. 1982. Food Microstructure 1(1), 55-62. [Dept. Food Technol., Univ. of Lund, Box 740, S-220 07 Lund, Sweden].

The functional properties of different lipids in foods are demonstrated and related to the structure of lipid of lipid-water phases. On the basis of new X-ray data on the crystal structure of the β'-form and the α → β' transition in fats, the polymorphic transitions are considered as different lateral arrangements of triglyceride dimers. The physical properties of fat crystals can be explained from the structures, as well as possibilities to influence the polymorphic transitions.

Molecular interaction between polar lipids and proteins or starch is discussed, and the effect of the amylose-lipid inclusion complex on gelatinization temperature and water penetration of starch is demonstrated.

Aqueous phases of polar lipids can form different structures, and the lamellar liquid-crystalline phase is the most important one with regard to functionality in foods. The role of this phase in emulsification and in foam stabilization is considered. The effect of lipids in the bread-making process can be fully explained on the basis of foam stabilization by lipid monolayers provided by a dispersed lipid-water phase. A cubic phase, which can solubilize large amounts of proteins, is described in addition.

TECHNIQUES

THE USE OF HIGH VOLTAGES AND THICK SECTIONS IN BOTANICAL ELECTRON MICROSCOPY
Harris N. 1982. In: New Frontiers In Food Microstructure, D.B. Bechtel (ed.), The Am. Assoc. of Cereal Chemists, Inc., St. Paul, MN 55121, U.S.A., 287-314. [Dept. Bot., Univ. of Durham, Durham DH1 3LE, U.K.].

A review of sample preparation techniques, botanical studies, 3-D recording and reconstruction, and quantitation. Many references.

MICROANALYSIS OF SEED TISSUE
Lott JNA. 1982. In: New Frontiers In Food Microstructure, D.B. Bechtel (ed.), The Am. Assoc. of Cereal Chemists, Inc., St. Paul, MN 55121, U.S.A., 317-338. [Biol. Dept., McMaster Univ., Hamilton, Ontario, Canada L8S 4K1].

A review with sections on wavelength dispersive spectroscopy, energy dispersive X-ray analysis, preparing samples for X-ray microanalysis, examples of X-ray microanalytical studies of seed tissues, studies of crystals and other mineral deposits, phytin deposits and heavy metal uptake or contamination, and electron energy loss spectroscopy.

STARCH ULTRASTRUCTURE
Hood LF, Liboff M. 1982. In: New Frontiers In Food Microstructure, D.B. Bechtel (ed.), The Am. Assoc. of Cereal Chemists, Inc., St. Paul, MN 55121, U.S.A., 341-370. [Dept. and Inst. of Food Sci., Cornell Univ., Ithaca, NY 14853, U.S.A.].

A review of SEM and TEM, including artefacts, illustrated with 40 figures.

QUANTITATIVE IMAGE ANALYSIS
Oney D. 1982. In: New Frontiers In Food Microstructure, D.B. Bechtel (ed.), The Am. Assoc. of Cereal Chemists, Inc., St. Paul, MN 55121, U.S.A., 373-385. [Cambridge Instruments, Inc., 40 Robert Pitt Drive, Monsey, NY 10952, U.S.A.].

Description of work using a Quantimet 900 digital image analyzer and LM and TEM micrographs.

ASPECTS OF SAMPLE PREPARATION FOR FREEZE-FRACTURE/FREEZE-ETCH STUDIES OF PROTEINS AND LIPIDS IN FOOD SYSTEMS. A REVIEW
Buchheim W. 1982. Food Microstructure 1(2), 189-208. [Inst. f. Chemie & Physik, Bundesanstalt f. Milchforschung, D-2300 Kiel, Federal Republic of Germany].

To select optimum specimen preparation methods and to correctly interpret freeze-fracture/freeze-etch micrographs of food systems, it is necessary to have detailed knowledge of the individual steps of preparation, i.e., chemical fixation of samples, their cryoprotective pretreatment, cryofixation, freeze-fracturing and freeze-etching, and replication and to understand their influence on the appearance of different constituents, especially proteins and lipids. Food

systems show great variation in composition, structure and especially in their content of water, e.g., molecular and colloidal solutions, oil-in-water and water-in-oil emulsions, gel suspensions, semi-solid systems such as cheese, dried systems such as milk powders, thus requiring a careful variation of preparatory conditions.

MISCELLANEOUS

[EFFECT OF COEXISTENCE OF GELATIN ON GELATION OF AGAROSE] [In Japanese]
Watase M, Nishinari K. 1983. Nippon Shokuhin Kogyo Gakkaishi 30(6), 368-374. [Chem. Res. Lab., Fac. Lib. Arts, Shizuoka Univ., Ohya Shizuoka City, 422, Japan].

Mixed agarose (2%) and gelatin (4 to 40%) gels, pH 6.86, were subjected to stress relaxation and dynamic viscoelasticity measurements and to SEM.

ULTRASTRUCTURAL CHANGES IN STRAINS OF FODDER YEASTS CULTIVATED IN THE PRESENCE OF FURFUROL
Losseva LK, Mihailova LI, Katranoushkova HS. 1982. Doklady Bolgarskoi Akademii Nauk 35(12), 1705-1707. [Inst. Microbiol., Acad. Sci., 1113 Sofia, Bulgaria].

The structure of fodder yeast cells (Candida tropicalis and C. diddensii) was severely altered upon cultivation in the presence of furfurol (0.05 and 0.02%, respectively) in wikerham's synthetic medium. TEM of thin sections revealed that cellular walls were thicker, some cells were elongated, cellular division was disturbed, cellular cytoplasm acquired uneven electron density, and most cells were intensely vacuolized.

THE USE OF THE PLASMA CHEMISTRY UNIT AS AN AID TO THE SCANNING ELECTRON MICROSCOPE STUDY OF AVIAN EGG-SHELL STRUCTURE
Reid J. 1983. British Poultry Science 24(2), 233-235. [Dept. Vet. Anat., Univ. of Glasgow Vet. School, Bearsden Rd., Bearsden, Glasgow G61 1QH, Scotland, U.K.].

In order to study the mammillary layer of the avian egg shell by SEM, it is necessary to separate the outer shell membrane from the calcified shell. Chemical methods of effecting membrane removal are difficult to standardise due to variations in the strength of the membrane-shell bond. The use of reactive gas (oxygen) plasma for ~3 h provides an alternative, more efficient method for removing membranes without the risk of damage to underlying crystalline structures.

ELECTRON MICROSCOPY OF FOODS
Kalab M. 1983. In: Physical Properties of Foods, M. Peleg and E.B. Bagley (eds.), AVI Publ. Co., Inc., Westport, Connecticut, U.S.A., 43-104. [Food Res. Inst., Agric. Canada, Ottawa, Ontario, Canada K1A 0C6].

A review with numerous references and examples of SEM and TEM of various foods.

PHYSICAL CHARACTERISTICS OF FOOD POWDERS
Peleg, M. 1983. In: Physical Properties of Foods, M. Peleg and E.B. Bagley (eds.), AVI Publ. Co., Inc., Westport, Connecticut, U.S.A., 293-323. [Dept. Food Eng., Univ. of Massachusetts, Amherst, MA 01003, U.S.A.].

A review, in which SEM has been used as one of many techniques to characterize various kinds of food powders.

PHYSICAL PROPERTIES OF SYNTHETIC FOOD MATERIALS
DeMan JM. 1983. In: Physical Properties of Foods, M. Peleg and E.B. Bagley (eds.), AVI Publ. Co., Inc., Westport, Connecticut, U.S.A., 267-291. [Dept. Food Sci., Univ. of Guelph, Guelph, Ontario, Canada N1G 2W1].

A review discussing the microstructure of synthetic food materials illustrated with numerous SEM micrographs.

ELIMINATION D'UN PROPHAGE DANS LES SOUCHES MONO- ET MULTILYSOGÈNES DE STREPTOCOQUES DU GROUPE N [Prophage curing of mono- and multilysogenic group N streptococcal strains]
Chopin M-C, Rouault A, Rousseau M. 1983. Le Lait 63(625-626), 102-115. [Lab. Rech. Tech. Lait., 65, rue de Saint-Brieuc, 35042 Rennes Cedex, France].

Four lactic streptococci strains out of 12 were cured of their prophage by using mitomycin C and ultraviolet light. After treatment, two of them were no more inducible. The two others, multilysogenic, were only cured from one prophage. Their immunity or their quantitative aptitude to allow phages development was modified by loss of one prophage. Acidification rate of strains in milk was not modified by prophage loss. The phages were negatively stained with phosphotungstic acid at pH 7.2.

FOOD MICROSTRUCTURE: AN INTEGRATIVE APPROACH
Davis EA, Gordon J. 1982. Food Microstructure 1(1), 1-12. [Dept. Food Sci. & Nutr., Univ. of Minnesota, 1334 Eckles Ave., St. Paul, MN 55108, U.S.A.].

The integration of information at all levels of organization in a food system - atomic and molecular through macroscopic properties - is illustrated with cake batters as an example of a formulated food and bovine muscle as an example of biologically intact, non-formulated food. Direct examples are given using macroscopic data collected in heat and water transport studies followed by integration of microscopical data for interpretive purposes.

The contribution of starch gelatinization to the characteristics of water loss in batter is related to events such as loss of birefringence as seen by polarizing microscopy, differential heat input as seen by scanning calorimetry, batter component morphological changes as seen by freeze etching, viscosity differences as characterized by viscometric data, and volume differences of the final baked product. The contribution of myofibrillar protein denaturation to the characteristics of water loss by drip and evaporation is related to events such as changes in sarcomere banding patterns and length as seen by TEM, differential heat input as seen by scanning calorimetry, and by overall muscle sample length shrink.

THE ACTION OF 1,4-β-D-GLUCAN CELLOBIOHYDROLASE ON VALONIA CELLULOSE MICROCRYSTALS. AN ELECTRON MICROSCOPIC STUDY
Chanzy H, Henrissat B, Vuong R, Schülein M. 1983. FEBS Letters 153(1), 113-118. [Centre de Rech. Macromol. Végétales (CNRS), 53 X - 38041 Grenoble Cédex, France].

The interaction between 1,4-β-D-glucan-cellobiohydrolase I (CBHI) from Trichoderma reesei and microcrystalline cellulose from Valonia macrophysa was investigated by EM which allows to visualize the individual enzymes and their strong adsorption at the substrate surface. The microcrystals are slowly degraded and decrystallized by erosion and fibrillation while soluble products are released and characterized by HPLC. CBHI is thus able to break down Valonia microcrystals without the help of any endo-β-1,4-glucanase activity. [Copyright 1983 by The Federation of European Biochemical Societies].

[EFFECT OF PREPARATION METHODS OF YEAST PROTEIN ISOLATE ON EMULSION STABILITY] [In Japanese]
Asano M, Yamaguchi S, Shibasaki K. 1983. Nippon Shokuhin Kogyo Gakkaishi 30(4), 228-234. [Dept. Food Chem., Fac. Agric., Tohoku Univ., Tsutsumidori, Amamiya-machi, Sendai, 980, Japan].

Emulsion stability of yeast protein isolate I was superior to that of soy protein or caseinate, particularly in acidic and alkaline media. However, yeast protein isolates II and III (different preparation procedures) had low emulsion stabilities, comparable to the other proteins mentioned. The particle sizes of the emulsions which had good emulsifying properties were smaller than particles in poor emulsions.

INFLUENCE OF WATER ACTIVITY ON GROWTH, METABOLIC ACTIVITIES AND SURVIVAL OF YEASTS AND MOLDS
Beuchat LR. 1983. Journal of Food Protection 46(2), 135-141. [Dept. Food Sci., Univ. of Georgia Agric. Exp. Station, Experiment, GA 30212, U.S.A.].

The behavior of yeasts and molds as influenced by water activity (a_w) is reviewed. Fungal spoilage of foods occurs more often than bacterial spoilage at a_w 0.61-0.85 not because fungi grow faster at reduced a_w but rather because the competitive effects of the vast majority of bacteria are absent. Higher a_w is generally required for spore formation than for spore germination. The range of a_w permitting germination of spores is greatest at an optimum temperature, but optimum availability of nutrients tends to broaden the range of a_w and temperature at which germination and growth will occur. The minimum a_w levels for growth of fungi are lower than those required for mycotoxin production. It is imperative that diluents and enumeration media with reduced a_w be used to detect xerotolerant fungi in foods. Otherwise, vegetative cells and spores may be killed by osmotic shock or remain dormant when exposed to high a_w associated with diluents and media routinely used for mycological analyses.

REVIEWING PROCEDURE
AND
DISCUSSION WITH REVIEWERS

Each paper in this volume contains a Discussion with Reviewers. This discussion follows the text and should be read with the paper. Each paper submitted to SEM, Inc. for publication is reviewed by at least three, up to an average of five, reviewers. The reviewers are asked to separate their comments from their questions. The comments are useful in determining the acceptability of the papers as submitted. Although the comments require no written response, in several cases, the authors have included responses to comments, or to questions phrased from, or based on, comments (either as a result of editorial suggestions or on the author's own initiative). Based on these comments approximately 15% of the submitted papers were not accepted for publication; while almost all of the others were asked to make changes involving from minor to major revisions.

The questions, for the most part, originate as a result of statements included in our cover letter accompanying each paper sent to the reviewers. The reviewers are asked to suppose they are attendees at a conference where this paper, as written, is being presented, and then ask relevant questions which would occur to them resulting from the presentation. From the questions so asked, some are not included with the published paper because the authors attended to them by text revisions. In some cases, editorial and/or space considerations may exclude inclusion of all questions asked by reviewers. The authors are asked to prepare their Discussion with Reviewers section in a camera-ready format. In some instances the authors edit the questions and/or combine several similar questions from different reviewers to provide one answer. While all efforts are made to check that the questions in the printed version faithfully follow the views of the specific reviewer, the editors apologize, if in some instances, the actual meaning and/or emphasis may have been changed by the author.

The cover letter to the reviewers states:

"1. Your name will be conveyed to the author with your review UNLESS YOU ASK US NOT TO.

2. The questions published in the Journal will be identified as originating from you UNLESS YOU ADVISE OTHERWISE..."

In all cases sincere efforts are made to respect the reviewer's wishes to remain anonymous; however, in nearly 95% of the cases, the reviewers have given permission to be identified; so their names are conveyed to the authors and are included with the questions printed with each paper. An overall list of reviewers is provided in the opening pages of each SEM part. We apologize for any error/omissions which may occur.

Finally, readers are urged to be cautious regarding the weight they attach to the authors' replies, since the answers to the questions represent the authors' unchallenged views--except for minor editorial changes--the authors generally have the last word. Also, please consider that the questions were, in most cases, relevant to the originally submitted paper, and they may not have the same significance for the revised paper published in this volume.

If you disagree with the results, conclusions or approaches in a paper, please send your comments, as a Letter to Editor, typed in a column format (each column is 4-1/8 inches wide and 11-1/2 inches long; i.e., 10.5 by 29.3 cm.). Your comments along with author's response will be published in a subsequent issue.

The editors gratefully thank the authors and reviewers (see p. xi & 202) for their contributions, invite your comments on ways to improve this procedure and seek qualified volunteers to assist with reviewing papers in the future.

ERRATA: Despite the best efforts of authors, reviewers and editors, errors may remain. Please help by pointing out errors that you notice. Please provide enough information to locate each error (volume, page, column, line, etc.) and indicate suitable correction.

The Editors
Food Microstructure

REVIEWERS LIST

The help of the following reviewers for papers published in the second volume of FOOD MICROSTRUCTURE is gratefully acknowledged.

Addis, P.B.	Univ. Minnesota, St. Paul
Arnott, H.J.	Univ. Texas, Arlington
Ashraf, M.	Univ. Cincinnati Sch. of Med., OH
Bair, C.W.	Frito-Lay, Inc., Irving, TX
Bell, Jr., P.B.	Univ. Oklahoma, Norman
Betschart, A.A.	USDA Western Reg. Res. Ctr., Berkeley, CA
Boyde, A.	University College, London, U.K.
Britt, B.A.	Univ. Toronto, Ontario, Canada
Caeseele, L.V.	Univ. Manitoba, Winnipeg, Canada
Carroll, R.J.	USDA Eastern Reg. Res. Ctr, Philadelphia, PA
Cassens, R.G.	Univ. Wisconsin, Madison
Chabot, J.F.	Cornell Univ., Ithaca, NY
Christianson, D.D.	USDA Northern Reg. Res. Ctr., Peoria, IL
Cohen, S.H.	US Army R & D Lab, Natick, MA
D'Appolonia, B.L.	North Dakota Univ., Fargo
Davies, F.L.	Natl. Inst. for Res. Dairying, Shinfield, U.K.
Davis, E.A.	Univ. Minnesota, St. Paul
Dexter, J.E.	Canadian Grain Comm., Winnipeg, Manitoba
Dieckert, J.W.	Texas A & M Univ., College Station
Earp, C.F.	Texas A & M Univ., College Station
Fuwa, H.	Osaka City Univ., Japan
Glennie, C.W.	CSIR--Sorghum Beer Unit, Pretoria, S. Africa
Gold, C.A.	US Army R & D Lab, Natick, MA
Gordon, J.	Univ. Minnesota, St. Paul
Hayes, T.L.	Univ. California, Berkeley
Hofsten, A.V.	Univ. Uppsala, Sweden
Holcomb, D.N.	Kraft Inc., Glenview, IL
Humphreys, W.J.	Univ. Georgia, Athens
Irvine, D.M.	Univ. Guelph, Ontario, Canada
Irving, D.W.	USDA Western Reg. Res. Ctr., Berkeley, CA
Kalab, M.	Agriculture Canada, Ottawa, Ontario
Kikuchi, K.	Sugiyama Chem. & Ind. Lab., Yokohama, Japan
Lee, C.M.	Univ. Rhode Island, Kingston
Locker, R.H.	Meat Industry Res. Inst. of New Zealand, Hamilton
Lundström, K.	Swedish Univ. Agric. Sciences, Uppsala
Mandigo, R.W.	Univ. Nebraska, Lincoln
Mills, J.T.	Agriculture Canada, Winnipeg, Manitoba
Molder, W.	Agriculture Canada, Ottawa, Ontario
Moss, R.	Bread Res. Inst., North Ryde, N.S.W., Australia
Munck,L.	Carlsberg Res. Lab, Copenhagen, Denmark
Newell, C.A.	Univ. Illinois, Urbana-Champaign
Norris, K.H.	USDA - Agriculture Res. Ctr., Beltsville, MD
Olson, N.F.	Univ. Wisconsin, Madison
Roach, J.	US Army R & D Lab, Natick, MA
Ross, W.E.	US Army R & D Lab, Natick, MA
Müegg, M.	Dairy Res. Inst., Liebefeld, Switzerland
Schmidt, D.G.	Netherlands Inst. Dairy Res., Ede
Segars, R.	US Army R & D Lab, Natick, MA
Seideman, S.C.	USDA - Meat Animal Res. Ctr., Clay Center, NE
Simmonds, D.H.	CSIRO Wheat Res., North Ryde, N.S.W., Australia
Sosulski, F.W.	Univ. Saskatchewan, Saskatoon, Canada
Squire, J.M.	Imperial College, London, U.K.
Stanley, D.W.	Univ. Guelph, Ontario, Canada
Sullins, R.D.	Frito-Lay, Inc., Irving, TX
Tamime, A.Y.	West Scotland Agric. Col., Auchincruive, U.K.
Taranto, M.V.	ITT Continental Baking Co., Rye, NY
Vaughan, J.A.	Queen Elizabeth College, London, U.K.
Venable, J.H.	Colorado State Univ., Fort Collins
Voyle, C.A.	ARC-Meat Res. Inst., Bristol, U.K.
Wolf, W.J.	USDA Northern Reg. Res. Lab., Peoria, IL
Young, O.A.	Meat Industry Res. Inst. of New Zealand, Hamilton

SUBJECT INDEX

Aleurone layer 13, 143, 165, 175, 183
Amylase 13
Ascospore morphology 143
Autofluorescence 183
Avacado leaves 67
Bacteria, in yoghurt 51
Barley 13
Batter, cake 153
Batter, wiener 27
Bean, winged 175
Bovine muscle 91, 119
Brabender viscosity 153
Bubbles (in whey protein gels) 161
Cakes 153
Casein 43, 51
Cereal foods 1, 153
Cheese 43
Coconut 81
Cocos nucifera L. 81
Contracture band 111
Corn leaves 67
Cotyledon cell 143, 175
Cotton leaves 67
Critical point drying 23, 161
Cryofracture 1, 23
Cryo-sectioning 81, 135, 165
Cultivars 183
Cytoskeleton 99
Dehydration 23
Desmin 99
Dough 1
Durum wheat 1
Electrophoresis, gel 91
Embedding 81, 165, 175, 183
Emulsions, meat 23, 27
Endosperm 13, 81
Enzymes 13, 91, 135, 183
Fat 23, 27, 81
Fibers, meat 111, 135
Field spectroscopy 67
Flour 1, 153
Flour, chlorinated 153
Fluorescence microscopy 143, 165, 183
Fluorochromes 183
Frankfurter 23, 27
Freeze-drying 13, 43, 143
Freeze-fracture 1, 23, 51, 143
Freon 23, 43
Gel, protein 161
Germination 13
Glucans, beta 183
Glucuronidase 91
Gluten 1
Halothane test 111
Image analysis 27
Immunofluorescence 99
Infrared spectroscopy 67
Lactoglobulin 51
Lettuce leaves 67
Leaf structure 67
Light microscopy 27, 81, 99, 135, 143, 165, 175, 183
Lysosomal enzymes 91
Meal, rapeseed 165
Meat 23, 27, 91, 99, 119, 135
Micelles 43, 51
Microphotometry 135
Milk, powder 43
Milk, Gelation 51
Morphometry 27, 135
Mucogenic bacteria 51
Muscle, bovine 91, 119
Muscle, cytoskeleton 99
Muscle, fibers 111, 135
Muscle, pork 111, 135
Mustard 143
Myofibrillar distortions 111
Nematospora 135
Oat leaves 67
Pasta 1
Plasmodesmata 175
Porcine stress syndrome 111
Pork 111, 135
Prerigor, muscle 91
Protein, cheese 43
Protein coagulation 1, 51, 161
Protein detection 67
Protein, gels 151
Protein, meat 23, 27
Protein solubility 1, 43
Protein, whey 51, 161
Psophocarpus tetragonolobus 175
Radiometry 67
Rapeseed 165
Reflectance 67
Replicas 1, 43
Rice flour 1
Rotary shadowing 51
Sarcolemma 99
Scanning electron microscopy 1, 13, 23, 51, 67, 81, 99, 111, 119, 143, 153, 161, 165
Scanning light microscopy 135
Sectioning 27, 135, 175
Seed morphology 143, 165
Sensory evaluation 119
Soft brine cheese 43
Soy 119
Spaghetti 1
Spectroscopy 67
Spice 143
Sorgum bicolor 183
Staining 33, 81, 143, 165, 175
Starch 1, 153, 175
Stereology 27, 135
Succinate dehydrogenase 135
Texture 99, 119
Thickening agents 51
Transmission electron microscopy 1, 43, 51, 81, 91, 111, 175
Transport, heat and water 153
Viscosity 143, 153
Wheat, durum 1
Wheat, flour 1, 153
Wheat leaves 67
Wheat, soft 1
Whey 43, 51, 161
Whey protein concentrate 161
Wieners 23, 27
Winged bean 175
X-ray microanalysis 23, 153
Yeast infection 143
Yoghurt 51
Z-line in muscle 91, 99

AUTHOR INDEX

Allan-Wojtas, P. 51
Altosaar, I. 165
Anglemier, A.F. 91
Basgall, E.J. 23
Basrur, P.K. 111
Bechtel, P.J. 23
Beveridge, T. 161
Brach, E.J. 67
Buchheim, W. 43
Cardello, A.V. 119
Chapman, J.A. 81
Cohen, S.H. 119
Davis, E.A. 153
Doherty, C.A. 183
Dushnicky, L. 13
Earp, C.F. 183
Elgasim, E.A. 91
Elkhalifa, E.A. 91
Frombach, S. 111
Fulcher, R.G. 165, 183
Geissinger, H.D. 111
Gordon, J. 153
Grider, J. 153
Heathcock, J.F. 81
Holley, R.A. 143
Jones, L. 161
Kalab, M. 51
Kempton, A.G. 27
Kennick, W.H. 91
Koohmaraie, M. 91
MacGregor, A.W. 13
McDonell, W.N. 111
McKeith, F.K. 23
Nakano, Y. 175
Nicholls, P.B. 13
Omar, M.M. 43
Pagani, M.A. 1
Phipps-Todd, B.E. 51, 143
Resmini, P. 1
Rooney, L.W. 183
Rosenkrans, R. 119
Saio, K. 175
Secrist, J. 119
Segars, R.A. 119
Smith, J. 119
Stanley, D.W. 99
Swatland, H.J. 135
Trupp, S. 27
Tung, M.A. 161
Uemoto, S. 175
Yiu, S.H. 143, 165

Copyright © 1983 Scanning Electron Microscopy, Inc.,
except for contributions in the public domain.
All rights reserved.

See statement on the inside front cover.

Permission is granted to quote from this volume in scientific works with the customary acknowledgement of the source. To print a table, figure, micrograph or other excerpt requires, in addition, the consent of one of the original authors and notification to SEM, Inc. Republication or systematic or multiple reproduction of any material in this volume (including the abstracts) is permitted only after obtaining written approval from SEM, Inc., and in addition, SEM, Inc. requires that permission also be obtained from one of the original authors.

Every effort has been made to trace the ownership of all copyrighted material in this volume and to obtain permission for its use.

FOOD MICROSTRUCTURE
INSTRUCTIONS TO AUTHORS

Papers for publication in Food Microstructure can be offered at any time. Papers intended for oral presentation at the Annual Food Microstructure meeting in April are due January 15th. Only papers acceptable for publication are allowed oral presentation.

In a letter accompanying the paper, authors must provide names and complete addresses of at least **four persons competent to review their paper**. Please note: **a.** Suggested reviewers must neither be from authors current or recent affiliations, nor coworkers; **b.** preferably suggested reviewers should be amongst active researchers in the field (e.g., whose work is being extensively referred); and **c.** Authors are neither expected to personally know nor required to contact the suggested reviewers. From the names suggested by the authors and SEM's advisors, editors **will select** the most suitable reviewers irrespective of their geographical location. Each paper will be intensely reviewed by at least three, and often more, reviewers.

The **initial paper (hereafter referred to as 'paper')** should conform to **these Instructions.** However, to be published after reviewing, **the final manuscript (hereafter referred to as 'manuscript'), must be submitted on model sheets conforming to the Manuscript Submission Guidelines; these guidelines and model sheets (a sample model sheet is available on request)** will be mailed **along with the reviewers' comments**. In addition to all the text, the **manuscript** must also contain author's publishable responses to questions raised by the paper's reviewers. (See, e.g., discussion with reviewers in this issue.)

Three types of papers can be offered. The authors must indicate type of paper and carefully adhere to the applicable definition, since the reviewers and editors judge the paper accordingly:

CONTRIBUTED PAPER: Presents new unpublished findings.

REVIEW PAPER: Includes an extended literature review and complete bibliography, **emphasizes author's new unpublished findings** and in an extended discussion puts the topic in proper perspective.

TUTORIAL PAPER: Contains an **organized comprehensive review** and bibliography of **ALL** relevant published material as for a teaching lecture.

INSTRUCTIONS FOR SUBMISSION OF PAPERS

Type paper in **double-spaced** format on 8½ x 11 inch (or similar size) paper. **A length limit is not imposed on papers. Short, but complete, papers are welcome.**

The paper should include title page, abstract, all headings and text. On the **title page** include a **short title** which accurately reflects the contents of the paper; *an informative running head consisting of no more than 50 characters, including spaces between words;* **names and affiliations** of all authors; **name and complete work and home address and phone numbers of the person to contact**, and **10 key words/phrases** suitable for subject index. **For review papers the title page must indicate page numbers containing new material** (e.g. "new material will be found on pages .").

An **Abstract** (of 100-250 words) is required for all papers. The abstract should be a concise statement of the purpose of the paper and of the major results obtained. **It must be self-explanatory**, and free of phrases such as "will be described", "is discussed", "are presented", etc.

The **Introduction** to the paper **must** contain a clear, concise statement of the purpose of the paper and the relationship of this paper to what is already in the literature. As applicable, a **Materials and Methods** section, with **complete specimen preparation** information must be included so that the work can be duplicated by others.

Equations should be numbered consecutively, using arabic numerals. Each **symbol and abbreviation** should be defined when first used. **SI (metric) units must be used.** U.S. customary (English) or other metric units, if used, must be given in parentheses.

REFERENCES

Include all references relevant to paper. Do not use too many of your own references. References can be made only to readily available published work and to papers in press. Work in progress, manuscripts in preparation, manuscripts submitted, unpublished experiments, and personal communications, must be excluded from the reference list, but may be acknowledged in the text (in parentheses).

The reference list at the end of the paper must be organized in alphabetical order by the first authors' names. Full titles of papers and inclusive pagination must be included.

In the text, cite references in one of the following two styles:

a. Cowley (1967) or (Cowley, 1967) or Crewe and Wall (1970). If there are three or more authors, use the form Venables et al. (1978). If more than one paper is published in the same year by the same author (or group of authors) use the form (Rose, 1974a), etc.

b. As long as there is consistency, either superscript[1] or full size numberals in brackets [1] can be used. In this case, the numbering must be in sequence in the reference list, but the references will generally not appear in sequence in the text.

Examples of acceptable reference formats are:

(i) **For a Journal**—(use standard abbreviations). Holt DB, Datta S. (1980). The cathodoluminescent mode as an analytical technique: Its development and prospects, Scanning Electron Microsc. 1980; I: 259-278. **(For papers from past issues of SEM, use this format only)**. Precht D, Buchheim W. (1980) Electron microscopic studies on the physical structure of spreadable fats. Milchwissenschaft, **35**, 684-687, 690.

(ii) **For a Book**—(include range of pages or chapter, do not refer to entire book). Heidenreich, RD. (1964). Fundamentals of Transmission Electron Microscopy, Interscience, NY, 332-356.

(iii) **For a Proceeding or Compilation**—(publisher or full availability information must be included). Pease DC. (1973). Substitution Techniques, in: Advanced Techniques in Biological Electron Microscopy, J.K. Koehler (ed.), Springer-Verlag, NY, 35-36.

ILLUSTRATIONS AND TABLES

Number each figure and table with **an arabic numeral and refer to them in sequence in the text**. Several illustrations within a figure must be designated a, b, c, etc. Each table must have a title. ***Each figure must have a caption***—either on its own page or all captions should be placed together on separate pages. **Very important: Use arrows or letters to identify features referred to, and so indicate in the caption.** Illustrate text with the fewest photographs possible. Indicate magnification on photos by a line of, e.g., 1μm, 10μm, 100μm, or 1 mm length; identify either on the photo or in the caption. Use nm, μm, or mm, not μ, u or -X.

Quality of Illustrations. *Photos should be clear, clean, unscreened,* (screened photos are not acceptable), *black and white glossy prints.* **Color photographs** can be published by prior arrangement between the author and the managing editor, whereby the author will be asked to pay the additional cost.

Size. For the *manuscript*, illustrations and tables should preferably be 10.5 cm wide. The maximum permissible length for photographs will be 9 cm (3.5"); line drawings and tables may be longer than 9 cm but not wider than 10.5 cm. All letters and symbols on illustrations and tables must be larger than 2.0 mm. **THE ILLUSTRATIONS, TABLES AND LETTERING INCLUDED WITH THE PAPER MUST CONFORM TO THESE SIZES.** *Permission for larger illustrations and/or tables, must be requested when the paper is submitted.*

SUBMISSIONS AND COMMUNICATIONS

Submit 4 copies of the paper. Each of the 4 copies must include its own set of illustrations and clear glossy prints of all photographs. (Retain the best set of prints for your manuscript, since illustrations sent with paper will not be returned.) Papers containing photocopies (Xerox, etc.) of photographs will not be processed for reviewing, manuscript containing photocopies of tables and illustrations are not accepted. All illustrations must be organized in sequence (must not be mounted on cardboards); and placed in separate envelopes. Place each copy of the paper, *(together with its envelope of illustrations), in separate, unsealed, ready-to-mail envelope,* so that the paper can be directly sent to its reviewers.

For **submission** of papers and **inquiries** contact: one of the editors, or **Dr. Om Johari**, managing editor, **(phone 312-529-6677)**, P.O. Box 66507, AMF O'Hare, IL 60666 USA. **(Street address**, if needed is: 1034 Alabama Dr., Elk Grove Village, IL 60007, USA).

OTHER IMPORTANT ITEMS

Reprints. 15 complimentary tear sheets are provided. Information for ordering 50 tear sheets and additional reprints is sent with the complimentary tear sheets.

Copyright. Food Microstructure is a copyrighted publication. Letters granting permission to use other copyrighted material must accompany the **manuscript**.

FOOD MICROSTRUCTURE

An International Journal on the Microstructure and Microanalysis of Foods, Feeds and their Ingredients

VOL. 2, NO. 2 (1983)

TABLE OF CONTENTS

SENSORY AND INSTRUMENTAL TEXTURE PROPERTIES OF FLAKED AND FORMED BEEF
A.V. Cardello, R.A. Segars, J. Secrist, J. Smith, S.H. Cohen and R. Rosenkrans 119

MORPHOMETRY OF MEAT BY SCANNING LIGHT MICROSCOPY
H.J. Swatland 135

INFECTION OF ORIENTAL MUSTARD BY NEMATOSPORA: A FLUORESCENCE AND SCANNING ELECTRON MICROSCOPE STUDY
R.A. Holley, B.E. Phipps-Todd and S.H. Yiu 143

EVALUATION OF SELECTED PROPERTIES OF CHLORINATED WHEAT FLOURS IN A LEAN CAKE FORMULATION
J. Grider, E.A. Davis and J. Gordon 153

STRANDED STRUCTURE DEVELOPMENT IN THERMALLY PRODUCED WHEY PROTEIN CONCENTRATE GEL
T. Beveridge, L. Jones and M.A. Tung (Short Note) 161

THE EFFECTS OF COMMERCIAL PROCESSING ON THE STRUCTURE AND MICROCHEMICAL ORGANIZATION OF RAPESEED
S.H. Yiu, I. Altosaar and R.G. Fulcher 165

MICROSTRUCTURE OF WINGED BEANS
K. Saio, Y. Nakano and S. Uemoto 175

ß-GLUCANS IN THE CARYOPSIS OF *SORGHUM BICOLOR* (L.) MOENCH
C.F. Earp, C.A. Doherty, R.G. Fulcher and L.W. Rooney 183

Abstracts of Food Microstructure Papers 189

Discussion with Reviewers 201

Reviewers List 202

Subject Index 203

Author Index 204

Instructions to Authors ..... Inside back cover